Murine Gap Junction Remodelling Induced By Subdiaphragmatic Pacing

A Thesis Submitted to Imperial College London for the degree

Of Doctor of Philosophy

Dr Andrianos Kontogeorgis

CID 00462074

May 2013

National Heart and Lung Institute

Imperial College London

St Mary's Campus

[1]

Abstract

This thesis aims to adapt and develop a mouse model for stable dyssynchronous pacing and systematic investigation of mechanisms of structural gap-junctional remodelling (GJR) and correlation to functional changes. GJR, an altered abundance or localisation of connexin proteins strongly correlates with arrhythmogenic substrates.

Wild type Cx43$^{+/+}$ and heterozygous Cx43 knockout Cx43$^{+/-}$ (66% mean reduction in Cx43) mice were paced *in vivo* subxiphisternally at 10-15% above anaesthetised sinus rates for one to six hours avoiding intubation, vascular access, thoracic or mediastinal disruption.

In Cx43$^{+/+}$ mice, pacing resulted in electrical and mechanical dyssynchrony. Echocardiographic (ECHO) and electrocardiogram (ECG) indices, ventricular effective refractory period (VERP) and arrhythmia inducibility were not significantly altered. Pacing attenuated transmural gradients of Cx43 immunosignal in the LV free wall. Significant reductions in Cx43 mRNA abundance at the LV free wall occurred. Cx43, its isoforms and interacting protein expression were unchanged. Fractionation studies of 6hr-paced hearts demonstrated reduced Cx43 in membrane fractions while cytosolic fractions increased significantly. Cx43 degradation studies demonstrated substantially increased ubiquitinated forms with pacing.

Cx43 protein expression in paced and unpaced Cx43$^{+/-}$ mice hearts was unchanged. In contrast to Cx43$^{+/+}$ cells, Cx43$^{+/-}$ mice demonstrated significantly shorter action potential durations (APD), increased steady-state (Iss) and inward rectifier (IK$_1$) potassium currents. Pacing prolonged action potential duration (APD) at 50ms and 90ms increased VERP at 80ms/100ms and significantly reduced Iss in Cx43$^{+/-}$ vs. unpaced Cx43$^{+/-}$ hearts.

Pacing induces electro-mechanical dyssynchrony in wildtype Cx43 (Cx43$^{+/+}$) hearts, results in remodelling of the cardiac gap junctions without sustained measurable effects or increased arrhythmia inducibility. Transgenic hearts (Cx43$^{+/-}$) respond quite differently to pacing, which may be relevant in cardiac disease, where Cx43 is focally reduced. Pacing could lead to the remodelling of repolarisation currents in regions of reduced Cx43, enhancing dispersion of refractoriness and potentially creating a substrate for arrhythmia re-entry.

Copyright Declaration

[4]

Statement of Originality

In accordance with Imperial College London regulations I declare that all the work within this thesis is my own unless specified otherwise with appropriate references in the text.

Dr Andrianos Kontogeorgis

2013

Acknowledgements

later Cx43$^{+/-}$ and Cx40$^{-/-}$ immunoblotting experiments with Marc Ponzio. Dr Edward Fisher participated in the design of the study and helped coordinate the qRT-PCR experiments that I executed together with Jonathan Feig.

Michael Rindler of the Cell Biology department at NYU helped design, oversee and interpret the cell lysate fractionation and immunoprecipitation experiments that were executed by Dr Gutstein, myself, Marc Ponzio and Pritha Gupta. I assisted Marc Ponzio with some of the cell isolation and provided cells to Dr Xiadong Li who kindly performed the patch clamp experiments; I observed, assisted where possible and aided in data collection, analysis, interpretation and creation of the graphs with Dr Gutstein. I also assisted with the optical mapping experiments in the Cx43$^{+/-}$ mice to assess epicardial activation breakthrough patterns and correlated this data with ECHO, PES and structural data. I performed all the immunostaining of the Cx40$^{+/+}$, Cx40$^{+/-}$ and Cx40$^{-/-}$ atrial tissue and quantitatively assessed the immunosignal on a regional (RAA vs. LAA) and age dependent basis and correlated this with functional, optical mapping data generated from the Morley lab.

Finally, I am indebted to my brother Dimitri, my family, and my wife for everything.

This work is dedicated to my family and loved ones.

Publications arising from this period of study:

Kontogeorgis A, Kaba RA, Kang E, Feig JE, Gupta PP, Ponzio M, et al. Short-term pacing in the mouse alters cardiac expression of connexin43. BMC Physiol 2008;8:8.

Kontogeorgis A, Li X, Kang EY, Feig JE, Ponzio M, Kang G, et al. Decreased connexin43 expression in the mouse heart potentiates pacing-induced remodeling of repolarizing currents. Am J Physiol Heart Circ Physiol 2008 Nov;295(5):H1905-H1916.

Roepke TK, Kontogeorgis A, Ovanez C, Xu X, Young JB, Purtell K, Goldstein PA, Christini DJ, Peters NS, Akar FG, Gutstein DE, Lerner DJ, Abbott GW.FASEB J. 2008 Oct;22(10):3648-60. Epub 2008 Jul 4. Targeted deletion of kcne2 impairs ventricular repolarization via disruption of I(K,slow1) and I(to,f).

Leaf DE, Feig JE, Vasquez C, Riva PL,Yu C, Lader JM, Kontogeorgis A, Baron EL, Peters NS, Fisher EA, Gutstein DE, Morley GE.Circ Res. 2008 Oct 24;103(9):1001-8. Epub 2008 Jul 3 Connexin40 imparts conduction heterogeneity to atrial tissue.

Malester B, Tong X, Ghiu I, Kontogeorgis A, Gutstein DE, Xu J, Hendricks-Munoz KD, Coetzee WA.FASEB J. 2007 Jul; 21(9): 2162-72. Epub 2007 Mar 6. Transgenic expression of a dominant negative K (ATP) channel subunit in the mouse endothelium: effects on coronary flow and endothelin-1 secretion.

Abstracts accepted and oral presentations

Kontogeorgis A, Kaba R, Peters N, Gutstein D. Short-term pacing results in sustained dyssynchrony and prolonged repolarization in connexin43 heterozygous knockout mice. BJCA 2007 abstract

Kontogeorgis A, Kaba R, Peters N, Gutstein D. Short-term pacing in the mouse heart alters expression of connexin43. BJCA 2007 abstract

Kontogeorgis A BCS June 2008 and Young Research Workers Prize accepted for presentation. Decreased connexin43 in heterozygous knockout mice potentiates pacing induced remodeling of repolarizing currents

Kontogeorgis A ECAS April 2008 accepted for presentation. Short-term pacing results in sustained dyssynchrony and prolonged repolarization in connexin43 heterozygous knockout mice.

Kontogeorgis A.18 June 2009 National Heart and Lung Institute Postgraduate Research Day oral presentation. Decreased Cx43 in heterozygous knockout mice potentiates pacing induced remodeling of repolarizing ion channels.

Awards and Prizes

Runner Up: Young Research Workers Prize –British Cardiovascular Society; Manchester

June 2008.

British Heart Foundation PhD Student Grant 2005-2007.

Table of Contents.

[16]

List of Figures

[18]

List of Tables

Abbreviations

AF	Atrial fibrillation
aLQTS	acquired long QT syndrome
APD	Action Potential Duration
4-AP	4-Aminopyridine
ANOVA	Analysis of variance
AVN	Atrio ventricular node
AWTs	anterior wall thickness at end-systole
AWTd	anterior wall thickness at end-diastole
cAMP	cyclic adenosine monophosphate
CKO	Conditional knockout.
CL	Cytoplasmic Loop
CRT	Cardiac Resynchronisation Therapy
CT	carboxy terminus
Cx40	Connexin 40
Cx43	Connexin 43
Cx43$^{+/+}$	Wild type Cx43
Cx43$^{+/-}$	Heterozygous Cx43
Cx45	Connexin 45
EBZ	Epicardial Border Zone
ECG	Electrocardiography
ECHO	Echocardiography
EF	Ejection Fraction
EL 1	Extracellular loop 1
EL 2	Extracellular loop 2
ER	Endoplasmic Reticulum
ESC	European Society of Cardiology
FS	Fractional shortening
GA	Golgi apparatus

GAPDH	Glyceraldehyde 3-phosphate dehydrogenase
GJ	Gap Junction
GJIC	Gap Junction Intercellular Communication
GJR	Gap Junction Remodelling
HPS	Haemotoxyline- phloxine- saffron.
IDD	intraventricular dimensions at end-diastole
IDS	intraventricular dimensions at end-systole
Ito	transient outward potassium current
Iss	steady state potassium current
Ikr	Inward rectifier potassium current
Kv channel	Voltage-gated potassium channel
LQTS	Long QT Syndrome
LV	Left Ventricle
MiRP	MinK-related peptide
mRNA	messenger RNA
MI	Myocardial Infarction
NSVT	Non sustained ventricular tachycardia
NT	N Terminus
NYU	New York University
OCKO	Heart specific Cx43 conditional knockout
PBS	Phosphate buffered saline
PCR	Polymerase Chain Reaction
PES	Programmed Electrical Stimulation
PKA	Protein Kinase A
PKC	Protein Kinase C
PP1	Protein phosphatase 1
PP2A	Protein phosphatase 2A
PR	PR interval
PTH	Parathyroid Hormone

PWTd	posterior wall thickness at end-diastole.
PWTs	posterior wall thickness at end-systole
qRT- PCR	Quantitative Real Time PCR
QRS	QRS interval
QRSa	QRS amplitude
QT	QT interval
QTc	corrected QT interval
RMP	Resting Membrane Potential
RNA	Ribonucleic Acid
RV	Right Ventricle
SAN	Sino atrial node.
SEM	Standard Error of Mean
SPWMD	Septal- to- Posterior Wall Motion Delay.
TEA	Tetraethyl ammonium;
TGF β	Transforming growth factor beta.
TNF	Tumour Necrosis Factor
VAMC	Veteran Affairs Medical Centre
VERP	Ventricular Effective Refractory Period
Wnt -1	proto-oncogene protein wnt-1 (encoded by WNT1 gene)
ZO 1	Zonnula occludens 1

Chapter 1.

Overview

The focus of the work in this thesis is the establishment of a novel murine model of sub diaphragmatic pacing and the study of electroanatomical effects i.e. aberrant electrical activation (dyssynchrony) on architectural and more specifically gap junction remodelling (GJR). The effects of pacing induced dyssynchrony are tested in mice with naturally occurring levels of connexin 43 ($Cx43^{+/+}$) and genetically reduced Cx43 ($Cx43^{+/-}$). To further explore the functional electrophysiology effects of gap junction remodelling, I quantify connexins and their cardiac isoforms in wildtype Cx40 ($Cx40^{+/+}$), $Cx40^{+/-}$ and Cx40 knockout ($Cx40^{-/-}$) mice and correlate findings to functional atrial electrophysiology data from optical mapping experiments.

In this chapter, I outline the key observations in the gap junction biology field on which the aims and hypotheses of this thesis are based. I present the current knowledge base for the molecular process driving gap junction remodelling with dyssynchrony. I include key, relevant concepts in the gap junction biology field as relates to their structure, function, bio assembly, modulation, phosphorylation, altered gap junction intercellular communication, their role in action potential propagation and how their remodelling alters electrophysiology and results in atrial and ventricular arrhythmias.

The clinical relevance of dyssynchrony and gap junction remodelling, is that they strongly correlate with arrhythmic sudden death, the commonest cause of mortality in western societies e.g. in the USA and the UK.

In Chapter 2, I present the establishment of the subdiaphragmatic pacing model. In Chapter 3, I outline the electrocardiographic measurements at baseline and after pacing or sham-pacing

in $Cx43^{+/+}$ wildtype mice as well as $Cx43^{+/-}$ mice. Chapter 4 presents the echocardiography findings at baseline, during pacing and after pacing in $Cx43^{+/+}$ and $Cx43^{+/-}$ mice. Subsequently, Chapter 5 explores the arrhythmia inducibility with programmed electrical stimulation and ventricular effective refractory period at baseline and after pacing in $Cx43^{+/+}$ mice and $Cx43^{+/-}$ mice. Chapter 6 correlates the anatomical data with electrophysiology at baseline and after pacing in $Cx43^{+/+}$ as well as $Cx43^{+/-}$ mice. Chapter 6 also includes data quantifying connexins and their cardiac isoforms in wildtype Cx40 ($Cx40^{+/+}$) and Cx40 knockout ($Cx40^{-/-}$) mice and correlates these to atrial optical mapping data. Chapter 7 integrates the findings throughout the thesis to draw some conclusions.

Aims and Hypothesis

Scope of Thesis and Rationale of studying dyssynchrony induced pacing.

The Hypotheses and Aims of the set of studies in this thesis are based on the following key observations:

1. Prolonged aberrant ventricular electrical activation has been associated with focal structural gap junction remodelling. Animal models of dyssynchrony demonstrate this observation; gap junction remodelling in canine models induced by pacing, localised to the pacing probe; whilst radiofrequency ablation of the canine left bundle branch resulted in no change to total Cx43 expression, however subcellular location was redistributed in late-activated myocardium from intercalated discs to lateral myocyte membranes(1-4).

2. Gap Junction Remodelling (GJR) due to altered Cx43 (as well as Cx40, Cx45 isoform) patterns of distribution and expression is associated with altered patterns of electrical conduction, activation and arrhythmia propensity; as in the cardiac specific Cx43 knockout mouse (CKO), the central common pathway of figure of eight re-entrant arrhythmia circuits in myocardial infarction (MI) models and altered contractility patterns (as in the chimeric Cx43 CKO mouse)(5-8). Cx43 normally localises to the intercalated disc, primarily situated at the terminal ends of healthy cardiac myocytes whereas in cells from the infarct border zone Cx43 is distributed throughout the lateral surface of the cardiac myocyte; much emphasis has been placed correlating gap junction *lateralisation* and arrhythmia substrates(8;9).

3. Cx43 demonstrates rapid trafficking and turnover with a short biological half-life of 1.5 hours and responds dynamically to changing external factors e.g. areas of gap junction

remodelling were observed in dog hearts after 21 days of pacing(1); strikingly, less than an hour of ischaemia-reperfusion in an isolated rat heart demonstrated redistribution of Cx43(10). It therefore seemed possible that pacing-induced gap junction remodelling might also occur over a short time between 1.5- 6 hours.

4.Prior studies have indicated that in the diseased heart Cx43 abundance can be variable, with focal areas of reduced expression corresponding to hibernating and ischaemic zones; such structural alterations affect other cellular membrane components such as connexin isoforms, other proteins which form part of the gap junction nexus and related ion channels(9;11-13).

5. Gap junction remodelling is also accompanied by altered ion channel expression, which occurs in a chamber, species-specific manner and strongly correlates with atrial and ventricular arrhythmias e.g. the central common pathway of figure of eight re-entrant arrhythmia circuits in MI models(12). It represents a common endpoint for several disease states such as ischaemia, infarction, hibernation, heart failure and atrial fibrillation (8;14-16).

6.A simple small-mammal in vivo model that avoids the risks of blood loss, ischemia, thoracotomy and ventilation for prolonged ventricular pacing has not been available (3).

7.Short-term pacing reduces connexin expression; this has previously been described by Sambelashvili et al, however, this has been in the setting of strong electric currents, up to 100 times greater representing a model of cardiac tissue damage rather than altered activation suggesting a voltage-dose response(17).

8. GJR due to altered connexin isoform expression e.g. Cx40 has been correlated in atrial and ventricular arrhythmia.

9. The developing heart demonstrates spatiotemporal gap junction remodelling while further age related cardiac membrane changes also occur (5;18;19). These models have furthered our

[27]

understanding of adaptive mechanisms driving gap junction remodelling and raised important questions regarding variations in age related myocardial electrical conduction.

This thesis has the following specific and novel goals:

1.To develop and refine an in vivo subdiaphragmatic murine pacing induced dyssynchrony model that allows prolonged pacing, with 100% stable capture, is well tolerated and reproducible without thoracic, abdominal, vascular or cardiac injury, without need for intubation and in the absence of ischaemia or hypothermia.

2. To demonstrate feasibility of the pacing protocol, undertake a set of experiments designed to test the duration of pacing tolerated in wildtype mice:

> Over the short term i.e. 15, 30, 45 and 60 mins.

> Over the longer term i.e. 4hr and 6hr.

3. To demonstrate survival of animals after 1hr pacing experiments in wildtype mice

> immediate survival experiment- 4.5hr survival study (3 half-lives)

> Long-term survival experiment-2 week survival study.

4. To establish whether there is any effect of subdiaphragmatic pacing on cardiac function, assess the following measurable parameters in wildtype $Cx43^{+/+}$ mice

> 4.1 Characterise ECG parameters, at baseline, and after pacing at 15, 30, 45 mins, 1hr, 4hr and 6hr.

> 4.2 Characterise ECHO parameters, at baseline, during pacing and after 1hr and 6hr pacing.

> 4.3 Characterise arrhythmia inducibility testing using PES and determine the VERP, at baseline and after 1hr and 6hr pacing.

4.4 Characterise the pacing threshold at baseline and after 1hr, 4hr and 6hr pacing.

5. Repeat all of the above measured parameters and determine functional effects in transgenic Cx43$^{+/-}$ mice:

5.1 Characterise ECG, parameters at baseline and after 6hr pacing.

5.2 Characterise ECHO parameters at baseline and after 6hr pacing

5.3 Characterise arrhythmia inducibility and VERP at baseline and after 6hr pacing.

5.4 Characterise the pacing threshold at baseline and after 6hr pacing

5.5 Characterise functional effects, if any, and whether sustained after a period of recovery (2hr).

6. To determine the epicardial breakthrough activation pattern and conduction velocity post pacing using optical mapping in Cx43$^{+/+}$ and Cx43$^{+/-}$ mice (and Cx40$^{+/+}$ mice).

7. Characterise cellular electrophysiology (using patch clamp) in Cx43$^{+/+}$ wildtype as well as Cx43$^{+/-}$ mice at baseline and after 6hr pacing and look at the following measurable parameters:

7.1 Resting membrane potential,

7.2 Action potential duration at 50ms and 90ms.

7.3 Activation and repolarisation kinetics

7.4 At baseline and post 6hr pacing in the Cx43$^{+/+}$ and Cx43$^{+/-}$ mice.

[30]

8. To determine the effects of subdiaphragmatic pacing on cardiac architecture/structure.

8.1 Macroscopic study of whole heart and cellular architecture:

After 1 hour of pacing (using HPS staining to determine macroscopically whether there are features of cellular injury due to the electrode or pacing).

8.2 Establish a semiquantitative method (using immunohistochemistry) for assessing Cx43 cellular and tissue immunofluorescence in wildtype Cx43$^{+/+}$ and Cx43$^{+/-}$ mice

8.2.1 Assess measurables at baseline and after 1hr, 4hr and 6hr pacing.

8.2.2 Mean Cx43 Immunofluorescence Index

8.2.3 Assess Cx43 Distribution using Cx43 immunosignal/tissue area as well as Cx43 lateralisation study

8.2.4 Cx43 plaque numbers

8.2.5 Size of Cx43 plaques.

9. Assess these parameters outlined in 8.2 in whole heart and on a regional basis to determine if there is local or spatial Cx43 heterogeneity post sham-pacing and pacing in Cx43$^{+/+}$ and Cx43$^{+/-}$ mice.

9.1 LV vs. RV

9.2 LV Base vs. Mid vs. Apex

9.3 LV septum vs. LV free wall

9.4 Epicardium vs. Mid-myocardium vs. Endocardium.

10. Utilise the semi quantitative method for assessing Cx43 and Cx40 colocalisation in a Cx40 transgenic model i.e. Cx40$^{+/+,}$ Cx40$^{+/-}$ and Cx40$^{-/-}$ mice.

11. Characterise changes in Cx43 protein expression levels (using immunoblotting) after sham-pacing and after pacing in wildtype Cx43$^{+/+}$and Cx43$^{+/-}$ mice:

      11.1 At baseline and after 6hr pacing and sham-pacing

      11.2. Determine Cx43 expression using immunoblotting

            11.2.1. at baseline and after 6hr pacing.

            11.2.2 on a regional basis

                  LV epicardium and endocardium.

                  LV free wall and LV septum

                  LV Base and Apex

12. Assess rates of Translation at baseline and after 6hr pacing in whole heart lysates from Cx43$^{+/+}$ and Cx43$^{+/-}$ mice and assess Cx43 mRNA on a regional basis (using qRT-PCR) in

          12.1.   LV free wall epicardium

          12.2.   LV free wall endocardium

13. Assess Cx43 distribution at baseline and after 6hr pacing using Cell fractionation techniques to assess Cx43 trafficking between membrane associated and cytosolic pools.

14. Assess degradation of Cx43 in Cx43$^{+/+}$ mice after 6hour sham-pacing and 6hr pacing using immunoblotting for ubiquitin (with Cx43 coimmunoprecipitation).

15. Examine the relationship of Cx43 with other connexin isoforms (Cx40, Cx45) and its binding partners e.g. cadherin (using immunofluorescence colocalisation methods) after 6hr sham-pacing and 6hr pacing

    15.1 In wildtype mice

    15.2 In Cx43$^{+/-}$ mice

16. To correlate structural remodelling (aims 8-15) in wildtype Cx43$^{+/+}$ and Cx43$^{+/-}$ mice post 6hr pacing and sham-pacing with functional effects (aims 4-7).

17. To characterise the Cx43 and Cx40 immunosignal in a Cx40 transgenic model

    17.1 in RA, RAA, LA and LAA

    17.2 in young and old hearts

    17.3 correlate structural data with optical mapping measured regional conduction velocity of Cx40$^{+/+}$, Cx40$^{+/-}$ and Cx40$^{-/-}$ mice.

These specific and novel goals enable addressing the following specific and novel Hypotheses:

PRINCIPAL HYPOTHESES

Hypothesis 1.

In a model of reproducible short-term (less than six hours) *in vivo* right ventricle (RV) pacing without the need for intubation, or thoracic disruption using the sub diaphragmatic route without effects of ischaemia, or heart failure, I hypothesise that RV pacing with resultant aberrant electrical activation would generate gap junction remodelling (GJR) due to disruption in connexin trafficking and correlate with increase arrhythmia propensity and/or impaired cardiac contractility.

Hypothesis 2.

In the setting of additional stress to the cellular anatomical architecture of the model e.g. genetically reduced basal levels of Cx43, (or the *action potential prolonging* effect of drug e.g. 4-AP) dyssynchronous pacing would correlate with more profound effects on cardiac function and cellular electrophysiology.

Hypothesis 3.

I hypothesise that gap junctional remodelling in $Cx40^{+/+}$, $Cx40^{+/-}$ and $Cx40^{-/-}$ mice results in altered Cx43 expression, conduction velocity and pattern of propagation in an age and chamber specific manner.

Subhypotheses

1. Pacing induced Gap junction remodelling in wildtype mice demonstrates Cx43 immunosignal lateralisation.

2. Remodelling of Cx43 at a structural level correlates with changes in regional transcription in wildtype and Cx43$^{+/-}$ mice after 6hr dyssynchronous pacing.

3. Gap junction remodelling occurs at a structural level and demonstrates differences on a regional and chamber specific basis thus creating connexin heterogeneity as a consequence of pacing induced dyssynchrony in wildtype Cx43$^{+/+}$ and Cx43$^{+/-}$ mice.

4. Gap junction remodelling correlates with altered trafficking and degradation of Cx43 protein

5. Pacing induced dyssynchrony alters phosphorylation state of Cx43 and alters Cx40, Cx45 and cadherin protein abundance at the intercalated disc.

6. Short-term dyssynchronous pacing of the murine heart demonstrates features of cardiac memory.

7. Altered activation of the ventricle would alter the relationship of gap junctions in subcellular and membrane pools and result in changes in the distribution of Cx43 utilising cell fractionation and immunostaining (colocalisation studies) to determine whether this occurs by disassociation from its scaffolding proteins e.g. cadherin at the adherens junction.

Rationale of study and clinical relevance

Human Models of Dyssynchrony

Heart Failure

Heart failure remains the leading cause of morbidity and mortality in westernised societies, with majority of patients having impaired cardiac systolic pump function, and a significant proportion, cardiac dyssynchrony with associated conduction delay (20;21). Estimates place this proportion of patients at 30% for having electrical dyssynchrony i.e. a widened QRS on ECG (LBBB), however as high as 60% for mechanical dyssynchrony i.e. with ECHO or MRI metrics of dyssynchrony.

Dyssynchrony is an independent risk factor for morbidity and mortality in heart failure beyond the traditional risks that predict poor outcomes. Dyssynchrony creates a heterogeneous workload with late and early activated myocardial regions demonstrating differences in work efficiency, perfusion, glucose requirements and metabolism with adaptive changes to cellular architecture (22;23). Therapies aimed at restoring synchrony have shown clear clinical benefits both in improving symptoms and survival in patients with dyssynchrony(3).

Ischaemia

Regional myocardial ischaemia, caused by atherosclerotic narrowing in coronary arteries is affected by reductions in blood flow which may either be dynamic e.g. ischaemia caused on exertion or after a heavy meal; or it may be chronic or fixed in nature as in the case of an old myocardial infarction. However, the resultant oxygen-demand mismatch results in altered cellular function e.g. due to altered Ca^{2+} state in the local tissue with altered mechanical function resulting in regional wall motion abnormalities, a form of dyssynchrony.

Ectopy and Tachyarrhythmia:

Spontaneous ectopy in the ventricle can occur often as a result of multifocal sources in diseased hearts or a unifocal source as is the case in a structurally normal heart e.g. with unifocal outflow tract generated Ectopy. These aberrant sources of depolarising cells can result in mechanical dyssynchronous activation, which in time may alter the cardiac architecture. The rate at which they depolarise can result in sustained tachyarrhythmia. Sustained tachyarrhythmia as a model is a well described entity resulting in structural impairment (in the case of tachycardia induced cardiomyopathy), mechanical dyssynchrony, and associated structural and gap junction remodelling.

In humans, data from studying cohorts of patients subjected to cardiac pacing (a form of artificially induced ectopy and dyssynchrony) either with a single chamber or dual chamber device highlight the importance of dyssynchrony induced by pacing the RV alone. Such clinical studies have emphasised the deleterious effects of dyssynchrony and have stirred interest in alternate site pacing and programming that minimises right ventricular pacing(24;25). Contrastingly, specialised pacing that restores synchrony improves mortality and functional parameters in those with heart failure induced dyssynchrony(4).

Animal Models of cardiac Dyssynchrony

Left bundle branch block (LBBB) induced Dyssynchrony.

Animal models have been designed to study dyssynchrony- Eppinger and Tothberger 100 years ago achieved a prolonged QRS by incising the interventricular septum in canine hearts and their canine work represents the very first model of a proximal bundle branch lesion.

Such a model of dyssynchrony has been observed in humans with LBBB as well as monkeys and pigs (23).

Important differences exist between species at the anatomical level of the left bundle branch with ox and sheep demonstrating thicker bundles extending to the epicardial surface while rabbits have fine subendocardial sheets as a left bundle. Canines appear to model the human LBBB model closest with doubling of their QRS duration when surgically disrupting the left bundle. A more recent study using catheter ablation of the LBBB in a canine has opened the possibilities for a less invasive approach. Other animal models e.g. pigs, using LBBB disruption combined with RV pacing only achieve a 50% prolonged QRS duration and have therefore been less favoured for modelling studies of human dyssynchrony(23).

An important difference in these animal models is that they are all usually free of any underlying disease processes thus differing substantially from human models of cardiac dyssynchrony (where cardiac disease is present). Incision of the proximal bundle in animal models, however, disrupts the ventricle, which must be opened to allow access to the left bundle; making this model unsuitable for the study of haemodynamic effects of dyssynchrony. This paved the way for alternative strategies e.g. catheter ablation of the Left bundle and the use of pacing as a model of dyssynchrony (26).

Pacing Induced Dyssynchrony

Wiggers et al in 1925 used an artificial stimulus and in the canine left ventricle demonstrated: 1.slowing in rise of interventricular pressure, 2.lengthening of the isometric contraction phase, 3.lowering of maximum systolic pressure and 4.an increase in the duration of systole. A set of elegant experiments performed by Prinzen et al in 1999 and 2002 demonstrated the

effects of multisite pacing on haemodynamics and showed that RV pacing delays transeptal and intraventricular conduction with haemodynamic change comparable to LBBB models(20).

An important difference with RV apical pacing is that it 1.Induces slow intramyocardial conduction instead of fast conduction through the purkinje fibres and 2.the site of stimulation-induced breakthrough differs from the intrinsic breakthrough site. This latter effect alters LV depolarisation through the interventricular septum compared to LBBB.

A more recent canine model of LBBB has utilised proximal ablation of the LBBB to generate a model of LBBB dyssynchrony combined with CRT pacing(20).

Structural remodelling with Dyssynchrony and electromechanical delay.

In the human and animal models outlined above, there is an interrelationship between altered work and mechanical load and adaptive structural changes that take place i.e. the ventricle must adapt to the change in workload that dyssynchrony imposes and this usually results in changes in extracellular matrix, myocyte hypertrophy and alterations in structural proteins such as gap junctions. In the context of pacing induced dyssynchrony, hypertrophy is observed in the wall furthest from the pacing site i.e. the late activated region. Contrastingly, thinning appears nearest to the site of pacing i.e. the early activated segment (20).

The mechanism behind these adaptive changes is unclear though cardiac load and neurohumoral factors are thought strong contributors. Ventricular asynchrony results in redistribution of mechanical work and alters perfusion and oxygen demand. During pacing

there is a reduction in regional myocardial perfusion and O2 consumption nearest to the pacing site.

Models of electrical stimulation, altered perfusion and ischaemia/hypoxia have been shown to result in gap junction remodelling in cell cultures, tissue and at the whole heart level. The duration of exposure to such noxious stimuli is an additional factor predicting severity of GJR. Thus, if dyssynchrony is sustained over a sufficient length of time it results in structural change.

Gap Junctions-specific key observations on which hypothesis and aims of thesis are based

In this next section, I will lay out key concepts from the gap junction biology field that are relevant to the hypothesis and aims of this thesis. These key observations form the basis of my work in the study of dyssynchrony induced gap junction remodelling, with possible alterations in gap junction intercellular communication and cellular coupling. Observations in the field may assist understanding the mechanisms driving dyssynchrony induced GJR. I will:

(i)   Define gap junction remodelling and present the structure of a connexon.

(ii)   Present how gap junctions as well as individual connexins are organised and distributed in the normal heart.

(iii)   Share with readers how assembly of gap junctions occurs and how this relates to their function vis. gap junction intercellular communication (GJIC).

(iv)   Contrastingly, I will also describe the process that remodels gap junctions in the heart's adaptive response to external stimuli

(v)   Present the process of oligomerization, intracellular trafficking and targeting to the cell membrane.

(vi)   Describe the regulatory process affecting internalisation and degradation.

(vii)   Include the regulatory effect of phosphorylation in these sub-cellular compartments will also be considered since they all affect the expression of gap junctions.

(viii)   Introduce the connexin gene family, in addition to translational and post-translational modifications that also alter gap junction expression.

(ix)   Describe how gap junctions modulate the propagation of the action potential

(x)   Present evidence from animal and human models of cardiac disease examining the role of gap junction remodelling in the genesis of arrhythmias within atrial and ventricular tissue.

(xi)   Describe the role of connexin binding partners and protein-protein interactions, which integrate into a gap junction nexus and their role in disease.

Connexins forming Gap Junctions:

Gap Junctions are dodecamers formed from protein subunits called connexins: six connexins form one connexon and two connexon hemi-channels make up a gap junction (27;28). Connexons are targeted to the membrane to form gap junction channels when they dock with connexons of neighbouring cells (see Figure 1 and Figure 7). Multiple channels cluster to form plaques of varying size.

It is generally accepted that connexins alone generate gap junction channels (29-31). Experimental work demonstrated sequences consistent with integral membrane proteins with a transmembrane domain as well as the reconstitution of connexins into artificial membranes and in heterologous (e.g. yeast) systems. Furthermore, electron microscopy and immunocytochemical studies localised connexins to gap junction plaques (32;33). The term "gap junction" has prevailed from the electron microscopy work of Revel and Karnovsky appearing as a small gap of 2-3nm where the plasma cell membranes of adjacent cells are closely apposed (33;34).

Initially, it was thought that all gap junctions contained the same protein, however, differences in electrophoretic mobilities of bands detected by SDS-PAGE (21-70kDa) resulted in the current nomenclature system using the word connexin (abbreviated Cx) and followed by a suffix indicating the molecular mass of the polypeptide connexin in kilodaltons (kDa)(35;36).

The existence of such gap junctions as a low resistance pathway was first postulated by Weidmann well before the discovery of the gap junction structure when he observed that the space constant for the spread of current between strips of myocardium exceeded the expected value for a single Purkinje fibre(37). Robertson's studies provided evidence for a neuronal

junction structure responsible for intercellular electrical transmission(33) while others

working in excitable tissues observed the presence of a junctional structure (38).

Connexin Isoforms and genes coding for connexins

The connexin family consists of 21 gene members in humans and 20 genes in mice (see Table

1), though not all are expressed in the heart. Connexins are tissue-specific e.g. hepatocytes

express Cx26 and Cx32 (39-41) while cardiomyocytes express Cx40, Cx43 and Cx45

(42;43). They are co-expressed in distinct combinations, which influence structure and

function (30;44;45). The presence of two or more connexins in each tissue type is a consistent

principle, which seems to allow for compensatory mechanisms in order to overcome loss or

mutation (see Table 1)(46-49).. They also exhibit the principle that there are certain functions

that cannot be compensated for despite the co-expression of two or more connexins, so called

"non-redundant" functions (50).

Of all connexin family members, Cx43 is the most ubiquitously expressed and can be found

endogenously expressed in 35 distinct tissue and cell types, some of which include

cardiomyocytes, astrocytes, keratinocytes, endothelial cells and smooth-muscle cells(51). The

connexin genes are located on a variety of chromosomes with a clustering of connexin genes

on murine chromosome 4, which is similar to a region on human chromosome 1. Genes

encoding connexins appear to have a first exon containing the 5$^{'}$-untranslated sequences and

a large second exon with the complete coding region as well as remaining untranslated

sequences. There are exceptions to this gene structure e.g. Cx32, Cx36 and Cx45.

Furthermore, variations in the number of introns and exons have been described.

Channels formed from two Connexons
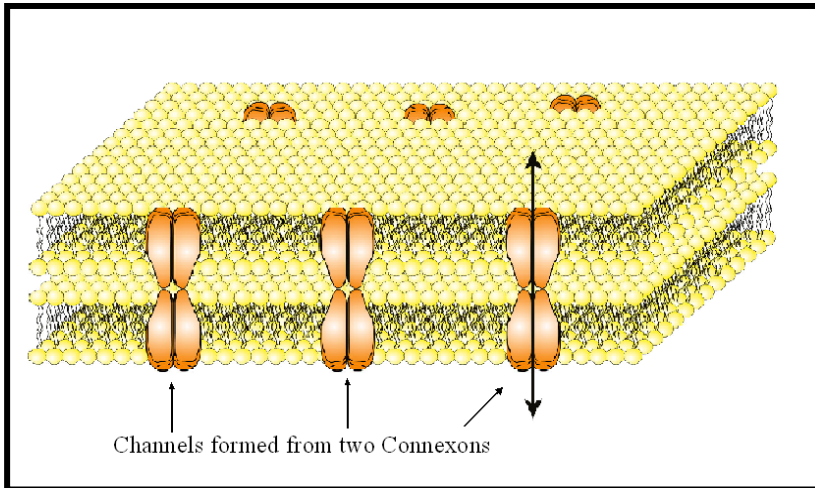
Figure 1 -A schematic diagram of a group of gap junction channels

Each cell contributes a hemichannel (connexon), which spans the lipid bilayer (representing the cell membrane; in yellow) to dock with the opposing connexon to form the complete gap junction channel. Each hemichannel is formed by six protein subunits, called connexins (Courtesy of Dr Rasheda Choudhury).

Mouse Connexins	Human Connexins	Mouse tissue/organ	Mouse cell type
Cx23	Cx23	-	-
	Cx25		
Cx26	Cx26	Liver, skin	Hepatocytes, keratinocyte
Cx29	Cx30.2	Brain	Oligodendrocytes
Cx30	Cx30	Skin	Keratinocytes
Cx30.2	Cx31.9	Testis	Smooth-muscle cells
Cx30.3	Cx30.3	Skin	Keratinocytes
Cx31	Cx31	Skin	Keratinocytes
Cx31.1	Cx31.1	Skin	Keratinocytes
Cx32	Cx32	Liver, Nervous	Hepatocytes, Schwann cells
Cx33		Testes	Sertoli cells
Cx36	Cx36	Retina, Nervous	Neurons
Cx37	Cx37	Blood vessels	Endothelial cells
Cx39	Cx40.1	Developing muscle	Myocytes
Cx40	Cx40	Heart, Skin	Cardiomyocytes, Keratinocytes
Cx43	Cx43	Heart, Skin	Cardiomyocytes, Keratinocytes
Cx45	Cx45	Heart, Skin	Cardiomyocytes, Keratinocytes
Cx46	Cx46	Lens	Lens fibre cells
Cx47	Cx47	Nervous	Oligodendrocytes
Cx50	Cx50	Lens	Lens fibre cells
	Cx59		
Cx57	Cx62	Retina	Horizontal cells

Table 1 Mouse and homologous human connexin family members;

Representative tissues and cell types where mouse connexin family members are found.

Reproduced with permission from D.W.Laird (2006) Life cycle of connexins in health and disease *Biochemical Journal,* **394(3)** 527-543. © the Biochemical Society (51).

Molecular Topology of Connexins

Amino acid sequencing experiments have aided in predicting the structure of connexins, which include four hydrophobic transmembrane domains and a hydrophilic carboxy terminus (CT) tail (see Figure 2;see inset 2 in Figure 7). Three hydrophilic domains separate the hydrophobic regions such that there are two extracellular loops (EL) and another on the intracellular aspect (IL or cytoplasmic loop CL). Sensitivity to proteases of isolated liver and heart gap junctions and oligonucleotide antiserum to segments of Cx26, Cx32 and Cx43 have been used to map connexin topology (31;35;41;52-57). The CT tail has been identified as a key component to the remodelling process of gap junctions.
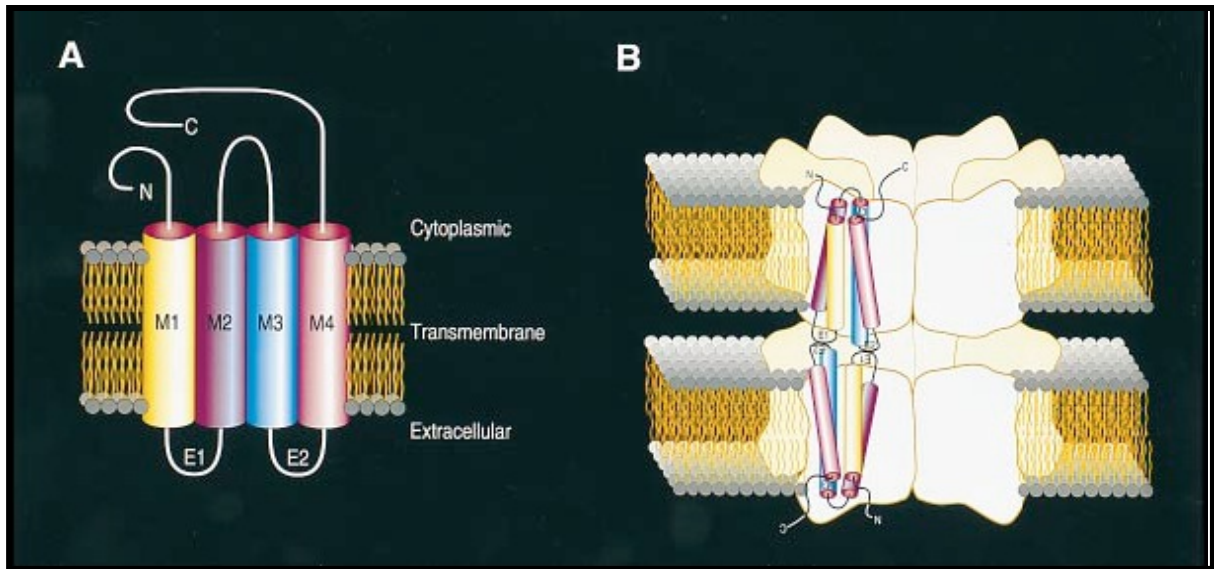
Figure 2 -Molecular Topology of Connexins

Panel A-Illustration of the four transmembrane domains (M1-M4), two extracellular loops
(E1-2), N and Carboxy (C) tail terminus of a connexin protein. Panel B- a superimposed
connexin molecule forming the pore unit within each of two adjoining connexons in yellow.
With permission from Kumar et al (28).

Gap Junction organisation in the normal heart:

Gap Junction Distribution and Expression:

Connexins in the heart are expressed in distinct combinations and relative quantities in a chamber and site-specific manner. Connexin 43 is the predominant connexin expressed by ventricular and atrial cardiomyocytes. Cx40 and Cx45 are co-expressed though in lower total quantities than Cx43 see figure 3,4 and 5 (5). The orientation of the connexon at the polar ends of the cell, particularly in the heart facilitates electrical transmission in the orientation of the fibre axis (see Figure 5) (58;59).

Diversity in gap junction function occurs as a consequence of different constituent connexins-Cx40, Cx43, and Cx45 in the heart (see Figure 3 and Figure 6) (5;43). This diversity is further enhanced due to differences in regional expression. This leads to functional heterogeneity and adaptively alters gap junctional conductance. Gap junctions may also be modulated by chemical or voltage gating, thus altering channel gating properties and the molecular transjunctional selectivity (see Figure 3 and Figure 4) (5;43).

Although, at first glance this may seem counterintuitive, this broad range of mechanisms for modulating connexon function influences the physiological role of the underlying tissue e.g. in the heart, the specialised conduction tissue (such as the common and right bundle branch as highlighted in figure 4) acts as a small electrotonic source of cells transmitting to downstream cells (the working myocardium). This reduced coupling property of Cx40 and Cx45 actually favour their role in coordinating downstream myocardial activation(58).

[49]
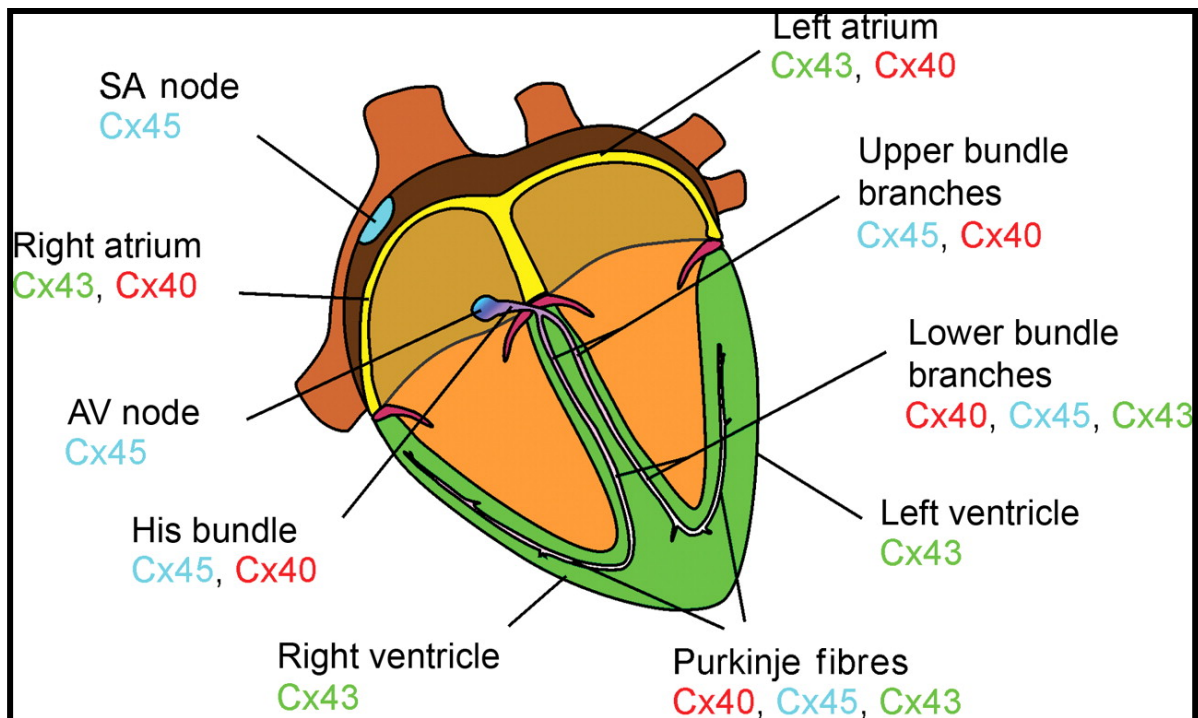
Figure 3 -Connexin expression in mammalian heart

Overview of typical connexin expression pattern of normal adult mammalian heart. With permission from Severs et al (5).
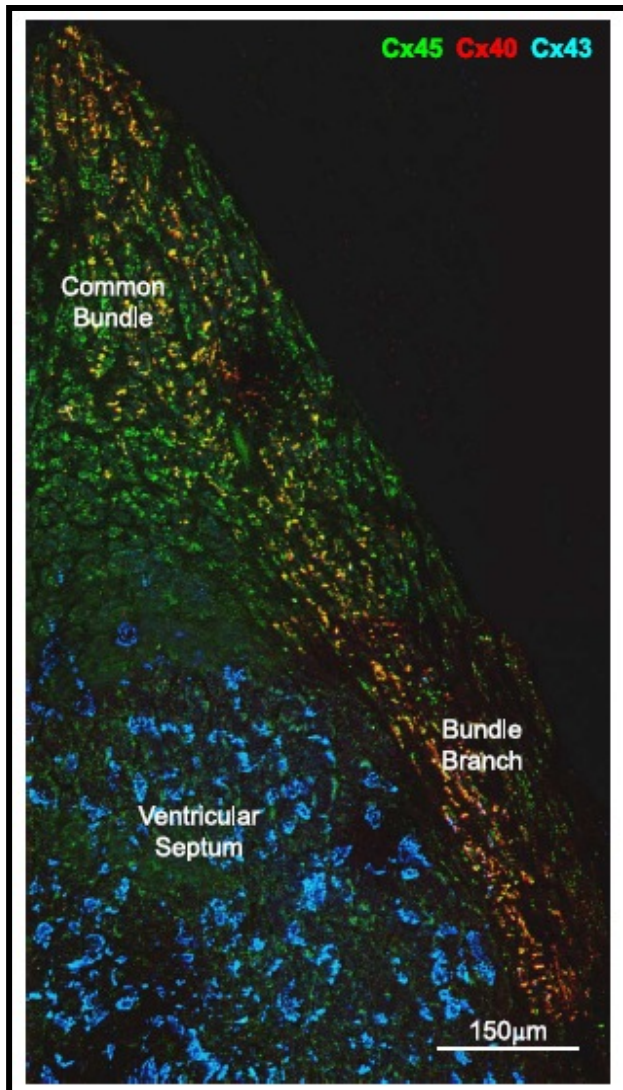
Figure 4 Connexin expression patterns in rat myocardium.

A triple labelled confocal merged image of Cx43 (blue), Cx40 (red) and Cx45 (green) showing the common bundle and right bundle branch which only express Cx40 and Cx45 whereas Cx43 is present in the adjacent working myocardium alone. With permission from Severs et al (60).
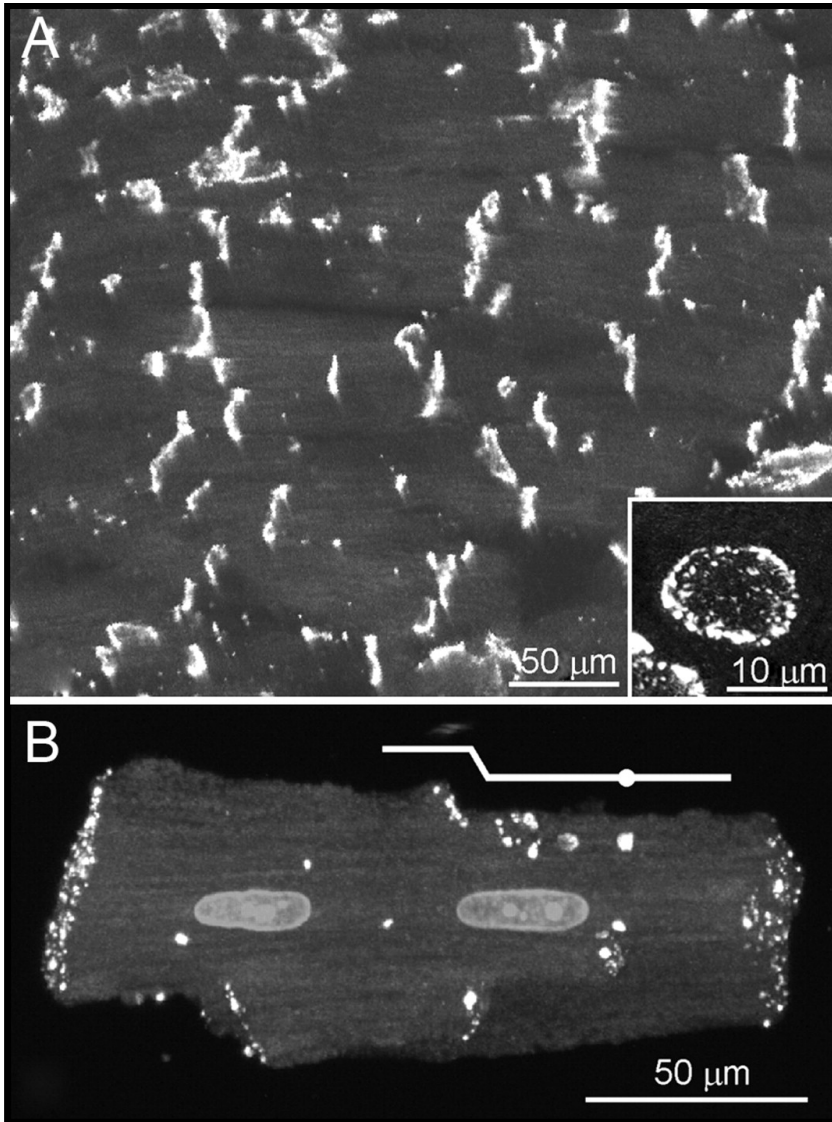
Figure 5 -Cx43 distribution pattern in ventricular myocardium.

In panel A (rat left ventricle; longitudinal section) gap junctions appear in rows and this corresponds to viewing an intercalated disc from an edge-on view. Contrastingly, a face-on view of human myocardial gap junction demonstrates larger peripheral gap junctions. In Panel B the white line denotes multiple discs of varying size from isolated rat myocytes. With permission from Severs et al (5).

Gap Junction Channel Configurations and their biophysical properties.

Connexons and hemichannels may be composed of six identical subunits (homomeric) or have two or more different subunits (heteromeric);(see Figure 6). Full gap junction channels may also exhibit various configurations with two identical connexons forming homotypic channels while two different connexons form heterotypic channels thus altering the permeability and conductance properties of the channels formed; (see Figure 6) (43;61;62).

These variations in expressed connexins modulate gap junction intercellular communication (GJIC) (63).Since each connexin subunit has its own unique gating and perm-selective properties it follows that different combinations of connexins yield gap junctions with new biophysical properties. In doing so this changes the interconnecting communication and electrical properties or coupling between cells(58).
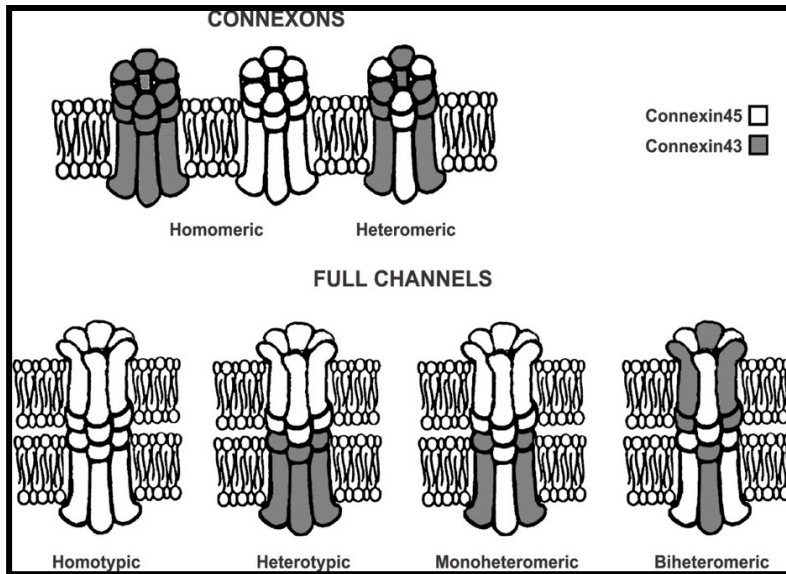
Figure 6 -Potential for gap junction channel diversity when combining constituent connexins

Varying combinations of connexins form connexons, hemichannels and gap junction channels. Cx45 is coded in white and Cx43 in grey. With permission from Moreno et al (43).

Electrophysiological properties of Gap Junctions:

Gap Junction Intercellular Communication:

Gap junctions are involved in communication, coupling cells electrically and metabolically, allowing non-specific communication, and passive diffusion of metabolites along electro-chemical gradients; peptides conjugated to fluorescent dyes in transfer studies have demonstrated the relative non-selective nature of the channel for molecules <1kDa in size (28;64). The passage of inorganic ions (Na^+, K^+, Ca^{2+}) and small molecules/ secondary messengers such as adenosine, ADP, ATP, cAMP and IP_3 are well described(27).

Factors that modulate communication include (i) the distribution and levels of expression of connexins, (ii) trafficking and degradation, (iii) the constituent connexins partaking in the formation of the channel and (iv)modulation of gating itself via voltage and chemical gating; ultimately affecting the numbers of channels and their open or closed configuration. In turn, this affects the propagation of action potentials between cells(58).

Electrophysiological role of Gap Junctions in Cellular Coupling.

Gap Junction and Action Potential Propagation.

Impulse propagation at the whole organ level of the heart is meticulously orchestrated. Initiation of the electrical impulse occurs at the SA node, spreads over the atria, and penetrates through the fibrous AV ring via the AV node and conduction system along the bundle branches and specialised *purkinje-ventricular* interface thus invading both ventricles. This results in the *synchronous* contraction of the working myocardium. When any disruption to this orchestrated process occurs, it results in *dyssynchrony* between the chambers of the heart with significant and deleterious electrical and mechanical effects; illustrated in more detail in the next section cardiac pathology induced gap junction alterations.

Impulse propagation in the heart interests clinicians and basic scientists because alterations in conduction velocity (θ) may contribute to cardiac arrhythmias(58).

 At a cellular level, 4 discrete elements affect local circuit currents and the propagation of an action potential:

1. Excitatory inward current channels i.e. Na^+, K^+ and Ca^{2+} (I_{Na}, I_K and $I_{Ca(L)}$ and $I_{Ca(T)}$); this is considered the source factor. It exerts its effect by the maximal upstroke velocity of action potentials, dV/dt_{max} .

2. Intracellular longitudinal resistance r_i = the sum of the cytoplasmic resistance (r_c) and gap junction (GJ) resistance (r_j); This is a sink factor and consumes charge.

3. Capacitance of the non-junctional membrane, cm. This is also a sink factor and consumes charge.

4. Extracellular longitudinal resistance ro. This is also a sink factor consuming charge.

These 4 elements determine the conduction velocity (θ) of an action potential and an approximation is that θ^2 is proportional to dV/dt_{max} and inversely proportional to ($r_o + r_i$). The space constant, λ, describes the tendency for current to spread between adjacent cells.

Though this is a reductionist approach it is useful and has been applied in mathematical and computer models to integrate experimental findings and predict likely outcomes (58;65).

Gap Junction Trafficking, Targeting, Turnover and Degradation:

An important factor modulating communication, as mentioned earlier, is the trafficking and degradation of connexins and the gap junctions they form. The biosynthetic study of connexins has been furthered with the advent of anti-connexin antibodies utilised in metabolic labelling and immunoprecipitation (66).

Pulse-chase experiments demonstrate that Cx43 is initially synthesised as a 40-42kDa polypeptide that is subsequently posttranslationally modified to forms with slower SDS-PAGE mobility due to phosphorylation of serine residues (67-70). Phosphates are added to Cx43 particularly at a serine-rich sequence near the carboxy terminus (CT) to yield phosphoform with degrees of phosphorylation (P0, P1 and P2) soon after translation. Various drugs that inhibit protein trafficking have been used to demonstrate that partial phosphorylation of Cx43 occurs before exiting the Golgi apparatus (71;72).

 The location at which connexins oligomerize into connexons appears connexin specific with Cx32 assembling at the endoplasmic reticulum (ER) while Cx43 assembles in the *trans*-Golgi network (73-77). Contrastingly, Cx26 hemichannels appear to be directly incorporated into the plasma membrane post translation(78) and in liver tissue, Cx26 appears in an ER/Golgi intermediate compartment while Cx26/Cx32 constructs are preferentially located in a Golgi membrane fraction (74).

This has raised an important concept in gap junction biology that connexins (including cardiac connexins) localise in subcellular pools and in doing so avail themselves to rapid trafficking when needed(79). There appear to be specific pathways for transporting newly synthesised connexins to the plasma membrane; a discovery achieved with chemical

inhibition experiments disrupting the Golgi compartment and that disassemble microtubules (75;80;80-82).

The role of the microtubules has emerged as an integral option to transporting packaged vesicles in association with motor proteins directly to the cell membrane (83). They are regulated by the microtubule plus-end binding proteins such as EB1 and p 150^{GLUED} which target Cx43 vesicles to specific membrane sub domains through interactions with the adherens junctions (AJ) complex (Figure 7) (83). Interestingly, EB1 is displaced from microtubules of stressed human and mouse myocardium limiting the delivery of connexons to the cell membrane (84;85).

So far, two important paradigms exist for the transfer of Cx43 vesicles: i) the direct targeting of gap junctions towards the intercalated disc/adherens junction complex and ii) the passive diffusion paradigm vis. Cx43 hemichannels are incorporated into the lateral plasma membrane and diffuse along towards the intercalated disc/gap junction complex(86).

The localization of Cx43 to the plasma membrane appears influenced by the cadherin/catenin complex(87;88) (especially Ca^{2+} dependent cadherin) and cell adhesion itself appears to play a role in phosphorylating Cx43 to its P2 isoform and restoring GJIC in S180 cells transfected with LCAM (E-cadherin)(70;89). Cell contact sites mediated by the cadherin/catenin complex act as foci for gap junction formation as shown by colocalisation of connexins with E-cadherin or β-catenin(87). Antibody studies directed to cadherin disrupt gap junction formation in Novikoff hepatoma cells.(90).

Recent data also supports the targeting of gap junctions to the periphery of GJ plaques while internalisation of centrally located GJ aggregates removes older gap junctions(91). The

mobility of connexins (Cx43 in particular) into discrete plasma-membrane domains appears

to be part of the process of GJ formation (see Figure 7)(92).
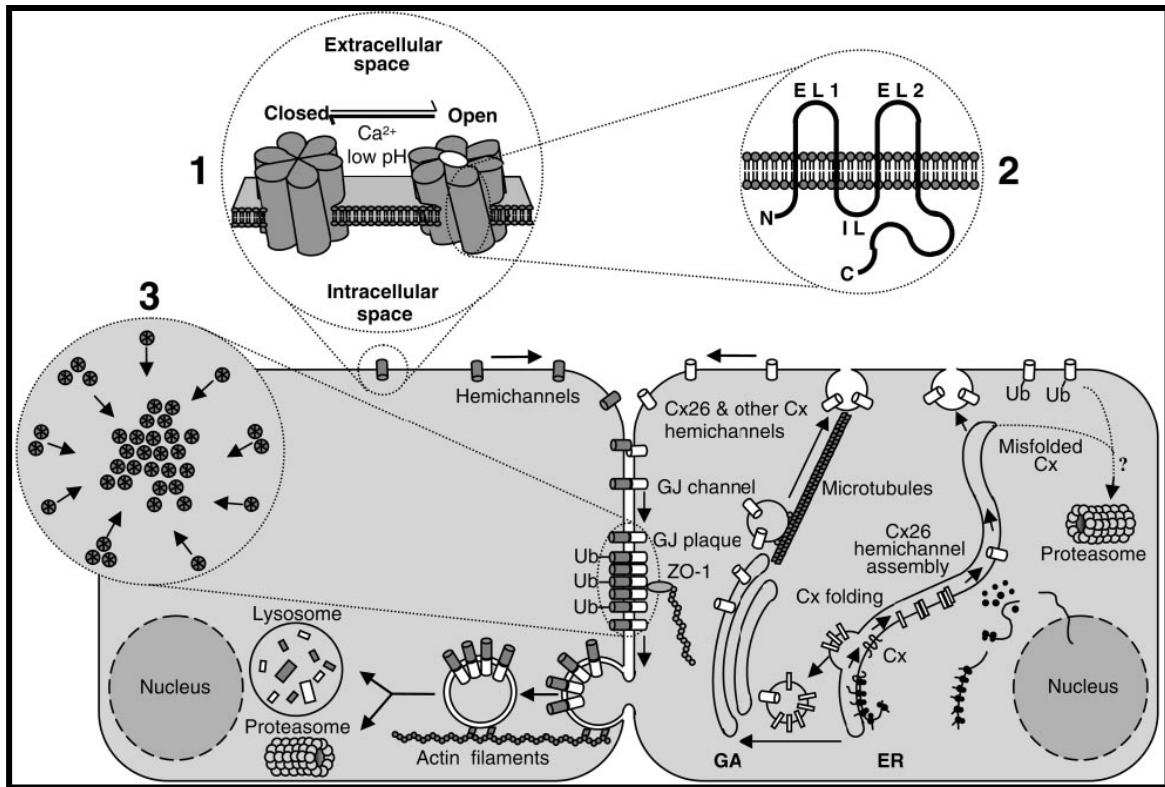
Figure 7-Connexin Trafficking and Targeting to Gap Junction Plaques

Connexin moieties (inset 2 showing molecular topology of connexin) are assembled into connexons ("hemichannels") in the endoplasmic reticulum (ER). Connexons are either inserted into the plasma membrane directly from the ER or, as is the case most often with Cx43, are packaged into vesicles in the Golgi apparatus (GA) and transported via microtubules to the membrane. The mechanism by which connexin hemichannels are subsequently targeted to the gap junction plaque (inset 3) is as yet undefined (inset 1 illustrating open and closed hemichannels on the lateral membrane) With permission from Saez et al (27).

Gap Junction Degradation:

In contrast to mechanisms for production and trafficking of connexins, degradation also modulates the gap junctions. The half-life of connexins is very short, 1-1.5 hours for Cx43 (93;94). Modulating the degradation of gap junctions alters the available channels at the GJ plaque in the cell membrane and directly affects intercellular communication (GJIC)(95;96). This is a key area of interest in the study of GJR.

Morphological and biochemical studies in models of ischaemia and remodelling have demonstrated that gap junctions are internalised into endosomes as "annular gap junctions" and followed by degradation in lysosomal or autophagosomal compartments (see Figure 7) (89;97-100). The ubiquitin pathway targets gap junctions for degradation (101-108).

Regulation of coupling and Biosynthesis of Gap Junctions;The role of Phosphorylation of Gap Junctions:

Connexins are phosphoproteins amenable to phosphorylation; with the exception of Cx26 due to its limited length and few C-terminal tail amino acids (highlighting the importance of the CT tail in phosphorylation state). Phosphorylation occurs either *in vivo* or in vitro at protein kinase consensus sites or can be directly incorporated (as in ^{32}P studies) and alters mobility on SDS page; of all connexins, Cx43 is most extensively investigated and modified by protein kinases and phosphatases (89;109;110).

Phosphorylation of Cx43 allows for sub states with altered dynamic properties and varying GJIC (30;111;112). Cx43 phosphorylation is mediated by protein kinases including v- and c-src kinase, protein kinase C, mitogen activated protein kinase, cyclin dependent kinase 2, casein kinase 1, and protein kinase A.   Balancing the dynamic interplay of phosphorylation and dephosphorylation are protein phosphatases such as PP1 and PP2A (112-114). This is illustrated in detail (see Figure 8).

Phosphorylation has been implicated in a broad range of mechanisms causing gap junction remodelling including connexin biosynthesis, trafficking, assembly, membrane insertion, channel gating, internalisation and degradation (27;109;110;115;116).
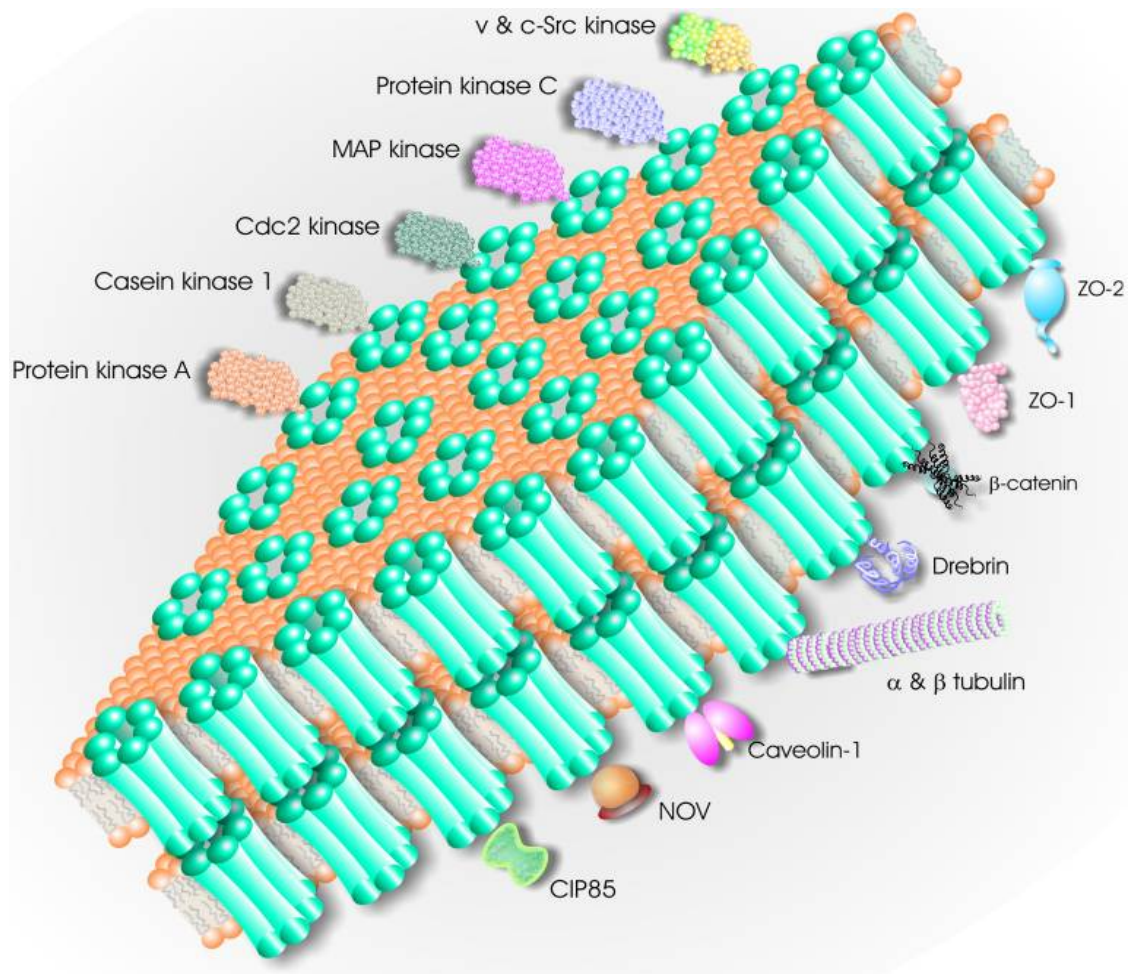
Figure 8 Cx43-binding proteins and proteins phosphorylating Cx43

Protein kinases that are known to phosphorylate Cx43- shown along the top of a diagrammatic gap-junction plaque. Scaffolding proteins and proteins of unknown function shown to bind directly or indirectly to Cx43 are illustrated along the bottom of the gap-junction plaque. It is not necessarily expected that all proteins shown here bind to Cx43 while it is a resident of the gap-junction plaque. MAP kinase, mitogen-activated protein kinase; CIP85, Cx43-interacting protein of 85 kDa. Reproduced with permission from D.W. Laird (2006) Life cycle of connexins in health and disease *Biochemical Journal,* **394(3)** 527–543. © the Biochemical Society(51).

Connexin Proteome, binding partners and Protein-Protein Interactions

The gap junctions appear to be closely related to neighbouring protein partners. Detergent extraction techniques in earlier studies stripped the associated signalling and scaffolding proteins and had erroneously suggested that there is autonomous connexon function. This paradigm has shifted in the field as increasing numbers of binding partners are identified and collectively called the "gap junction proteome" or "nexus". Combinational techniques such as coimmunoprecipitation, colocalisation, cofractionation, yeast-two hybrid and cell-free affinity binding studies have been employed in discovering partner proteins (51;117).

Given that Cx43 is the most ubiquitous of the connexin isoforms it has been the primary focus for most of this work. Therefore an important limitation to this data in understanding mechanisms of GJR is whether these interactions apply to all the other connexin isoforms; this has yet to be studied.

Broadly there are 5 major groups of interaction:

1. Inter-connexin interactions; structural and temporal coexpression of different connexins.

2. Post-translational modifiers; includes protein kinases (8 have been identified), protein phosphatases (3 have been studied), Nedd 4 ubiquitin ligase, organ of Corti protein 1 (OCP1) and ubiquitin (in response to phorbol esters and epidermal growth factors)

3.Scaffolding and cytoskeletal proteins form bridges to microfilaments and microtubules and cross-talk with occludin, claudins and N-cadherin to form a junctional nexus; they include zonula-occludens 1, 2, 3 (ZO-1, ZO-2, ZO-3) and ZO-1 associated nucleic acid binding protein (ZONAB), plakophilin-2 (PKP2), actin, spectrin, drebrin, cortactin, β catenin, tubulin

and EB1. This interaction plays a role in regulating gap junction distribution, gap junction plaque size and internalization.

4. Trafficking regulators.

5. Other molecules and growth regulators; an area, as yet, not easily classified protein partners which influence cell growth (NOV, CCN3, Disc large homolog 1), channel closure via Ca^{2+} (as in interaction with calmodulin) and other channel modifying agents Aquaporin-O (AQP-O), Acetylcholine receptor (AChR) and purinoceptor (PzX_7). A putative and controversial role linking connexins to mitochondrial function has been suggested by interactions with translocase of the outer membrane 20 (Tom20), heat shock protein 90 (Hsp90) and the adenine nucleotide transporter (ANT).

The arrangement of all these molecules and interrelationships is depicted in Figure 9.
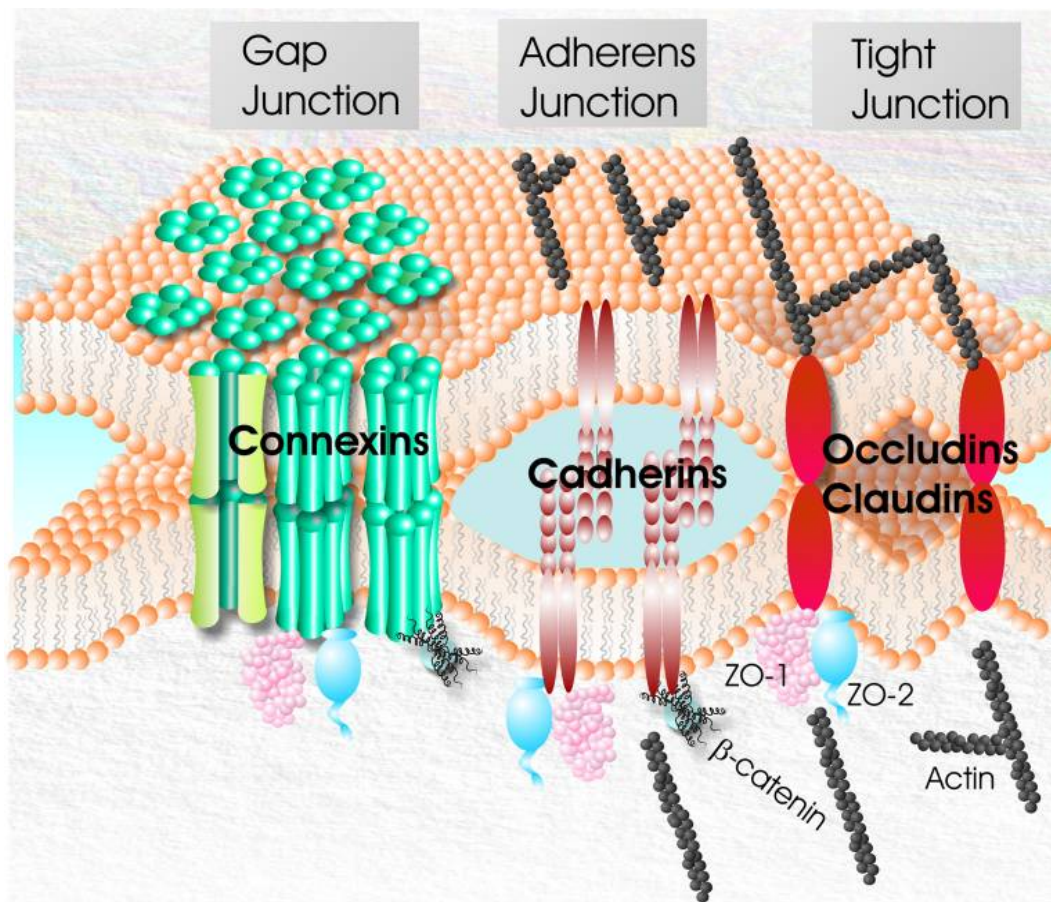
Figure 9 The arrangement of junctional complexes into a nexus

Gap junctions, adherens junctions consisting of cadherins and tight junctions made up of occludins and claudins often closely arrange in epithelial cells and share common binding proteins that scaffold to actin and microfilaments. Binding-protein-mediated cross-talk occurs. This allows these three junctional complexes to act as a nexus. They are governed by some common regulatory events. Reproduced with permission from D.W. Laird (2006) Life cycle of connexins in health and disease *Biochemical Journal,* **394(3)** 527–543. © the Biochemical Society(51).

Cardiac Gap Junction Remodelling in Human Cardiac Disease and in Animal Models.

Gap Junction Remodelling strongly associates with arrhythmogenic and disease substrates. GJR has been seen in mutated genes of congenital hearts and in the acquired forms of ischaemic heart disease, hypertrophy secondary to pressure and volume overload as well as dilated cardiomyopathy(9;14-16).

Gap junction remodelling due to mutations in connexin-encoding genes.

Developmental malformations in connexin knock-out mice suggest that the cardiac myocyte gap junctions have the potential to act as pathways for direct passage of signalling molecules and ions from cell to cell especially during cardiac morphogenesis(5). In humans much interest was generated by the observation of complex cardiac malformations and visceroatrial heterotaxia or hypoplastic left heart syndrome with mutations of the Cx43 gene affecting phosphorylation sites in the Cx43 carboxy tail (118;119). A range of Cx43 mutations are clearly associated with oculodentodigital dysplasia affecting the eyes, limbs, teeth, face and in some the heart (120-122). Anomalies of the aortic arch in a small proportion of cases are due to chromosomal and Cx40 gene deletion while somatic missense mutations and polymorphisms in the gene's regulatory region have been linked to atrial fibrillation (5;123-125).

Gap Junction remodelling in acquired adult heart disease.

1. Effects of acute cardiac ischaemia on gap junction remodelling

Occlusion of a coronary artery results in ischaemia with the affected territory of myocardium experiencing major alterations in impulse formation and propagation. Action potential upstroke velocity decreases, conduction velocity transiently increase then slows; changes in refractory period ensue with localized conduction block and re-entry arrhythmia. These are not uniform changes and ectopic foci also arise in ventricular myocardium.

Experimental animal studies demonstrate rapid dephosphorylation of Cx43, electrical uncoupling and altered distribution of gap junction immunolabelling to the sides of myocytes- referred to as "lateralization" (126;127). Immunolabelling using antibodies directed to different phosphorylation sites on Cx43 suggest that dephosphorylated Cx43 is associated with laterally distributed gap junctions while gap junctions that are at the polar intercalated disc orientation contain phosphorylated Cx43.

An important concept in the field which has yet to be fully clarified is whether the striking lateralized immunofluorescent signal is attributable to potentially functional gap junctions connecting side-by-side myocytes and what proportion represents vesicles of gap-junctional membrane internalised due to cellular stress (5;65).

Ischaemic preconditioning reduces the adverse effects of ischaemia on gap junctions raising a possible role by connexins extending beyond their electrical coupling. Possible mechanisms include the opening of hemichannels altering cellular swelling, releasing ATP and reducing membrane potential during ischaemia (128-130).Gap junction mediated passage of ionic/molecular signals appears responsible for the spread of ischaemia-reperfusion injury from myocyte to myocyte thus leading to cell rigour contracture and cell death (131;132).

This idea has been supported by the use of uncoupling agents such as heptanol during or prior to an ischaemic insult and the resulting reduced infarct size. Trafficking of Cx43 to mitochondria has been proposed as central to the role of Cx43 in preconditioning with numerous proposed candidate mechanisms (5;133). Conversely, agents such as AAP 10 and rotigaptide that maintain the open state of gap junctions have also been studied to challenge the paradigm in the translational sciences vis. that closed channels are beneficial (134-136).

2)Altered distribution and expression in heart failure

Cx43 gap junction immunosignal lateralization is a feature of the infarct border zone of surviving myocytes around the bordering scar tissue in the human ventricle and also in animal models of acute infarction (see Figure 10) (8).

Ultrastructure techniques such as electron microscopy have aided our understanding of the structural changes that this lateralized signal represents and reveal that both laterally disposed gap junctions connecting adjacent cells and internalized non-functional gap junction membrane contribute to this abnormal pattern.

A similar change has been found in models of rat ventricular hypertrophy and correlates with reduced longitudinal conduction velocity, a potential proarrhythmic feature. In a dog model of infarction the lateral gap junction label correlates spatially with electrophysiologically identified figure-of-eight re-entrant circuits(8). Gap junction changes distant from the infarct scar tissue, in particular reduction in the size and number of gap junctions per unit length of intercalated disc, and fewer side-to-side connections between cardiac cells characterize longer term remodelling events in dog myocardium.

 In idiopathic dilated cardiomyopathy, myocarditis, compensated hypertrophy due to valvular aortic stenosis and end stage human heart failure smaller areas of gap junction disarray have

been reported. Patches of few or absent gap junctions are seen amongst normally arrayed gap junctions in decompensated hypertrophy due to aortic stenosis and emphasise that even in the absence of infarcts, Cx43 gap junction distribution becomes heterogeneous. In hypertrophic cardiomyopathy, the commonest cause of sudden cardiac death due to arrhythmia in young adults there is a particularly disordered arrangement of gap junctions dictated by the haphazard myocyte orientation, which characterizes this disease(9).

In "hibernating myocardium" there is a unique form of gap junction remodelling where the large Cx43 gap junction typically found at the edges of the intercalated disc are smaller in size and the overall amount of immunodetectable Cx43 per intercalated disc is reduced, compared with normally perfused segments of myocardium within the same heart. This finding was the first indication that not only does gap junction remodelling contribute to arrhythmia in ischaemic heart disease but also impaired ventricular contraction(14).

In transplant patients (a treatment option for end stage heart failure), there is marked reduction in ventricular Cx43 transcript and protein levels and occurs irrespective of aetiology (ischaemic, non-ischaemic or valvular). The reduction is spatially heterogeneous and progressive over the course of the disease. This has been indicated by the pattern of change in pressure-overloaded hearts with aortic stenosis and its presence in non-failing hearts with ischaemic heart disease(5).

Does Gap junction remodelling and reduced Cx43 contribute to atrial and ventricular arrhythmia?

This is a critical question as it is commonly assumed that such reductions in Cx43 in the disease human ventricle lead to slowed conduction, and render the ventricle more susceptible to re-entry arrhythmia. Therapeutic interventions that increase coupling have been proposed, however experimental cell and theoretical models show that action potential propagation can fail in well coupled cells if these form a large mass or "sink" receiving a relatively small depolarizing "source" current i.e. a so called "source-sink mismatch". In these instances reducing the coupling in the sink can overcome conduction block. Thus the reduced Cx43 of sufficient magnitude to reduce coupling may represent a protective mechanism or response that increases the safety of conduction(5).

However, there is a surplus of gap junctions in the mammalian heart and computer models predict that even substantial reductions in content make relatively little difference to propagation velocity. In keeping with this theory, the magnitude of reduction associated with sudden cardiac death in the cardiac restricted Cx43 knockout mouse is in the order of 90%, much greater than the average reduction of ~50% observed in the failing human ventricle. Of course, there is considerable spatial heterogeneity in the extent of reduction with some regions of diseased hearts approaching >90% reduction of control values. Such heterogeneity is critical to both altered impulse propagation and contractile dysfunction. This was elegantly demonstrated experimentally in a chimeric mouse model generated to give patches of myocardium lacking Cx43. When combining areas with heterogeneous gap junction distribution with areas expressing reduced Cx43 levels they appear to act co-operatively to create an arrhythmogenic substrate at less severe levels of overall gap junction reduction than theoretical models predict. In selectively bred cardiac-restricted knock-out mice, 59%

reduction in Cx43 does not alter propagation velocity or susceptibility to arrhythmia, but when Cx43 reduction reaches 18% of control levels and appears heterogeneous there is a 50% slowing of conduction velocity and 80% of animals are inducible into lethal ventricular arrhythmias. Furthermore, the threshold for arrhythmia may be facilitated by other factors such as ischaemia e.g. halving the Cx43 content in transgenic mice and subjecting them to ischaemia is sufficient to increase the incidence, frequency and duration of ventricular tachycardia(65).

Extrapolating findings from mouse to man could be argued as being flawed due to the small size of the murine heart and its theoretical inability to accommodate large re-entrant circuits; however, in a dog model of heart failure it has been shown that a heterogeneous 50% reduction in Cx43 results in slowed transmural conduction and dispersion of action potential duration of magnitude sufficient for conduction block and re-entry(5).

Connexin 45, connexin 40 and the Purkinje/working ventricular myocyte interface.

Since Cx43 is the main focus of most arrhythmic models it raises the question as to the role of the other connexins and in particular Cx40 and Cx45 in the human heart. A report of elevated expression of Cx45 in the failing human ventricle alongside the reduced Cx43 significantly alters the Cx43:Cx45 ratio. Since co-expression and mixed assembly of gap junctions with Cx43 and Cx45 is possible this would predict channels with substantially different functional properties. Experimentally overexpressing Cx45 such that the Cx45:Cx43 ratio is substantially increased in transgenic mice has demonstrated increased susceptibility to ventricular tachycardia and reduced gap-junctional intercellular communication(65). Increased Cx40 expression has been found in the failing human ventricle in a regionally

[73]

restricted manner and confined to end-stage ischaemic heart disease. The endocardial surface and adjacent to purkinje fibres appears to be the site of Cx40 upregulation and highlights the purkinje/working ventricular myocardium as a potential site of altered electrical coupling that may trigger arrhythmogenesis. Amongst older surviving cardiac restricted Cx43 knockout mice there is increasing propagation across purkinje/myocyte junctions, which alters activation and favours wave-front collisions paralleling patterned cell culture experimental findings as classically described by Rohr. Nonetheless cautious interpretation is necessary since there are important differences between *in vivo* models, in vitro patterned cell cultures and species differences, as is the case between porcine, human and murine models. It appears that the architecture of the purkinje/myocardial interface is a complex structure with a zone of mediating cells, the transitional cells that connect the purkinje fibres to the myocardium(5).

Since, this process occurs from the endocardium the model utilised in this thesis is unique in that it not only induces dyssynchrony between the ventricles but it also reverses the activation pattern across the transmural surface of the myocardium. This is very relevant as it stands in contrast to the ex vivo LV wedge preparations utilised to study tissue dispersion and heterogeneity in understanding the mechanisms of arrhythmia(5).

Gap junction remodelling in atrial fibrillation

Intense interest abounds in understanding the commonest atrial chamber related arrhythmia, atrial fibrillation (AF) and the role of gap junctions. There are many contradictory findings in this area (in humans high, low and even unchanged levels of Cx43 and Cx40 expression in AF have all been described) and there is a challenge to find more refined and rigorous approaches to tease out the effects of gap junctions and connexins.

It is possible that differences between humans and animal models relate to differences in species, age differences, disparity of experimental protocols for AF induction and in humans dissimilar clinical sub-sets of patients with divergent associated pathological factors. Many aspects contribute to the pathophysiology of AF, including focal triggers and altered conduction, and there are important differences in the principal drivers between chronic AF (here gap junction remodelling may occur as part of AF-related remodelling) and paroxysmal or triggered AF (pre-existing features of connexin or gap junction expression act as a predisposing factor in AF occurrence)(137;138).

The issue is further complicated by the multi-factorial nature of AF and the relative importance of gap junctions as causal contributors may vary between patients. Technical deficiencies include the common lack of antibody specificity. Confusion persists due to considerable variation in the appearance of normal atrial myocardium and the gap junction arrangement observed both at the end of cells or lateralized to the plasma membrane in healthy samples.

Also heterogeneity as observed in the goat model of AF where patches of absent Cx40 have been described as AF-induced change resemble the natural appearance of human atria. This has complicated the development of reliable quantitative methods for comparing AF and

normal samples. The work by Allessie suggested changes in gap junctional gating, distribution and expression. Increased vulnerability to inducible AF has been demonstrated in animal models of heptanol induced gap junction uncoupling(139). Furthermore, altering cell coupling in a model of sterile pericarditis demonstrated a transmural gradient in the volume fraction of Cx40 and Cx43 which favoured atrial conduction abnormalities (140). Cx40 knock-out mice and Cx40 genetic polymorphism association studies in humans have identified higher AF susceptibility and emphasised the role of Cx40 in AF (124;125;137;138;141;142).

The contribution of Cx43 in AF is less clear with contradictory results reported with increased levels in the canine model but unchanged levels in the goat model. The inflammatory molecule tumour necrosis factor (TNF) overexpressed in a mouse model is also implicated in AF susceptibility through its role in fibrosis and remodelling with reduction in Cx40 levels (138;143).

An important distinction to make is that the sub diaphragmatic pacing induced dyssynchrony model does not utilise the rapid rates of firing utilised to pace the goat. Tachycardia is a well-recognised entity that alone induces heart failure with the passage of time likely due to cellular oxidative stress and an inability to cope with the contractile and therefore energy demands imposed on the cell. There are also changes in calcium handling which result in overload (4;23). However, clinical studies of physiological atrial pacing have also highlighted an increased propensity to atrial fibrillation though cautious interpretation is needed as the original pacing indication may suggest other underlying heart disease that affects the conduction system or the atrium (144-146). The sub diaphragmatic pacing model bypasses these issues in generating the hypothesis and tests it without tachycardia or any apparent underlying disease process.

Gap Junction Remodelling and Ventricular arrhythmia

Gap junctions have been implicated in uncoupling cells during the *acute* and *subacute* phase of myocardial ischaemia resulting in conduction slowing. The predominant mechanism of ventricular tachycardia (VT) in *acute*, *subacute*, and *chronic* phases of myocardial ischaemia is re-entry; focal triggers contribute less so (8;12;147-149). Re-entry is due to dispersion of action potential duration in the *acute* phase or anisotropy in the *chronic* phase of myocardial ischaemia. The epicardial border zone of healing canine infarcts has disturbed Cx43 distribution and correlates with re-entrant ventricular tachycardia circuits (see Figure 10).

The inverse relationship between Cx43 levels and arrhythmia is highlighted in the cardiac restricted Cx43 transgenic mice, which despite structurally normal hearts appear to succumb to sudden cardiac death at around 2 months from lethal ventricular arrhythmias(6).

Disordered Cx43 staining pattern in peri-MI zone

Absence of Cx43 signal in scar

Lateralized Cx43 signal in peri-MI zone
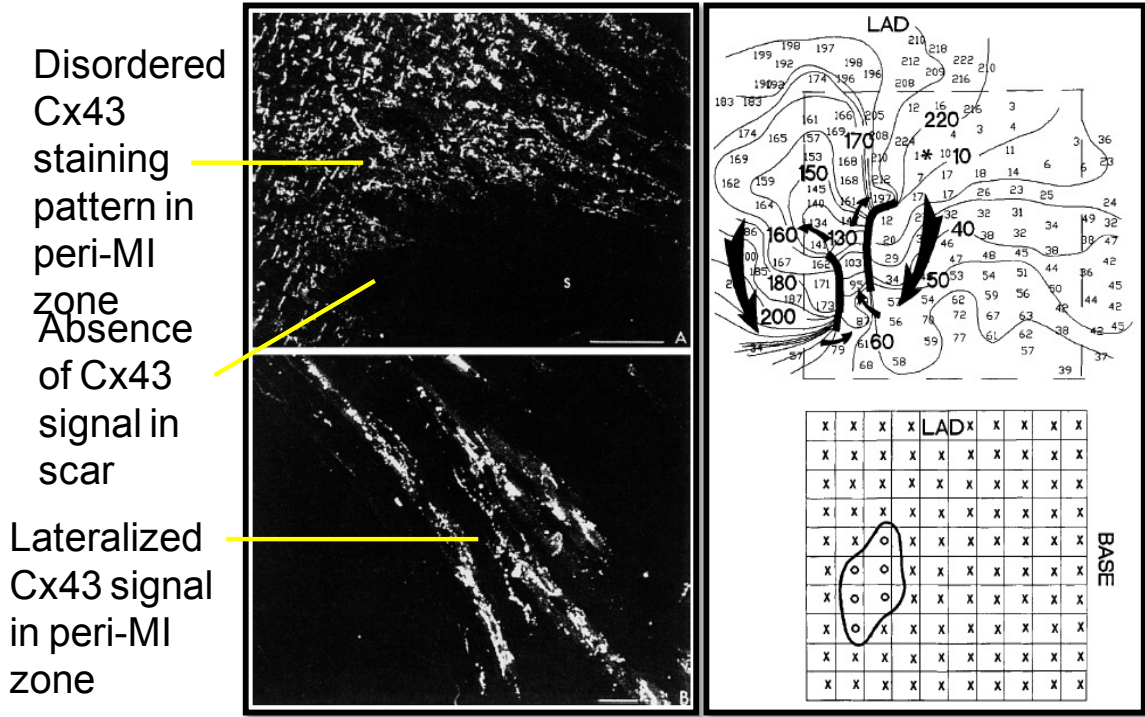
Figure 10 Gap Junction remodelling in epicardial border zone of healing canine infarct.

Gap Junction remodelling in epicardial border zone of healing canine infarct correlates with the location of figure-of-eight re-entrant tachycardia circuit. Reproduced with permission from Peters et al (8).

Co-expression of multiple connexins: non-canonical properties

The predominant nature of Cx43 in the ventricle has facilitated observation that gap junction remodelling predisposes to arrhythmia. Co-expression of Cx40 has unexpected functional effects (as seen in atrial tissue and the purkinje/myocardial interface). In vitro expression has consistently found that expressing Cx40 alone makes high conductance gap junctions and it's been assumed that co-expression with Cx43 *in vivo* would elevate cell-to-cell coupling.

However, this has not been borne out. Cultured neonatal atrial myocytes from heterozygous Cx43 and Cx40 knockout mice, with 50% reduction of Cx40 levels, demonstrate an increased propagation velocity. With near zero levels expressed, Cx40 propagation increases even further. This inverse relationship between Cx40 levels and propagation velocity against a background of Cx43 expression helps explain previous contradictory findings in the human atrium(5).

Cellular mechanisms of gap junction remodelling as derived from disease models

As with all proteins, connexin expression may be regulated at the transcriptional and post-transcriptional levels. The interaction of transcription factors with their target elements to control transcript expression has advanced as our knowledge of the structure of the genes encoding Cx43, Cx40 and Cx45 has progressed. In a recent study the role of microRNA-1 in silencing GJA1 (the gene encoding Cx43) and KCNJ2 (K+ channel subunit Kir 2.1) in ischaemic heart disease has been identified as a post-transcription regulator. These microRNAs are endogenous non-coding RNAs that interact with target mRNAs to prevent translation; levels appear elevated in diseased human ventricle and antisense blocking of this elevation prevents arrhythmia in a corresponding animal model (51;117;117;150).

Apart from connexin synthesis, regulatory mechanisms may affect assembly into connexons, channels and gap-junction plaques as well as degradation. Extracellular signalling pathways leading to altered connexin expression in disease may be triggered in part by mechanical forces and involve cAMP, angiotensin II, and growth factors such as VEGF, activated via protein kinases such as focal adhesion kinase and c-Jun N-terminal kinase (JNK). JNK activation in a transgenic mouse model leads to down-regulation of Cx43, slowing of ventricular conduction, contractile dysfunction and congestive heart failure.

Research has focused on connexin partner proteins, which possess regulatory properties that interact with the carboxy-terminal domain of Cx43. This domain houses important residues involved in channel gating and phosphorylation (which itself can affect a variety of processes from trafficking to assembly and degradation).

[80]

Several protein-protein interactions and binding partners have been discussed earlier and it is worth noting again the role of zonula occludens-1 (ZO-1) and tubulin. Binding sites at the carboxy-terminus exist for such motor proteins driving the trafficking and targeting connexins to their destination. ZO-1 appears intimately involved in regulating gap junction size such that removal or blocking of this protein results in larger and more extensive gap junction plaques. An important finding given that consistent up-regulation of ZO-1 is observed in disease models with an increased proportion of interacting Cx43. Furthermore it is apparent this is not an isolated effect with likely "cross-talk" with adhesion junction partner proteins such as N-cadherin, β-catenin, γ-catenin, plakophilin-2 (PKP2) and desmoplakin. These proteins affect the stability and formation of gap junctions(51;117).

Not only can this "cross-talk" occur at the membrane level but also within the cytoplasm and interactions occur with other signalling pathways such as Wnt mediated by β-catenin. The carboxy-terminus domain again appears to be a critical link in these interactions and when truncated forms have been expressed in mice this has resulted in larger yet fewer gap junction plaques with altered spatial organization at the intercalated disc(51;117).

Limitations to understanding GJR

An important limitation in the gap junction field is that although interest in exploring interactions between connexins and adhesion junction molecules has exploded, the technique of immunofluorescence and co-localization of proteins lacks resolution to infer an interaction at a molecular level and it may merely reflect distant juxtaposition. There remain unanswered questions as to the exact site of interaction between adhesion junction proteins with gap junctions and clarifying the hierarchy of binding partner interactions(5).

Chapter 2

Development of the sub diaphragmatic model of pacing induced dyssynchrony

Overview

Dr Gutstein originally described sub diaphragmatic programmed electrical stimulation; this gave rise to the idea that adapting the same technique could facilitate dyssynchronous right ventricular pacing (151). Advantages of this approach include the ability to study the whole animal and whole heart in vivo under conditions of general anaesthesia and analgesia, with thermoregulation, without disruption of the thoracic structures or need for cardiac surgery, intubation or mechanical ventilation and without damage to abdominal or mediastinal structures. Furthermore, the safety and tolerability of programmed electrical stimulation using this approach allowed administration of intraperitoneal drugs e.g. amiodarone and to perform temporal studies (151).

By refining this approach, I aimed to achieve pacing of varying duration and elicit aberrant activation across the myocardial surface. I aimed to study the structural effects and determine whether gap junction remodelling (GJR) occurs. I also aimed to determine whether this resulted in functional changes.

The Fishman/Gutstein lab's transgenic mouse lines made the study of genetically modified mice such as the $Cx43^{+/-}$ cohort, with pacing, possible. It also allowed collaboration with other investigators interested in testing in vivo arrhythmia inducibility in their models (see other work arising from this period of study and publications).

In Chapter 2, I will present the project overview, the establishment of the model including adequate monitoring, analgesia and recording of electrocardiogram; safe positioning of the stimulating probe, adequate electrical capture, reproducibility of the protocol, absence of

visceral damage, demonstration of survival and measurement of the pacing threshold at baseline and after pacing in Cx43$^{+/+}$ mice. This addresses objectives 1-3 of the thesis.

Project overview

A series of experiments to assess functional parameters at the specified time points are presented in table 2; a summary of the study design. The 15-minute time point represents pilot experiments to establish technical feasibility of pacing, ECG and ECHO measurements.

Table 2. Overview of study design and time points selected for duration of dyssynchrony (Y=Yes).

Duration of Pacing	15 min	30min	45 min	1hour	4hour	6hours
ECG data	Y	Y	Y	Y	Y	Y
ECG axis sub study	Y	-	-	Y	-	-
ECHO data	Y	-	-	Y	-	Y
PES	-	-	-	Y	-	Y
Immunohistochemistry(IHC) and Quantification	-	-	-	Y	Y	Y
Thresholds	Y	Y	Y	Y	Y	Y
Drugs (4-AP)		-	-	Y	-	-
Survival Study:						
4.5hours survival				Y	-	-
2 weeks survival				Y	-	-

IACUC approval, wild type murine strain and age

The studies were performed in accordance with the regulations of the Institutional Animal Care and Use Committee (IACUC) of the New York University (NYU) School of Medicine. Dr Gutstein and Ms F Liu coordinated access to animal resources and arranged surgical space, (kindly accommodated in the adjoining microbiology lab of Prof Martin Blaser and Dr Guillermo Perez-Perez at the Veteran Affairs Medical Centre (VAMC) and commercial vendors supplied oxygen and isoflurane.

For Wildtype experiments the C57BL/6J strain (Jackson Lab, Maine, USA) was used. Adults were 3-4 months in age and sex matched. C.C. Little originally developed these mice in 1921, from a mating of Miss Abby Lathrop's stock that also gave rise to strains C57BR and C57L. These became available through Charles River in 1974 when they were acquired from NIH. Animals were housed in the animal facility of the Veteran Affairs Medical Centre (VAMC) where the development of the model took place.

$Cx43^{+/-}$ mice.

Mice with reduced basal levels of Cx43 were kept at the VAMC having been previously produced. They were housed with their WT littermates and maintained in mixed background consisting of C57BL/6J, SV129 and FVB strains.

Design of Monitoring and analgesia

Initial experiments were performed to anaesthetise mice directly under a nose cone both for induction and maintenance of anaesthesia. Handling involved a manoeuvre of pinching the nape of the neck and distal tail simultaneously and then orientated to maintain a supine position. The nose of the mouse once placed in the nose cone resulted in rapid anaesthesia though was associated with some degree of animal resistance. Furthermore, this arrangement resulted in leakage of anaesthetic gases in the local area. Refinements included use of carbon scavengers in the anaesthetic circuit. Animals were immobilised once under general anaesthesia with adhesive tape applied to all 4 limbs. This also stabilised the limbs for ECG recordings and avoided movement artefact. Surgical tape was applied to each of the paws against a firm glass plate surface (see figure 14)

Initial pilot experiments only allowed study of single animals at any time. Earliest experiments were performed in series for 1 hour-using 12 mice (6 paced and 6 sham paced for 1 hour) thus resulting in a 14 hour day. Further refinement included duplication of the set up to expedite throughput; initially 2 sets of nose cones were set up joined to the vaporiser via a T tube (with 2 separate anaesthetic gas scavengers) with a 3-way tap system. This allowed diversion of anaesthetic gases with the higher doses for induction being piped to one animal and then switching the supply of gas to both mice. Where one mouse was already asleep, there would be a period of some seconds where the circuit was switched off to allow induction of the second mouse. In the event of higher dosing of anaesthetic gas, this posed a risk of apnoea in either of the two mice and required extreme vigilance in managing these experiments since airway access and therefore manual ventilation was not available. Maintenance continued on lower concentration of isoflurane necessitated positioning animals

180 degrees apart due to concerns over the short tube length and dead space constraints. These refinements meant that longer duration experiments including the 4 hour pacing protocol and 6 hour pacing protocol were possible.

In 2006 a final refinement to the scalability model was made when we transferred to the Smilow Institute at Tisch hospital. A bench top Biopac system was set up using AcqKnowledge software for Mac from Dr Fishman's lab and MP 100 boxes. I refined anaesthetic management with veterinary staff at Vetequip (Vetequip, Inc. Pleasanton, CA.) with introduction of an induction chamber, vaporiser with multi-procedural tubing, taps and activated charcoal filters to ensure consistent levels of anaesthesia, animal safety, comfort and higher throughput (up to 4 experiments could be performed in a 6-8 hour time window). Inhaled isoflurane (4% volume induction) achieved general anaesthesia of mice inside an induction chamber and the mice were then transferred to a nose cone for maintenance (1.5 vol % maintenance; Baxter, Deerfield, IL) inhalation of a mixture of oxygen and isoflurane. Adhesive tape applied to each of the limbs immobilised animals on a glass plate lying on top of a Gaymar® (Gaymar Inc. NY, USA) heating pad set at a constant 37°C and expanded circuit of the Gaymar® Pump to maintain 2 heating pads for a total of 4 mice at any one time. A ground electrode was attached to either the ear or subdermally across the manubrium sterni. Removal of hair was achieved using Nair® to expose the smooth ventral epidermis. The epidermis was then cleaned with alcohol prior to any surgical procedure.

Figure 11- Bench top small mammal anaesthesia set up as provided by Vetequip.

Vaporiser, tubing and induction chamber (reproduced with permission courtesy of Vetequip);

http://www.vetequip.com/images/big-901806.jpg).

A cohort of CD-1 mice (Charles River Lab, Wilmington, MA, USA) were used for the immunoblotting of ventricular lysates and quantification of mRNA expression experiments.

Recording of electrocardiograms for monitoring.

Pilot experimental ECG recording involved using surgically tunnelled leads. A refinement included an ECG setup that could be moved between the animals using commercially available ECG electrodes that had a sharp needle insertion (see figure 12) and proximal connector that could be clipped off thus avoiding repeated surgical removal and insertion of the ECG leads at different stages of the pacing experiments.

Electrode leads were applied to each of the four limbs, signals amplified and digitally monitored and stored on PC or Mac. Using Ponemah physiology software and/or Biopac MP 100 we were able to record data points at baseline, during pacing to document 1:1 capture and following cessation of pacing. This data could then be analysed offline at a later time.

Application of the stimulating electrode for pacing or sham pacing

After the baseline electrocardiogram recording, the ventral epidermis was cleaned with alcohol and sterile instruments used to make a 1cm incision in the epigastric region and expose the xiphisternum and diaphragmatic aspect of the abdomen. Once the liver was safely retracted, a custom made UE-GM1 cardiac stimulating electrode with a 200μm monopolar platinum tip (Frederick Haer & Co, Bowdoinham, ME) mounted on a micromanipulator and connected externally to the Medtronic stimulator was positioned on the right ventricular (RV) surface.

A limitation to the project was a limited number of pacing probes. These were fragile and prone to bending at the tip. Any structural damage to the probe if sufficiently severe resulted in ineffective pacing with damage to the diaphragm. Extreme caution was necessary at this point to avoid damaging the abdominal, and critically thoracic structures as the thoracic integrity maintained negative pressure for spontaneous respiration. Subtle micromanipulations adjusted the angle, depth and height of the stimulating probe.
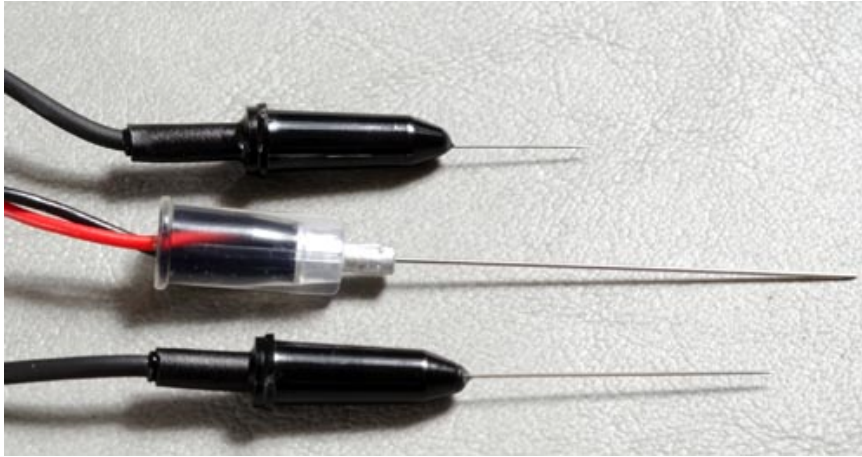
Figure 12 Example of pin electrodes supplied by Biopac;

The distal pin electrodes illustrated were accompanied with a detachable extension clip on the proximal end of the leads for ease of application and removal. (Reproduced with permission from Biopac website;http://www.biopac.com/research.asp?SubCatID=59&Main=Electrodes).

Confirmation of capture

Capture with pacing during experiments was confirmed with electrocardiographic monitoring in real-time throughout the duration of the experiment. Pacing was performed using a Model 2352 Medtronic Programmable Stimulator (Medtronic, Minneapolis, MN) and this device was also used for programmed electrical stimulation after a pacing experiment. The stimulating output was set at a fixed pulse width of 1.0ms and twice the diastolic threshold. The paced cycle length was set, maintained and adjusted throughout experiments to ensure a 10-15% faster heart rate than the anesthetised sinus rate.

Managing fluid balance

Gauze soaked in PBS was applied across the open wound to minimise evaporative fluid and conductive heat loss. However, no additional fluid was administered during pacing.

Infection control and bleeding.

The experiments required a sterile field and appropriate surgical clothing was worn with sterile gowns and gloves, as well as clean surgical hats, masks and shoe covers. In the event of bleeding, as occurred when animal euthanasia was performed under anaesthesia with transection of the aorta, I managed this using gauze and absorbent disposable surgical pads (separate pads for each experiment).The pads also provided some cushioning for instruments and required a square to be cut in them to accommodate the glass plate on which the mouse was immobilised. Topical antibiotic ointment was used for experiments where survival was being assessed after closure and to avoid surgical site infection.

Regulator inspection

At least 2 pacing experiments (6 hour protocol) were performed from start to finish under

close supervision of animal inspectors who reviewed surgical and animal handling.
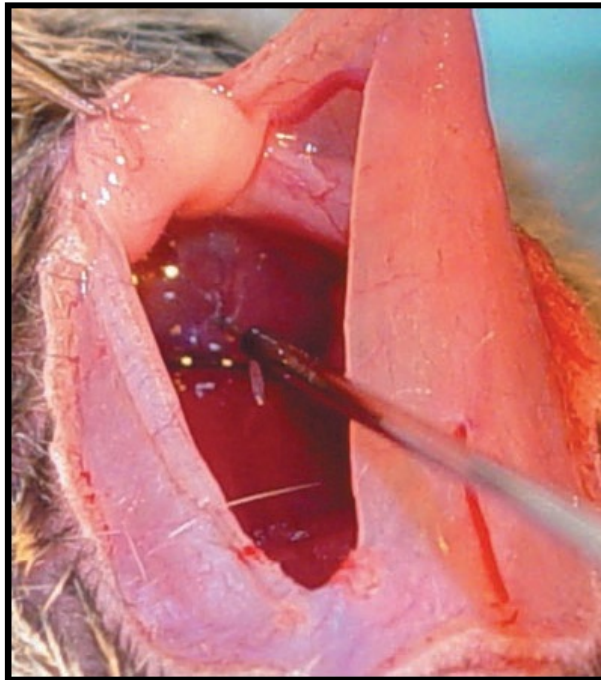
Figure 13 Stimulating electrode inserted through small subxiphoid incision into contact with the diaphragmatic surface of the RV.

This open area would be covered with PBS soaked gauze to avoid dehydration. Reproduced

with permission from Gutstein et al (151).
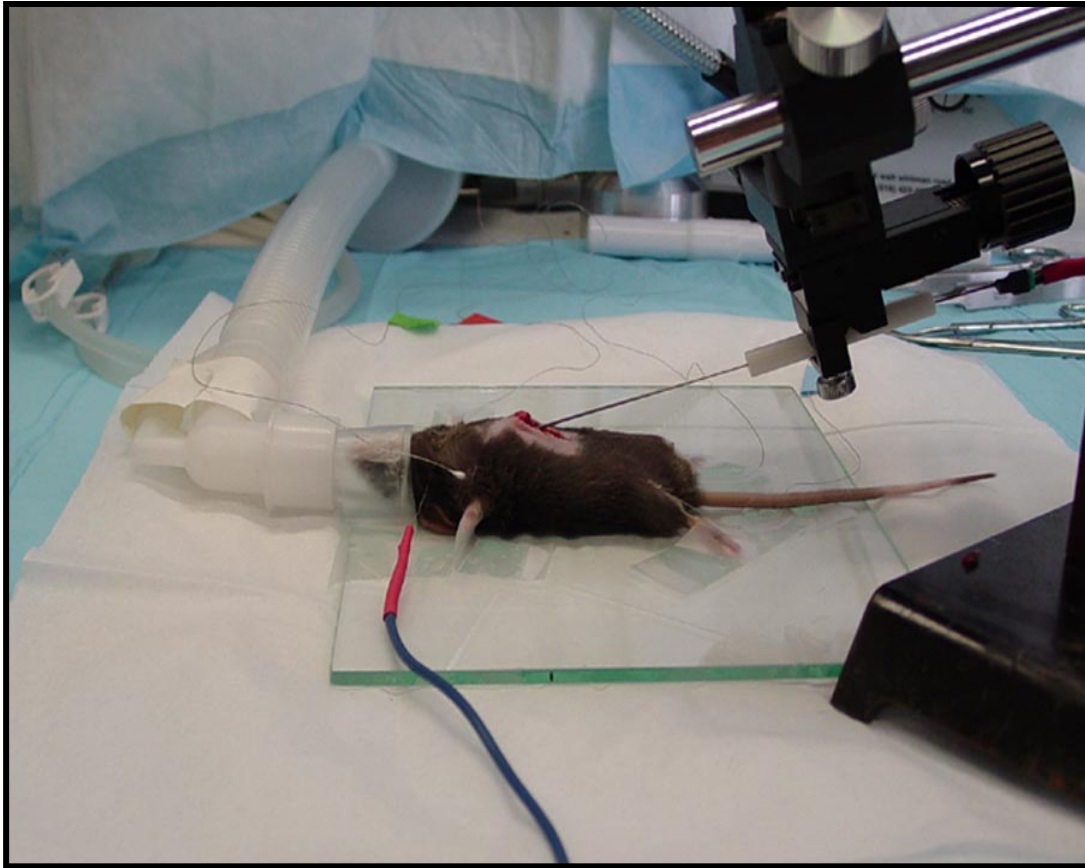
Figure 14-Pacing setup demonstrating positioning of the animal with pacing probe in situ.

The probe is connected to a micromanipulator and stand. The mouse is asleep via nose cone and limbs fixed with adhesive pad to glass plate. A warm pad lies beneath the disposable surgical pad and glass plate to keep body temperature constant at 37C. ECG electrodes are surgically implanted in each of the limbs; these are the older style electrodes illustrated (151).

Sham pacing

Age, sex and strain-matched control mice were prepared in the same way described above i.e. with the pacing electrode in contact with the heart but the programmable stimulator was not switched on.

Reproducibility of positioning the Stimulating Electrode:

In four animals, a midline sternotomy was performed at the end of the pacing protocol confirming that though the electrode traversed the diaphragm, it did not puncture the heart and was consistently positioned on the RV.

Mediastinal viscera are not disrupted or damaged by the pacing electrode.

The main advantage of the model was its consistent ability to avoid trauma to mediastinal structures; The heart, local structures (including the abdominal viscera i.e. liver, diaphragm and lungs) were not disrupted by the electrode.

Myocardial Tissue Appearance after short-term pacing and programmed electrical stimulation:

To determine whether microscopic damage resulted from subdiaphragmatic pacing and Programmed Electrical Stimulation, Hearts from a subset of six subdiaphragmatically paced and PES tested animals were removed on death, fixed in 10% formalin, and embedded in paraffin for histological evaluation. No evidence of fibrosis or intramyocardial haemorrhage was seen on haematoxylin-phloxine-saffron (HPS) - stained histological sections from these hearts.
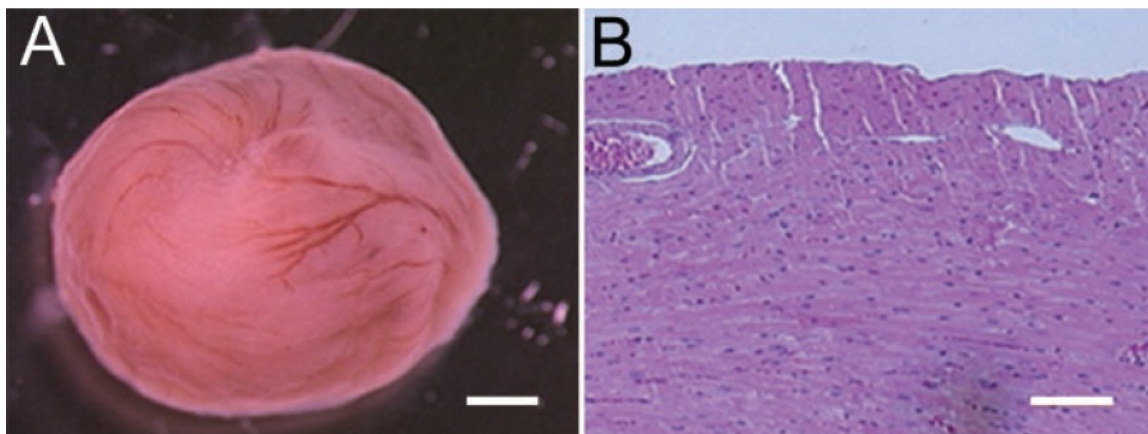
Figure 15 -Myocardial tissue appearance after electrophysiological study from a subdiaphragmatic approach.

A: apical surface of the heart of a study animal after electrophysiological study. No gross evidence of tissue damage is seen. *B*: haematoxylin-phloxine-saffron (HPS)-stained apical section from a study animal showing normal tissue architecture without evidence of disruption or injury. Scale bar = 1 mm (*A*); 100μm (*B*). Reproduced with permission from Gutstein et al (151)

Procedural Deaths:

A total of 400 mice were used for all experiments. Two procedural deaths occurred due to hypothermia; perforation of the heating pads by surgical instruments (with ensuing gradual loss of water and thermoregulation) resulting in hypothermia and asystole. Four episodes of pneumothorax occurred (n=4). Factors contributing to pneumothorax included: (i) loss of capture necessitating repositioning of the electrode within a few 100μm- 1mm and (ii) prolonged procedures with repeated placement of the stimulating electrode e.g. longer protocols were needed with 6hr pacing and (iii) repeated PES and (iv) repositioning of ECG limb leads . Where pneumothoraces compromised cardiorespiratory function and therefore the integrity of the preparation, experiments were terminated and the animal euthanized while under general anaesthetic. Other losses occurred due to liver injury n=1, apnoea due to excessive anaesthesia n=1. A total of 10 mice died .This gave a procedural all-cause mortality of 2.5 % though losses were greatest during the early stages of developing the model (see Table 3).

Cause of death	number	% of total
Early stages of training and ECG repositioning	2	2/400 (0.5%)
Hypothermia	2	2/400 (0.5%)
Pneumothorax	2	2/400 (0.5%)
Multiple Probe repositioning	1	1/400 (0.25%)
Long protocol	1	1/400 (0.25%)
Apnea/Excess anaesthesia	1	1/400 (0.25%)
Liver injury	1	1/400 (0.25%)
Total deaths	10	10/400 (2.5%)

Table 3 Procedural deaths from pacing sub diaphragmatically.

Total all cause mortality 2.5%.

Evaluation of mechanical and electrical capture:

Surface electrocardiograms demonstrated substantial widening of the QRS complex during pacing, suggesting aberrant interventricular electrical conduction. (Fractional shortening was marginally decreased from $44.2 \pm 2.0\%$ at baseline to $37.2 \pm 2.8\%$ during pacing ($p < 0.05$). Rather than measure aortic doppler velocities as had been done by the Kass group, I demonstrated mechanical capture on echo whilst the pacing stimulator was turned on.
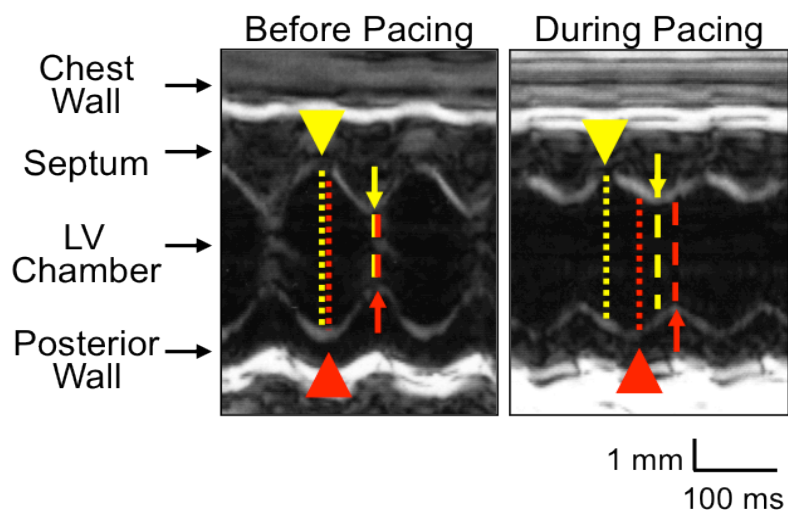
Figure 16 –Echo before and during pacing.

Echo demonstrating mechanical capture and mechanical dyssynchrony with septal to posterior wall motion delay. Reproduced with permission from Kontogeorgis et al (152).
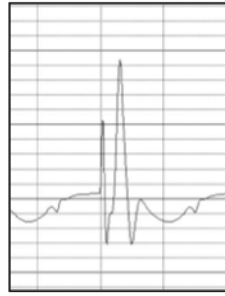
Before Pacing   During Pacing

Figure 17- Electrical capture and electrical dyssynchrony during pacing.

Electrical capture and electrical dyssynchrony during pacing as evidenced by broadening of

the QRS. (recorded from Biopac MP100 system). Reproduced with permission from

Kontogeorgis et al(152).

4.5hr, and 2 week Survival Study after 1 hr pacing.

The aim of this study was to determine the impact of the surgical procedure as well as the 1hour pacing protocol on the animals. Six mice were paced for 1hour and six sham-paced (the electrode was placed in contact with the RV surface sub diaphragmatically but the stimulator was turned off). At the end of the procedure the epigastric incision was sutured and the animals recovered. Within a few minutes, once the inhaled anaesthesia wore off, the animals began mobilising and became progressively more active in their cages. There were no signs of distress over the next few hours and days with good patterns of feeding and drinking as well as interaction with their fellow mice and when handled. After 4.5hrs 3 paced mice were sacrificed and their hearts examined macroscopically and immunostained for Cx43. Once again, no obvious qualitative macroscopic injury was observed and no difference on immunostaining for Cx43.

After 2 weeks the remaining 3 paced mice that were recovered were sacrificed. Their hearts were examined in a similar fashion. There were no signs of injury to other viscera (examined at the time of sacrifice). The Cx43 immunosignal was then qualitatively examined by me and Dr Gutstein in a blinded fashion. We were unable to distinguish the paced from the unpaced tissue samples. The sham-paced animals had an uneventful recovery and no losses were incurred as a result of the surgical procedure. These findings are consistent with the longitudinal studies previously undertaken by Dr Gutstein(151).

Measuring Threshold parameters at baseline, 1hour and after 6 hours pacing protocol

The objective was to model altered activation rather than induce tissue damage; hence the stimulator output was limited to approximately twice the stimulating threshold. The mean stimulator output was 0.366 ± 0.011mA. These levels were sufficient for stable electrical capture throughout all pacing experiments. The average threshold determined after 1hour sham-pacing was 0.21 ± 0.04mA (n=6) and after 1 hour pacing 0.191 ± 0.049mA (n=6) and this was not significantly altered (p=0.52). The average threshold prior to 6 hours pacing was 0.165 ± 0.007mA (n=65). In a subset of eight mice, the threshold was determined after 6 hours of pacing with an average post-pacing threshold of 0.162 ± 0.026mA (p=NS). The unchanged threshold values underscore the stability of the experimental preparation.
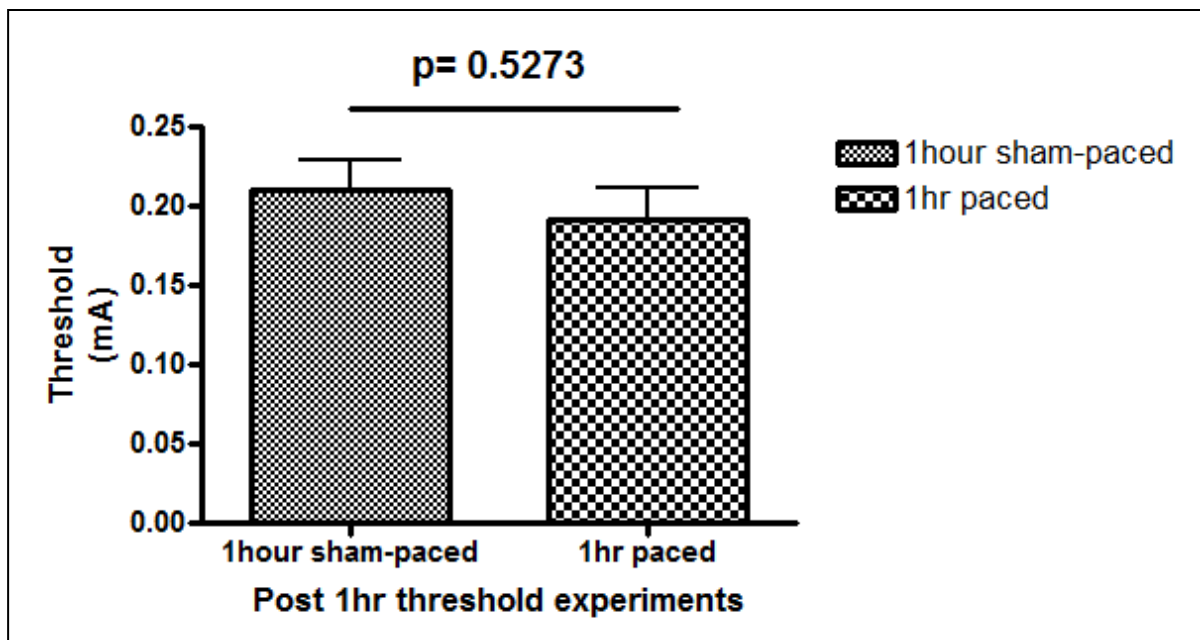
Figure 18 Pacing thresholds after 1 hour (n=6; p=ns).

No difference in pacing thresholds after 1hr pacing.
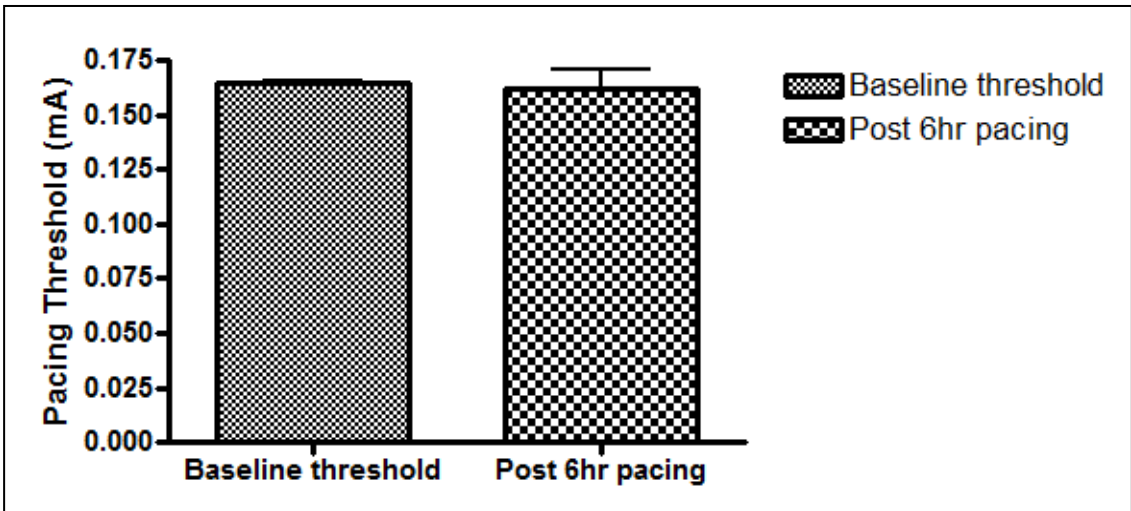
Figure 19-Pacing threshold at baseline (n=65) and after 6 hours pacing (n=8;p=ns).

No difference in pacing threshold after 6hr pacing.

Conclusion

In this chapter I have shown that the sub diaphragmatic model of pacing is a feasible approach to pacing the murine heart and inducing dyssynchrony. Cautious placement of the pacing probe avoids injury to the diaphragm and thoracic structures making pacing of the RV epicardial surface possible and safe. There is no need for intubation, vascular access and thoracotomy. Mice survive the surgery, are free of any obvious distress for up to 4.5 hours as well as 2 weeks after the 1hour pacing procedure. When pacing is switched off the mice also recovered well. There was no evidence of macroscopic injury to the heart and the HPS staining did not show any pacing related changes. Pacing capture thresholds remained stable throughout the experiments at 1 hour and 6 hours thus highlighting the stability of the preparation. Pacing achieved electrical and mechanical capture as demonstrated on ECG and ECHO with features of electrical and mechanical dyssynchrony.

Chapter 3

Electrocardiographic assessment in the subdiaphragmatic model of dyssynchrony

Introduction

In Chapter 3, I outline data from an experimental series performed at baseline, after sham-pacing and after pacing at 1hr, 4hr and 6hr intervals in C43$^{+/+}$ and Cx43$^{+/-}$ mice. This addresses objectives 4 and 5 of the thesis mentioned in Chapter 1.

The origins of the ECG can be traced as far back as the 19th century when in 1887 Augustus Waller demonstrated the amplification of the source voltage of the heart on the surface of the skin in humans(153). It wasn't until the 20th century before this became more widely applied in clinical medicine. Correlating the timing of ECG with mechanical events (such as heart sounds) in the heart followed in 1911 by T Lewis and other investigators such as H C Bazett in 1920 and Wiggers who had been working with dogs to correlate the onset of the R wave on ECG with systole (154-156).

ECG analysis in mice has been used extensively in the literature to study models of arrhythmia. Interest in the field of cardiovascular research has put the ECG as a central tool in analysing electrophysiology to characterise various models. The mouse poses some challenges to performing ECG (as well as programmed electrical stimulation) given its small size. The first *in vivo* attempt at programmed electrical stimulation required intubation and an open chest model by Berul et al(157). These investigators followed the convention of using needle electrodes implanted subcutaneously strapped the rodent limbs to minimise movement induced artefact. It has also been shown by Danik et al, using this same approach that there is a significant challenge in models of long QT syndrome to find consistency in the measurement of the QT interval such that the authors arbitrarily assigned 3 separate deflection points that may correlate with return to baseline denoting the end of repolarisation (13;148;151;158;159).

In the field of cardiac memory, mouse models have therefore not been favoured given that they differ substantially from large mammals in their shorter repolarisation profile. Yet, mice remain unique in that average sinus heart rates are in the order of 500-600 beats per minute and their need to sustain such rapid rates justifies this difference of rapid repolarisation in the action potential. When compared with that of humans its clear that the ion channels expressed by mice are different. Yet, within the human heart significant differences exist between ventricular and atrial ion channels expressed and therefore action potential morphology(fig 20). Understanding the electrophysiology in mice can be particularly helpful in understanding the high rates sustained by human atrial tissue during atrial fibrillation, for example. These regional heterogeneities are highly significant and considered contributory in the study of mechanisms of arrhythmia in disease models as well as in human disease (2-4;160).
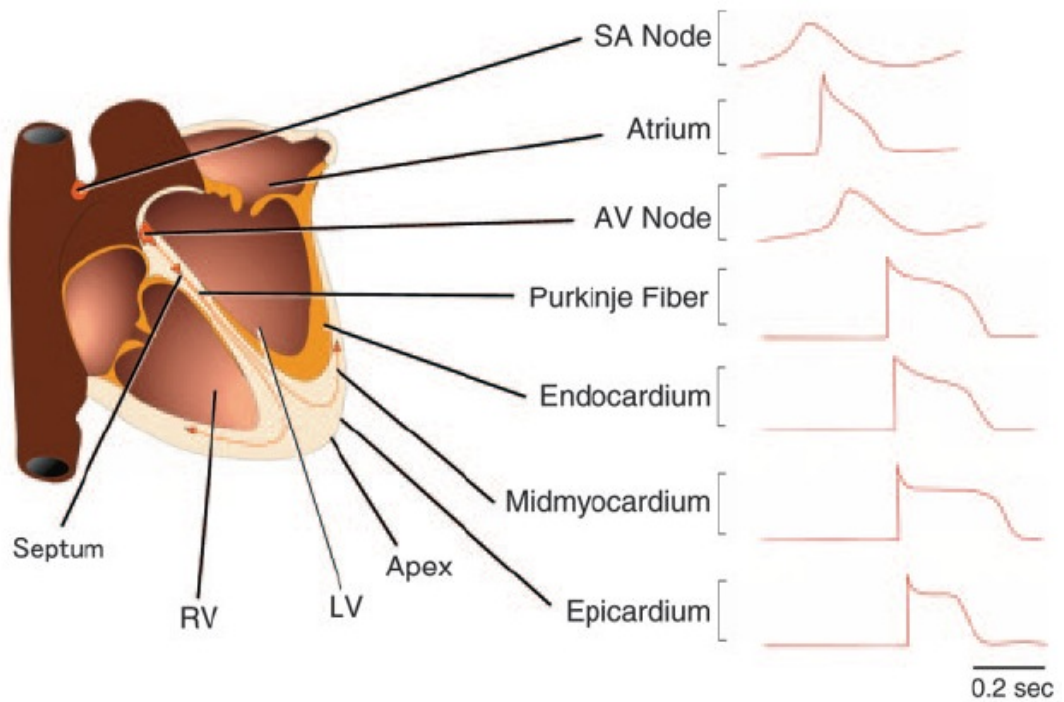
Figure 20 Schematic illustrating region specific differences in action potential morphology and duration.

Note altered rate of depolarisation or upstroke of SA node cells compared to rapid upstroke of atrial and ventricular myocardial cells. This is due to regional differences in the ion channels expressed at the cell surface. Reproduced with permission from Kass et al (160).
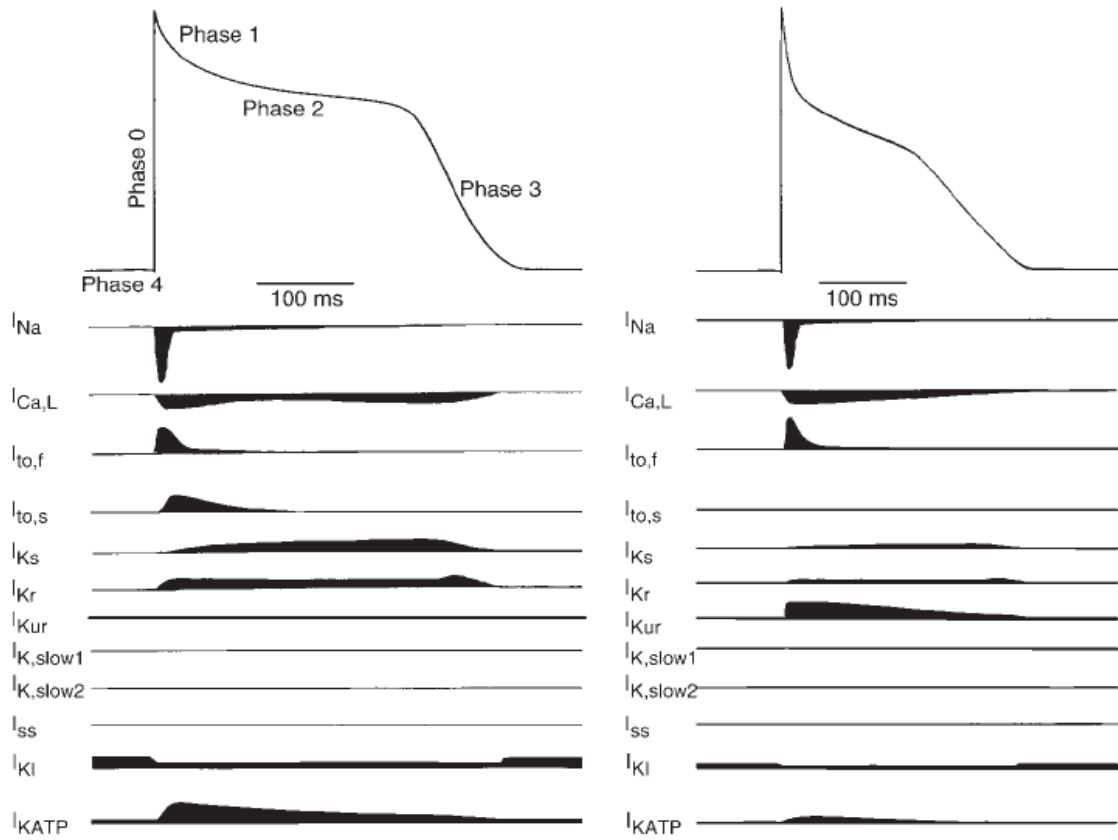
Figure 21 Figure illustrating differences in regional ion channel expression.

Differences in human ventricle (on left) and atrium (on right); Reproduced with permission from Kass et al (160).
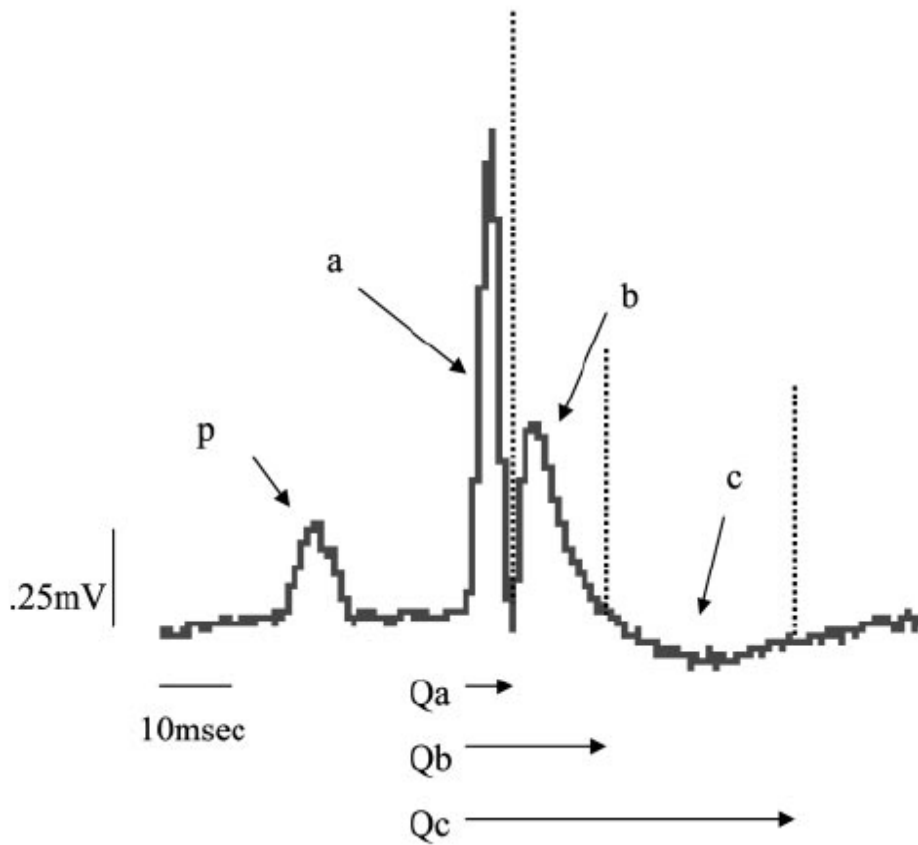
Figure 22 - Difficulty in identifying the QT interval on murine ECG.

One heartbeat on murine ECG with intervals demonstrated. After the p wave there are 3 deflection points that have been designated arbitrarily by Danik et al as Qa, Qb and Qc .Reproduced with permission from Danik et al(159).

Method:

Recording of electrocardiograms and application of the stimulating electrode for pacing

Electrode leads were applied to each of the four limbs, and signals were amplified and digitally monitored on PC or Mac. Using Ponemah physiology software and Biopac MP 100 I recorded data points at baseline, during pacing to document 1:1 capture and following cessation of pacing. This data could then be analysed offline.

In the preceding chapter describing the development of the model I have described the technique of positioning the pacing probe but here I present in more detail the method of ECG recording.

ECG recordings

Signals were amplified using a Honeywell ECG amplifier (Honeywell, Morristown, NJ), converted from analogue to digital with an ACQ-16 Acquisition Interface and recorded with Ponemah Physiology software (Gould; Valley View, OH). ECG Intervals, including p wave amplitude and duration, PR interval, QRS amplitude and duration, axis and QTc interval were calculated from limb leads I, II and III. These were recorded at baseline, during pacing and after completion of pacing and then analysed by myself offline to look for any changes in the ECG in the pacing model. In the next section I will present the data from these experiments.

Figure 23 -Biopac MP100 and AcqKnowledge ECG system.

Reproduced with permission from Biopac website;
http://www.biopac.com/Research.asp?CatID=43&Main=Systems.

Figure 24 - Ponemah Physiology Platform.

Upper and lower left panel (ACQ 16 unit) with permission from Data Science International

(**http://www.datasci.com/products/software/ponemah/ponemah-5-10**).**;**

http://www.datasci.com/products/signal-conditioners-and-amplifiers/acq-16-acquisition-interface-unit).

Right panel (Honeywell ECG amplifier) used in the first year of experiments.

Results:

Electrocardiographic assessment after short-term pacing at 1hr and 4hrs:

Pre and post-study six lead electrocardiograms in mice paced for 1, 4, 6 hours as well as sham-paced controls were analysed. No significant change from baseline values of PR interval, QRS duration, RR interval or rate corrected QT interval (QTc) in any of the paced groups was observed when compared with sham-paced controls. QRS amplitude was modestly but significantly diminished after 1 hour pacing when compared at baseline but not 4hour and 6 hour time points. See Table 4.
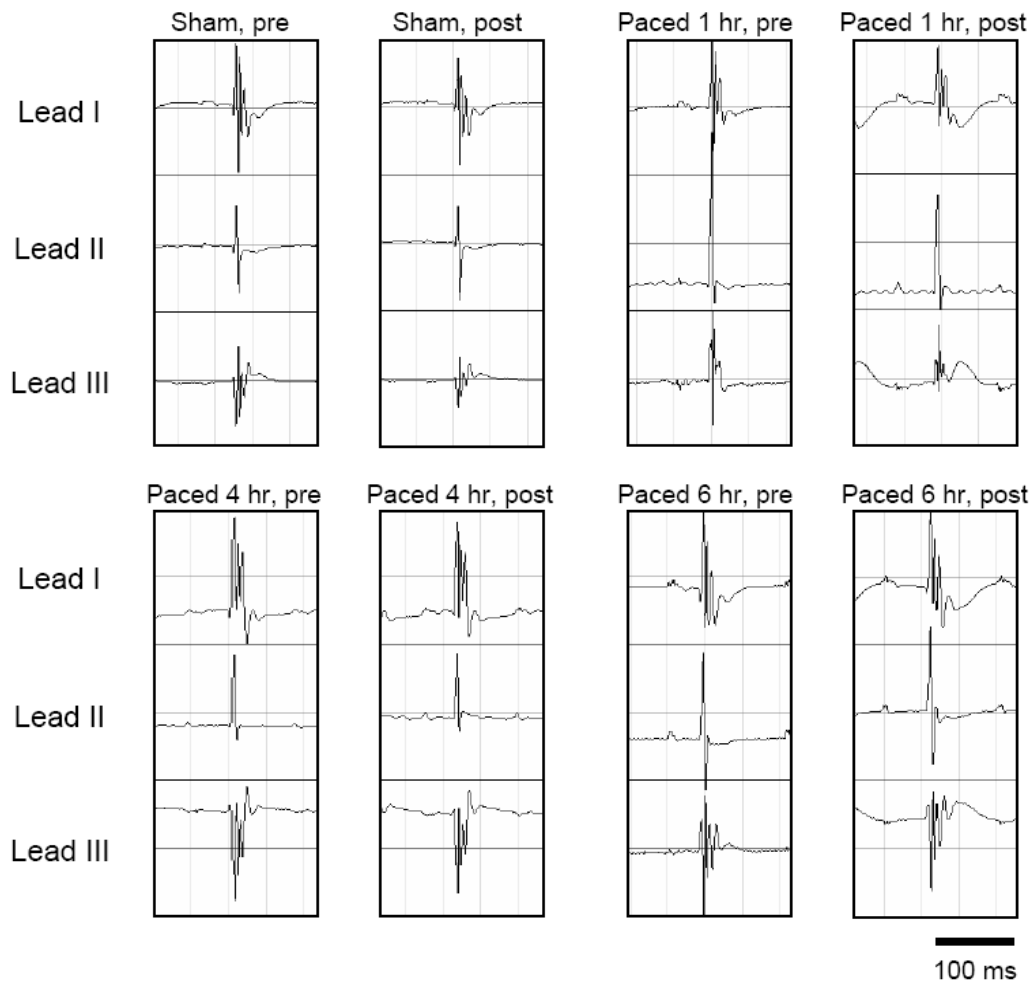
Figure 25 ECG at baseline and after sham pacing at 1hour, 4hour and 6 hours.

ECG morphology demonstrating "cardiac memory" at 1 hour and 6hour time point in lead I and III.

ECG Axis substudy at 1hour pacing time point

An additional 7 mice were paced and sham-paced for 1 hour and QRS amplitude analysed separately in each of six leads (I, II, III, avR, avL and avF). These experiments demonstrated no difference in QRS amplitude. This suggested that the effect observed may have been related to only studying lead II in the earlier analysis and that once combined with the other leads a correction of the error occurred given it was likely due to an ECG axis shift.

Electrocardiographic indices at 6hour time point:

No significant differences were observed in ECG parameters in paced and sham-paced mice after six hours. See Table 5. Electrocardiographic Indices in C57BL/6J Wildtype Sham-Paced and Paced Mice.

Table 4. Comparison of Electrocardiographic Data at 1hour, 4hour and 6 hour in Sham and Paced Mice

	Sham-paced, n=17	Paced 1 hr, n=11	Paced 4 hr, n=16	Paced 6 hr, n=14
PR Interval, ms	40.9 ± 1.1 (-1.2 ± 0.9)	44.5 ± 1.3 (+3.0 ± 1.7)	44.7 ± 2.4 (+1.8 ± 3.0)	49.4 ± 3.7 (+6.1 ± 3.6)
QRS Duration, ms	11.7 ± 0.4 (-0.4 ± 0.5)	12.0 ± 0.5 (+0.5 ± 0.6)	12.8 ± 0.5 (+0.4 ± 0.6)	14.1 ± 1.1 (+0.9 ± 1.1)
RR Interval, ms	140 ± 4.5 (+7.1 ± 4.6)	121 ± 3.2 (-11.1 ± 5.7)	137 ± 6.3 (+7.1 ± 5.6)	145 ± 4.7 (+0.9 ± 7.0)
QTc, ms	106 ± 3.2 (-2.8 ± 3.6)	122 ± 4.9 (+7.3 ± 5.7)	123 ± 2.9 (-3.7 ± 4.3)	106 ± 2.3 (+0.6 ± 4.1)
QRS Amplitude, µV (Lead II only)	114 ± 7.5 (+5.1 ± 5.9)	98.4 ± 6.9 (-30.8 ± 12.1)* **(p<0.01)**	118 ± 13 (+6.3 ± 7.8)	103 ± 7.9 (-7.8 ± 5.4)

Post-pacing data and changes from baseline (in parentheses) are presented as group means ± SEM. Comparisons between groups of changes from baseline were performed with ANOVA followed by Fisher's protected least significant difference test. *, $p < 0.01$ compared to Sham-paced and Paced 4 hr ($p = 0.05$ compared to Paced 6 hr).

Table 5. Electrocardiographic Indices in C57BL/6J Wildtype Sham-Paced and Paced Mice

	Sham-Paced, 6 hr (n=8)	Paced, 6 hr (n=14)
QRS Duration, ms	11.1 ± 0.7 (-1.3 ± 0.7)	14.1 ± 1.0 (0.9 ± 1.1)
RR Interval, ms	144.6 ± 8.0 (12.6 ± 8.3)	144.6 ± 4.7 (0.9 ± 7.0)
QTc, ms	97.7 ± 4.2 (-6.7 ± 5.7)	106.2 ± 2.3 (0.6 ± 4.1)

Post-pacing data (and changes from pre-pacing baseline) are presented as group means ± SEM. Comparisons between groups were performed with unpaired T-tests. For electrocardiographic indices, n = 8 sham and 14 paced. With permission from Kontogeorgis et al (179)

Table 6 Electrocardiographic Measurements at Baseline (Pre-sham and pre-pacing) in WT and Cx43$^{+/-}$ Mice

	WT pre-sham pacing (n=6)	WT pre-pacing (n=6)	Cx43$^{+/-}$ pre-sham pacing (n=7)	Cx43$^{+/-}$ pre-pacing (n=9)
QRS Duration, ms	11.7 ± 0.5	12.7 ± 0.8	10.4 ± 0.8	9.8 ± 1.1
RR interval, ms	131 ± 4.4	134 ± 2.4	137 ± 5.3	139 ± 6.0
QTc, ms	114 ± 7.4	126 ± 9.3	119 ± 7.3	119 ± 17.9

Data is presented as group means ± SEM. Comparisons between groups were performed with ANOVA.

Table 7 Electrocardiographic Indices after Pacing or Sham-Pacing Protocol in WT and Cx43$^{+/-}$ Mice

	WT sham paced(n=6)	WT paced (n=6)	Cx43$^{+/-}$ sham paced (n=7)	Cx43$^{+/-}$ paced (n=9)
QRS Duration, ms	12.0 ± 0.3 (0.3 ± 0.6)	13.2 ± 1.3 (0.5 ± 1.4)	9.8 ± 0.8*(p<0.05) (-0.6 ± 0.7)	10.1 ± 0.7*(p<0.05) (0.2 ± 1.4)
RR interval, ms	136 ± 4.3 (5.7 ± 6.3)	138 ± 6.9 (4.2 ± 7.3)	134 ± 9.8 (-2.9 ± 5.9)	142 ± 13.2 (2.9 ± 14.7)
QTc, ms	116 ± 3.7 (1.2 ± 6.0)	127 ± 5.3 (1.8 ± 9.2)	130 ± 11.1 (11.4 ± 13.0)	167 ± 23.3 (48.3 ± 34.6)

Post-pacing data (and changes from pre-pacing baseline) are presented as group means ± SEM. Comparisons between groups were performed with ANOVA. *, $p < 0.05$ compared with WT paced; compared with all other groups. For electrocardiographic indices, n = 6 WT sham paced, 6 WT paced, 7 Cx43$^{+/-}$ sham paced and 9 Cx43$^{+/-}$ paced. With permission from Kontogeorgis et al (179).

Table 8. Differences in Electrocardiograph Measurements, Delta, **in Wildtype and Cx43 Heterozygous KO Mice**

	WT sham- pacing delta (n=6)	WT post-pacing delta (n=6)	Cx43$^{+/-}$ post-sham pacing delta (n=7)	Cx43$^{+/-}$ post- pacing delta (n=9)
QRS Duration, ms	0.03 ± 0.001	1 ± 0.001	-1 ± 0.001	0.02 ± 0.001
RR interval, ms	6 ± 0.006	4 ± 0.007	2 ± 0.006	0.3 ± 0.015
QTc, ms	1 ± 0.006	2 ± 0.009	5 ± 0.013	4.8 ± 0.04

Data is presented as group means ± SEM. Comparisons between groups were performed with ANOVA. *, $p < 0.05$; **, $p < 0.01$ compared to matched wildtype littermates. No significant differences between groups.

Electrocardiographic parameters at baseline and after short-term pacing in Cx43$^{+/-}$ mice and deltas.

Surface electrocardiograms in Cx43$^{+/-}$ mice were compared to matched wildtype littermates at baseline (See Table 6). ECG in Cx43$^{+/-}$ mice and Cx43 sham-paced mice after 6hr pacing demonstrated a slightly but significantly reduced QRS duration in both paced and sham-paced mice (See Table 7). No significant differences in RR interval or QTc were noted (although paced Cx43$^{+/-}$ mice did appear to have longer QTc intervals). A comparison of ECG differences, deltas between wildtype Cx43 and Cx43$^{+/-}$ mice after 6hr sham-pacing or 6hr pacing demonstrated no significant change (See Table 8).

WT Unpaced   WT Paced   Cx43$^{+/-}$ Unpaced   Cx43$^{+/-}$ Paced
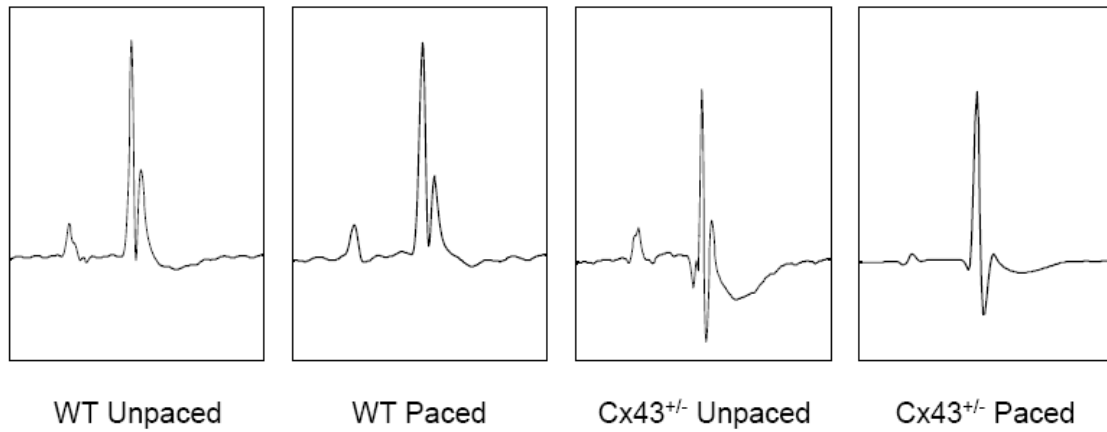
Figure 26 Surface electrocardiograms in Cx43$^{+/-}$ mice at baseline and after pacing were compared to matched wildtype littermates at baseline and after 6hr pacing.

The surface ECG demonstrates significant shortening of the QRS duration in unpaced and paced Cx43$^{+/-}$ mice relative to unpaced and paced WT mice. Reproduced with permission from Kontogeorgis et al (161).

Discussion:

The ECG data characterising the wild type Cx43$^{+/+}$ mice and Cx43$^{+/-}$ mice with pacing looked for differences that might suggest pacing induced dyssynchrony results in significant change to integrated action potential morphology at the body surface. The evidence for electrical capture confirms that the pacing probe exerted an electrical stimulus with altered activation across the myocardium.

The ECG figures at the 1hour, 4hour and 6hour time point suggest that changes consistent with cardiac memory could be observed as early as after 1 hour of pacing in lead I and III but without measurable differences in ECG parameters. This initially suggested that 1 hour of pacing alone may be a sufficient time point for the pacing model in order to study remodelling. Changes evident within lead II QRS amplitude appeared consistent with findings from previous work on the Cx43 transgenic line(6;7). However, a separate ECG axis sub-study was undertaken to explore whether this observed change in QRS amplitude might be due to a change of axis. All 6 limb leads were incorporated into the analysis. This further study aided in correcting for what was likely an axis shift in lead II rather than a true reduction in QRS amplitude.

Despite the difficulties in measuring the QT interval in mice, I consistently and manually measured this from all time points using the equivalent of deflection point Qc as described in the Danik et al paper. The calculation of the corrected QTc also followed the standard approach in the literature, which involves use of the Bazett formula(159).

The data for the p wave amplitude, duration and PR interval as well as QRS were also analysed. However, in the subdiaphragmatic pacing model, both wildtype and Cx43$^{+/-}$ mice

did not demonstrate conduction slowing or delay at the AV node as would be inferred by PR interval prolongation.

The most striking difference was noted in the surface ECG in Cx43$^{+/-}$ mice with shorter QRS duration at baseline and after pacing as compared to matched Cx43$^{+/+}$ mice as well as features suggestive of QTc prolongation which were not statistically significant.

Chapter 4

Echocardiographic assessment in the pacing induced dyssynchrony model

Introduction:

In Chapter 4, I determine the echo parameters at baseline, during pacing and after cessation of sham- pacing and pacing in Cx43$^{+/+}$ mice. I assess mechanical synchrony and evaluate mechanical capture and mechanical ventricular function. Furthermore, I evaluate echo parameters after sham-pacing and after pacing in Cx43$^{+/-}$ mice. Additional echocardiography experiments are performed after completion of a 2hour rest period following cessation of pacing to re-evaluate echo findings. This series of experiments addresses objectives 4 and 5 of this thesis as mentioned in Chapter 1.

History of Echocardiography

The use of ultrasound to assess myocardial contractility and non invasively assess blood flow with Doppler has gained widespread appeal both in clinical medicine as well as in cardiovascular research the full potential of which is yet to be realized. In some respects it gives humans the ability to copy the ability of some mammals who use high frequency ultrasound to navigate their environments as in the case of bats and water mammals. It was the early discovery of piezoelectricity by Curie and Curie that laid the foundation for the development of echo technology. Early pioneers of the technique were credited with patents in the case of Sokolov and Firestone. Experimentation following WWII by Wild meant he was first to examine the heart with ultrasound. However, it is Hertz and Edler who first used echo as we know it today(162).

Qualitative and Quantitative echo indices.

The commonly used measurements in echo include a qualitative assessment of cardiac movement on 2D echo as well as M mode. Quantitative measures include wall thickness, chamber volume and the calculated functional indices such as fractional shortening and ejection fraction. Regional wall motion abnormalities are considered highly significant in clinical practise and often are thought to reflect coronary perfusion abnormality. However, there are other causes including delayed activation of the myocardium. Wall motion abnormalities have been observed in studies of conduction system disease e.g. LBBB.

Echo is a vital tool in assessing patients with heart failure in reaching a diagnosis, assessing severity and in more recent years determining the presence of dyssynchrony. In heart failure if evidence for dyssynchrony exists this has important therapeutic implications for patients and expands their options to device based therapy such as CRT-P or CRT-D. National guidelines incorporate ECHO parameters for suggesting implantation of devices but have struggled to meet the expanding role for these devices. The evidence in favour of improving clinical outcomes as well as echo indices is extensive(3;21;163-165).

Echo in animal research

There is a wide literature base for echocardiography in various animal models as well as small mammals such as rodents. Apart from models of infarction where echo can assess the degree of infarct size it has also played a role in characterising models of dilatation, non ischaemic heart failure and pressure overload(6;7;15;22;162;166).

Role of echo in this thesis

 In this model I was interested in demonstrating that pacing achieved mechanical dyssynchrony and therefore mechanical capture during pacing and altered the activation of the myocardium. I used the method of Pitzalis et al rather than adopt that of Kass and investigators who looked at aortic Doppler velocities in their mouse model of chronic pacing (2). Since rodents are challenging to manage in the awake state, I elected to perform all these experiments under general anaesthesia which is a commonly adopted practise(4).

Furthermore since heart failure is known to result in mechanical dyssynchrony I was interested in using the model to characterise the functional effects in wildtype $Cx43^{+/+}$ mice as well as heterozygous $Cx43^{+/-}$ mice. I was keen to look for any altered echo indices that might suggest a correlation to adaptive functional effects at the 6 hour time point - ECG data suggested there may be some changes with shortening of QRS duration in $Cx43^{+/-}$ mice at baseline and prolongation after pacing.

Methods:

Echocardiography

As described earlier, once mice were anaesthetised and positioned on the heating pad with limbs immobilised and hair removed I proceeded to baseline echocardiography (Dr Gutstein also assisted and supervised). Measurements were obtained both online and offline for a blinded analysis. Review of the images from pacing induced mechanical capture and dyssynchrony were clearly not blinded. Parameters calculated included fractional shortening (FS), left ventricular volumes and ejection fraction (EF). Mice were imaged using a Philips HDI 5000 equipped with a 15MHz linear probe. Images were also printed and digitally captured on a flatbed scanner to allow blinded offline analysis.

Results:

Determining the effects of short-term pacing on mechanical synchrony, capture, myocardial dimensions and contractility.

Assessment of mechanical Synchrony

Mice were examined prior to and during pacing using echocardiography to determine whether short-term pacing influenced synchrony of cardiac contraction. The septal-to-posterior wall motion delay (SPWMD), an echocardiographic index of dyssynchronous contraction, increased significantly from 7.8 ±2.5ms before pacing to 27.9 ± 2.4ms during pacing ($p< 0.01$;n=6 each). Furthermore pacing significantly increased the delay in onset of systolic wall thickening measured from the septal to posterior walls (12.8 ± 1.1ms at baseline vs 31.6 ± 1.4ms during pacing, $p< 0.001$).

Evaluation of mechanical and electrical capture:

Surface electrocardiograms demonstrated substantial widening of the QRS complex during pacing (as demonstrated in figure17, chapter 2), suggesting aberrant intraventricular electrical conduction. Fractional shortening was marginally decreased from 44.2 ± 2.0% at baseline to 37.2 ± 2.8% during pacing ($p< 0.05$). In the previous chapter I have shown the effect of pacing on the echo parameter SPWMD (figure 16, chapter 2)

Table 9   Echocardiographic Measurements before Initiation of Pacing and During Pacing in Wildtype C57BL/6J Mice

	Pre-Pacing (n=6)	During Pacing (n=6) 1hour.
IDD, mm	3.8 ± 0.14	3.6 ± 0.08
IDS, mm	2.1 ± 0.10	2.2 ± 0.12
Fractional Shortening, %	44.2 ± 2.0	37.2 ± 2.8* (p<0.05)
AWTs, mm	1.1 ± 0.14	0.85 ± 0.08
AWTd, mm	0.53 ± 0.09	0.47 ± 0.05
PWTs, mm	1.4 ± 0.14	1.2 ± 0.10
PWTd, mm	1.0 ± 0.11	0.85 ± 0.13

Data is presented as group means ± SEM. Comparisons between groups were performed with unpaired T-tests. *, $p < 0.05$. IDD, IDS, intraventricular dimensions at end-diastole, end-systole; AWTs, AWTd, anterior wall thicknesses at end-systole, end-diastole; PWTs, PWTd, posterior wall thicknesses at end-systole, end-diastole. With permission from Kontogeorgis et al (179).

Evaluation of Ventricular Function

Pacing resulted in slight reduction of ventricular function though fractional shortening was not significantly altered after cessation of pacing. Left ventricular dimensions and thickness were not significantly changed in paced mice compared to matched sham-paced controls or compared to baseline values (Table 9). Short-term pacing was therefore associated with dyssynchrony during pacing and a slight decrement in ventricular function that normalized immediately after cessation of pacing in wild type mice (Table 10).

Table 10 Echocardiographic Measurements in C57BL/6J Wildtype Mice after Cessation of Short-Term (6hour) Pacing

	Sham-Paced, 6 hr (n=6)	Paced, 6 hr (n=6)
IDD, mm	3.1 ± 0.13 (0.3 ± 0.1)	3.2 ± 0.18 (0.1 ± 0.2)
IDS, mm	1.8 ± 0.12 (0.2 ± 0.1)	1.9 ± 0.12 (0.1 ± 0.2)
Fractional Shortening, %	43.8 ± 1.7 (-2.3 ± 1.7)	40.6 ± 2.4 (-1.1 ± 1.2)
AWTs, mm	1.2 ± 0.09 (-0.13 ± 0.13)	1.2 ± 0.12 (0.03 ± 0.08)
AWTd, mm	0.8 ± 0.07 (-0.07 ± 0.1)	0.8 ± 0.1 (0.07 ± 0.1)
PWTs, mm	1.6 ± 0.03 (-0.43 ± 0.08)	1.4 ± 0.16 (-0.43 ± 0.29)
PWTd, mm	1.0 ± 0.05 (-0.75 ± 0.12)	1.0 ± 0.13 (-0.42 ± 0.18)

Post-pacing data (and changes from pre-pacing baseline) are presented as group means ± SEM. Comparisons between groups were performed with unpaired T-tests. IDD, IDS, intraventricular dimensions at end-diastole, end-systole; AWTs, AWTd, anterior wall thicknesses at end-systole, end-diastole; PWTs, PWTd, posterior wall thicknesses at end-systole, end-diastole. With permission from Kontogeorgis et al (179).

Table 11 Post-Pacing Echocardiographic Measurements in WT and Cx43$^{+/-}$ Mice

	WT sham paced (n=6)	WT paced (n=6)	Cx43$^{+/-}$ sham paced (n=7)	Cx43$^{+/-}$ paced (n=9)
IDD, mm	3.4 ± 0.10 (-0.05 ± 0.10)	3.2 ± 0.19 (-0.12 ± 0.21)	3.3 ± 0.12 (-0.16 ± 0.21)	3.5 ± 0.15 (0.28 ± 0.14)
IDS, mm	1.9 ± 0.09 (0.08 ± 0.06)	1.8 ± 0.14 (0.05 ± 0.18)	1.8 ± 0.11 (-0.04 ± 0.18)	2.2 ± 0.21 (0.41 ± 0.13)
Fractional Shortening, %	43.9 ± 1.4 (-3.2 ± 1.7)	43.6 ± 1.2 (-2.8 ± 3.3)	45.8 ± 1.7 (-1.5 ± 2.7)	38.4 ± 3.5 (-7.0 ± 2.9)
AWTs, mm	1.0 ± 0.02 (-0.02 ± 0.07)	0.98 ± 0.06 (-0.20 ± 0.12)	1.1 ± 0.08 (-0.03 ± 0.08)	1.1 ± 0.08 (-0.02 ± 0.11)
AWTd, mm	0.81 ± 0.08 (-0.07 ± 0.08)	0.80 ± 0.08 (0.0 ± 0.12)	0.79 ± 0.06 (-0.03 ± 0.05)	0.88 ± 0.06 (-0.01 ± 0.08)
PWTs, mm	1.3 ± 0.09 (-0.23 ± 0.13)	1.6 ± 0.10 (0.03 ± 0.08)	1.4 ± 0.10 (-0.14 ± 0.15)	1.4 ± 0.08 (-0.17 ± 0.10)
PWTd, mm	0.83 ± 0.09 (-0.25 ± 0.17)	1.2 ± 0.14 (0.23 ± 0.18)	0.97 ± 0.08 (-0.19 ± 0.12)	1.1 ± 0.08 (-0.14 ± 0.12)
SPWMD, ms	6.2 ± 0.74 (1.7 ± 1.2)	4.3 ± 0.70 (-0.67 ± 1.1)	7.2 ± 1.5 (-3.0 ± 1.3)	17.7 ± 2.3** (8.6 ± 1.9)**

[138]

Table 11 Post-pacing data (and changes from pre-pacing baseline) are presented as group means ± SEM. Comparisons between groups were performed with ANOVA. **, $p < 0.01$ compared to all other groups. IDD, IDS, intraventricular dimensions at end-diastole, end-systole; AWTs, AWTd, anterior wall thicknesses at end-systole, end-diastole; PWTs, PWTd, posterior wall thicknesses at end-systole, end-diastole; SPWMD, septal-to-posterior wall motion delay. With permission from Kontogeorgis et al (161).

Echocardiographic assessment at baseline, post pacing in WT and Cx43$^{+/-}$ mice:

Cx43$^{+/-}$ mice imaged after cessation of 6hr pacing or sham-pacing had no significant differences (Table 11). Baseline echo characteristics including ventricular dimensions, fractional shortening, or wall thickness were not significantly different in the WT group (Table 9) and after cessation of 6hr pacing (Table 10). However, there was evidence of significant mechanical dyssynchrony after 6hour pacing in Cx43$^{+/-}$ mice compared to sham-paced Cx43$^{+/-}$, WT paced and WT sham-paced mice (SPWMD =17.7 ± 2.3 p<0.01) (Table 11).

2hour recovery period

The mechanical dyssynchrony was significantly sustained despite a recovery period of 2 hours (SPWMD =17.7 ± 2.3 p<0.01).

Discussion:

The echo data in this chapter underscore the absence of any overt disease process in these animals such as would be seen if there was impaired left ventricular function or altered wall thickness or volume dimensions. However, there is evidence here that pacing alters the activation pattern of the myocardium consistent with altered stress-strain during pacing with altered temporal relation between the interventricular septum and the posterior wall (SPWMD). In the canine model of LBBB induced dyssynchrony this had been suggested by an alternative imaging modality as in the case of MRI (26;167-170).

A limitation to consider here is that the echocardiography did not utilise colour flow doppler to assess any possible underlying functional mitral regurgitation which may have occurred as a consequence of the distorted activation sequence a well recognised (at least in clinical studies) possible complication. Furthermore no attempts were made to measure nor calculate any velocity time integrals using pulsed doppler as surrogates of cardiac output or index given the scale of the animal. Nonetheless, the data supports the conclusion that there is no significant impairment in cardiac function with pacing.

However, what is novel is the evidence of mechanical dyssynchrony at the end of the pacing procedure immediately after the stimulator was switched off. The measured SPWMD remained prolonged at 17.7ms immediately after cessation of pacing in all Cx43$^{+/-}$ animals that had been subjected to 6 hours of pacing. It seems reasonable to surmise that these experiments reflect some change in myocardial contractility due to a spatial and temporal heterogeneity within the affected area as measured on echo. Furthermore, this mechanical dyssynchrony was a sustained measurable after a 2 hour rest period possibly suggesting a

more permanent effect had taken place rather than a transient metabolic or ion overload effect.

Based on the ECG and ECHO findings, it is possible that some degree of electrical heterogeneity might account for these differences. The data support the likelihood of a change in repolarisation properties as observed by the ECG QRS duration which prolongs with pacing in the $Cx43^{+/-}$ group. However, without a further reductionist experiment to explore regional heterogeneity in Ca2+ or K+ ions it would be difficult to understand the mechanism behind such sustained mechanical effect. Furthermore, a detailed look at anatomical/structural effects was warranted to understand the mechanism of this observation.

In a subsequent chapter (chapter 6) I undertake a more in depth analysis of what was taking place at a structural level as well as a functional level. In the following chapter, chapter 5, I present the experiments that try to assess whether there are any associated changes in tissue refractoriness and increased arrhythmia inducibility utilising subdiaphragmatic programmed electrical stimulation.

Chapter 5

Programmed Electrical Stimulation and arrhythmia testing in the subdiaphragmatic dyssynchrony model.

Introduction:

In Chapter 5, I present the set of experiments performed to assess arrhythmia inducibility using programmed electrical stimulation and VERP after 1hour sham-pacing and pacing as well as when combined with 4-AP in Cx43$^{+/+}$ mice. Furthermore, I present the PES and VERP after 6hr sham-pacing, 6hr pacing in Cx43$^{+/+}$ and Cx43$^{+/-}$ mice. Finally, I evaluate PES and VERP in Cx43$^{+/-}$ mice after a 2hr recovery period following 6hr sham-pacing and 6hr pacing in Cx43$^{+/-}$ mice.

Principles of Programmed Electrical Stimulation(PES)

This technique is widely adopted in the clinical setting. Historically it was first performed by Wellens and Coumel in the late 1960s. Initially protocols were designed to induce and terminate supraventricular tachyarrhythmia (SVT) and aid diagnosis of the mechanism of these arrhythmias in individual patients to target ablation strategies. Their role expanded in subsequent years, the 1970s to induce ventricular tachyarrhythmia (VT) which correlated with clinical VT that post infarction or heart failure patients were experiencing(171). These studies furthered our understanding of the re-entrant nature of a large proportion of VT in the post infarction setting. It soon became a risk stratification tool to identify patients at risk of VT as inducibility became a recognised prognostic indicator of increased risk of sudden cardiac death (SCD) in post infarction patients. This became standard practise in recruiting patients for trials, testing efficacy of defibrillators and as a requirement in patient selection in published UK NICE guidelines.

The disadvantage of this approach in clinical practice is that the technique is a poor risk stratification tool given its sensitivity and specificity(171). This likely reflects differences in the mechanism of sudden cardiac death which may be due to non-reentrant mechanisms and

bradycardia and temporal changes in those at risk of sudden cardiac death which cannot be predicted due to underlying disease process such as progression of coronary disease or heart failure .

Nonetheless it has widespread use still in the clinical setting and in studying arrhythmia models in animal research. It allows a measure of the absolute refractory period which correlates with the refractory period of the action potential in the ventricle, called ventricular effective refractory period (VERP). The protocol originally designed by Wellens involves a pacing protocol of a train of beats at fixed cycle length (S1 drive train) followed by a first extrastimulus (S2) the coupling interval of which is progressively reduced until it falls on the refractory period of the last S1 beat. A second (S3) and occasionally a third extrastimulus (S4) has also been used and define progressively more aggressive protocols (151;171). Arrhythmia inducibility is thought to be triggered on the premise that one is activating myocardial tissue that has recovered from the last extrastimulus and a critical window allows re-entry (which may be functional or anatomical) to occur as other regions of myocardium recover and this sets-up re-entry.

In animal models, and in particular murine studies such provocation testing has been found to result in the induction of NSVT in up to 30% of normal wild type mouse hearts signalling a cautious interpretation of findings(151).

Methods:

Programmed Electrical Stimulation to assess

Ventricular refractoriness and arrhythmia inducibility

These experiments were performed by me once Dr Gutstein had taught me the protocol. Programmed electrical stimulation (PES) was performed in control and paced mice at baseline and at the end of the pacing protocol. Baseline ECG recordings preceded the incision and probe placement as described earlier (in contact with diaphragmatic RV surface). Contact was verified throughout the experiment by real-time ECG monitoring to ensure 1:1 capture. The Medtronic programmable stimulator was utilised with output set at 1.0ms pulse width and twice diastolic threshold for a burst of 8 beats (S1) at either 100ms or 80ms cycle length followed by a single extrastimulus (S2) with progressive shortening of the coupling interval S1S2 (i.e. pacing at shorter cycle lengths in 10 ms decrements until loss of capture occurred) for determination of ventricular effective refractory period (VERP). The longest cycle length at which S1S2 failed to capture defined the VERP. Arrhythmia inducibility was tested by adding two extrastimuli (S2S3), with progressively shorter (10ms, 5ms or 2ms decrements approaching VERP) coupling intervals after the burst of 8 beats at 100ms and 80ms respectively. Ventricular arrhythmias lasting between 3 beats and up to 30 seconds were considered non sustained (NSVT) while those lasting >30 seconds, sustained. Two separate sites, just 1mm apart were tested for VERP and the mean of the two sites determined for each cycle length.
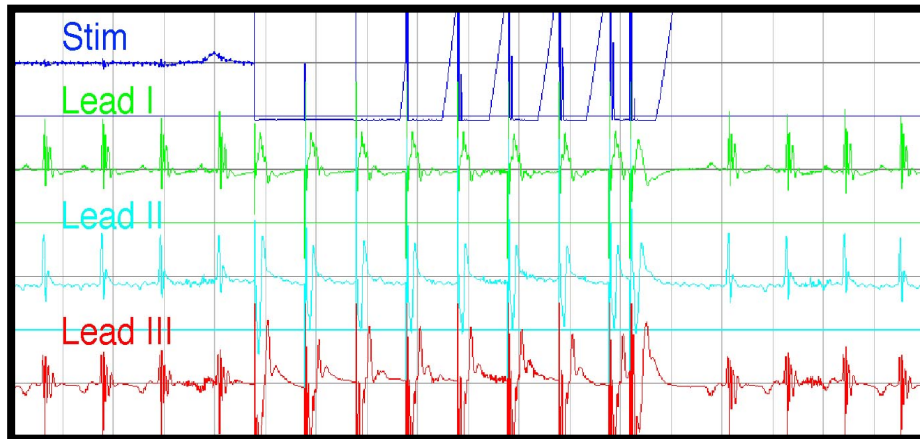
Figure 27 Programmed electrical stimulation *in vivo* demonstrating stimulus (in dark blue) and Lead I, II and III.

Pacing with a train of eight beats is followed by a single extrastimulus for the determination of ventricular effective refractory period (VERP). Double extrastimuli were added to test for inducible arrhythmias. Reproduced with permission from Gutstein et al (151).

Results

Programmed Electrical stimulation after 1hr pacing and combined with 4-AP in wildtype mice:

Following 1 hour of pacing and sham-pacing a set of 6 mice in each group were tested for arrhythmia inducibility and changes in ventricular refractory period at cycle lengths of 80ms and 100ms.No significant differences were found (see fig 28).

PES After 6 hr Pacing in WT mice

Similarly after six hour pacing there was no significant difference in refractory period and inducibility of ventricular arrhythmia (see fig 29).

At the outset of the project, experimentation using the shorter time period of 1 hour pacing and 1 hour sham pacing was used. I hypothesised that this would be of sufficient duration to modulate the degree of coupling between gap junctions and alter the conduction rendering them more prone to arrhythmia.

Given the propensity toward arrhythmia in models of disease, possible options for stressing the myocardial substrate during pacing included reducing the oxygen mixture to model hypoxia (I considered this too non-specific as it would affect other organs), perform myocardial infarction surgery (unfavoured as it would defeat the purpose of the subdiaphragmatic approach by breaching the integrity of the thorax) and use potentially proarrhythmic drugs e.g. 4-aminopyridine (4-AP), a K+ channel blocker (without a known Na+ or Ca2+ blocking effect) that is known to prolong the action potential. This could be administered via the intraperitoneal route. A set of 6 paced and 6 sham paced experiments were undertaken and followed by administration of the drug, a 15-minute waiting period and then followed by PES.

[148]

Despite the added combination of the 4-AP drug to 1 hour pacing this did not increase the propensity toward arrhythmia or alter whole heart refractoriness.
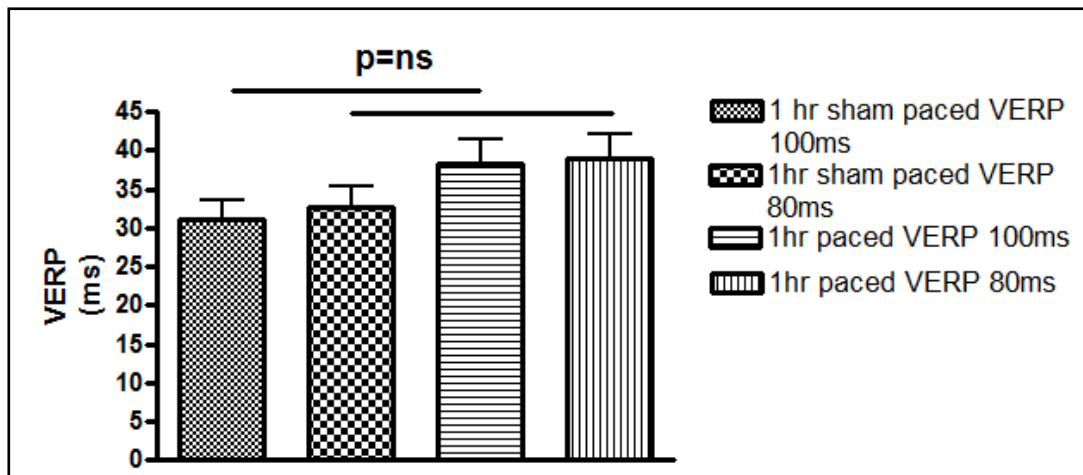
Figure 28 Programmed electrical stimulation to determine VERP after 1 hour paced and sham paced experiments.

Using an 80ms and 100ms drive train (p=ns) in WT mice.

No significant difference in VERP 80ms and 100ms after 1hr pacing.
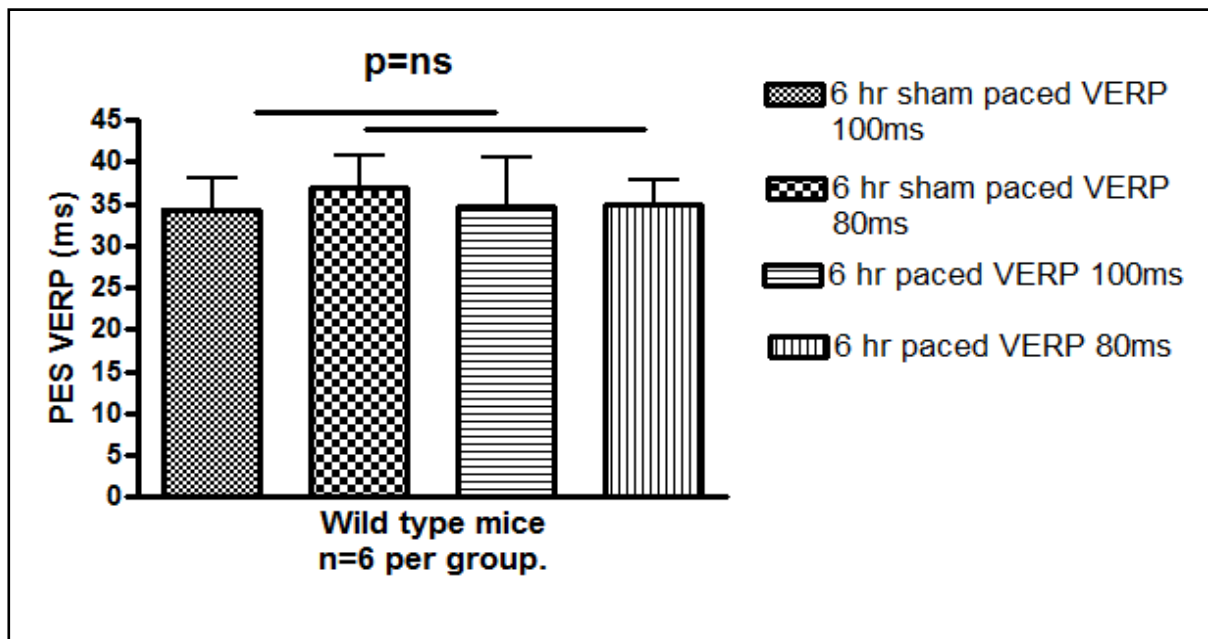
Figure 29 Programmed electrical stimulation after 6 hours of pacing to determine VERP.

Using an 80ms and 100ms paced drive train with single and double extrastimuli in WT mice.

No significant difference in VERP 80ms and 100ms after 6hr pacing.

In vivo electrophysiology after 6hour pacing

Wildtype mice

After pacing for a longer period of time i.e. 6 hours of dyssynchrony, wildtype mice did not show any significant prolongation of VERP 80 or VERP 100 and no arrhythmia propensity on inducibility testing (figure 29).

$Cx43^{+/-}$ mice

After pacing, the VERP at 100ms pacing cycle length prolonged significantly in $Cx43^{+/-}$ mice to 49.4 ± 5.1ms compared to unpaced $Cx43^{+/-}$ mice (30.3 ± 1.8ms;p<0.01), unpaced WT (36.6 ± 3.2ms) and paced WT(34.3 ± 1.9ms). Similar significant changes were observed at VERP 80ms (Table 12).

Programmed stimulation after 2hours rest in paced $Cx43^{+/-}$ mice.

The VERP remained elevated in the $Cx43^{+/-}$ mice despite a 2hour rest period after cessation of 6hr pacing. VERP 100= 50 ± 9ms and VERP80= 51.3 ± 7.4ms n=3.

Arrhythmia inducibility:

There were no differences between groups and although sustained arrhythmias could be induced with either single or double extra-stimuli they were in equal measure between the groups.

Table 12. Programmed Electrical Stimulation Measurements (post) in Wildtype and Cx43 Heterozygous KO Mice

	WT post-sham pacing (n=6)	WT post-pacing (n=6)	Cx43$^{+/-}$ post-sham pacing (n=6)	Cx43$^{+/-}$ post-pacing (n=6)
VERP100, mm	34.3 ± 3.6	34.7 ± 2.8	30.3 ± 1.8	49.4 ± 5.1*
VERP 80, mm	37 ± 3.7	34.8 ± 2.9	29.7 ± 1	49.8 ± 5.4*

Data is presented as group means ± SEM. Comparisons between groups were performed with ANOVA. *, $p < 0.05$ compared with WT post-sham pacing and $p < 0.01$ compared to WT post-pacing and Cx43$^{+/-}$ post-sham pacing. VERP (Ventricular effective refractory period). With permission from Kontogeorgis et al (161).

Discussion:

In this chapter I present the data from programmed electrical stimulation protocol performed via the subdiaphragmatic approach as originally described by Gutstein et al (151). The technique is a useful tool in testing for arrhythmia inducibility and testing for changes in action potential duration that might alter the refractoriness of the myocardium.

I found that after 1 hour of pacing and sham pacing there was no difference in the VERP and arrhythmia inducibility. The administration of intraperitoneal 4-AP did not increase the arrhythmia inducibility in wild type mice. This suggested that perhaps even if gap junction changes were taking place I was not observing a propensity to arrhythmia or sudden death. This would be consistent with the observations in the literature that suggest approximately > 90% loss of gap junctions is necessary to result in vulnerable arrhythmia in a mouse model(6). However, it has also been proposed that only smaller reductions in gap junctions, approx. 50% are required when accompanied by additional stressors eg structural changes. These affect the action potential, as is often the case in clinical disease models and together with the slightly reduced gap junctions may lower the threshold toward arrhythmia. Nonetheless, the addition of 4-AP did not unmask such a finding. I decided against an infarction in my model as it would defeat the purpose of a relatively non-invasive approach whilst global hypoxia with its systemic effects I considered too non-specific.

A longer duration of pacing for 6 hours in wildtype mice was therefore attempted in an effort to explore whether longer pacing periods might have more progressive and pronounced functional effects as measured by refractoriness and PES. Once again, in wildtype mice, perhaps due to the abundance of connexin protein at the outset, pacing induced

[153]

dyssynchronous activation appeared to be well tolerated and absorbed by the myocardium such that no apparent difference in VERP 80 or VERP 100, or arrhythmia propensity was noted.

The $Cx43^{+/-}$ mice were of particular interest as their baseline levels of Cx43 are reduced by 66% and they seem to respond differently to the effects of 6hr pacing.

It was soon apparent that there was clear prolongation in the VERP after six hours of pacing experiments. Yet, these mice were not prone to arrhythmias. These changes were sustained even after a rest period of 2 hours suggesting that adaptive structural or electrical remodelling of some kind had occurred.

Likely ion channel targets that might account for these changes included the primary drivers of murine repolarisation, K+ channels as well as possible changes in Ca2+. Together with the mechanical dyssynchrony presented in the earlier chapter, I initiated a set of experiments with Dr Morley and Dr Xiadong Li, to investigate further with optical mapping and patch clamp.

In Chapter 6, I present the structural correlates of tissue studies undertaken at 1hr pacing and 6hr pacing in wildtype mice after pacing as well as regional studies and further explore mechanisms for the observed differences in mechanical dyssynchrony and sustained VERP prolongation in $Cx43^{+/-}$ mice.

Chapter 6

Electroanatomical correlation in Wildtype Cx43$^{+/+}$, Cx43$^{+/-}$ mice and Cx40$^{-/-}$ mice

Overview:

Introduction

In the preceding chapter I have demonstrated that at least in WT $Cx43^{+/+}$ there is no overt inducibility into arrhythmia and no change in VERP. However, despite the lack of changes of ECG parameters, ECHO or inducibility testing I still needed to test whether at least some form of subtle remodelling may be occurring at a structural level. In chapter 6, I will show that this is indeed the case based on the immunostaining, immunoblotting and cell fractionation data in wildtype mice. In WT mice in particular it appears that there are changes at the endocardium of the LV free wall and to study this further regional immunoblotting, qRT-PCR and fractionation experiments were performed.

Separate to these experiments, I present a deeper look at the changes taking place in the $Cx43^{+/-}$ mice; suggesting that some form of remodelling is occurring and correlate this with the aid of data from experiments performed with Dr Li. My main intention in this chapter is to test the effects of pacing induced dyssynchrony on gap junctions at a structural level and correlate these with electrophysiology functional data at a cellular level.

The murine pacing model represents single lead ventricular pacing with the electrode placed in contact with the epicardial surface of the right ventricle. Furthermore, it is a model of fixed pulse-width (effectively rheobase) and twice the minimum threshold for the stimulus needed to capture the heart (chronaxie). It therefore represents a model of low current output with dyssynchronous activation rather than a current-injury model(17). The duration of pacing over the mentioned time course avoids temporal changes in threshold and I addressed any loss of capture immediately due to constant ECG monitoring in paced experiments. Pacing at cycle length only just above sinus rhythm also ensures that this is not a model of tachycardia-

induced changes (172-175). Since this is an *in vivo,* whole animal model, an additional advantage is that this does not denervate the heart but allows physiological effects of other systems such as the endocrine, higher autonomic and renin angiotensin system. Thus non-cardiac systems are integrated when making comparisons between controls, sham paced and paced experiments and the data for connexin interactions reflects these interactions.

I hypothesised that dyssynchronous activation may alter coupling properties between cells with electrotonic flow occurring through an unconventional direction e.g. epicardial to endocardial (and RV to LV) activation as opposed to the usual endocardial to epicardial activation. The orientation of cells in the myocardium, the transmural heterogeneity of gap junctions and the spatial heterogeneity of ion channels alter the coupling properties of the myocardium during normal activation. I hypothesise that pacing induced dyssynchrony likely alters and increases the spatial heterogeneity and alters coupling. Further, that gap junctions would adapt to this by altering their pattern of distribution or the absolute levels of connexins expressed through a disruption in trafficking.

My objective is to see whether any meaningful conclusions can be drawn from the relationship between structure i.e. hemichannels and fully formed gap junctions i.e. whether there are structural signs to suggest increased lateralisation of connexin immunosignal and attempt to correlate these with functional changes.

I test these using molecular tools such as immunostaining and apply a model of immunohistochemistry quantification which I developed. Data analysis was performed by Mr Ponzio and me. Also, immunoblotting for transcriptional levels of Cx43 expressed, were a joint effort with assistance from Dr Gutstein, Mr Ponzio, Ms Gupta and Dr Kang. I also assisted Mr Feig to perform a set of experiments and gather data to quantify transcriptional

effects using qRT- PCR. I will also test the effects of phosphorylation state with pacing and assess the relationship of Cx43 with its binding partners.

Methods:

Collection and Storage of murine myocardium:

Exposure of the heart was undertaken at the end of all experiments by midline thoracotomy followed by mobilising mediastinal structures and euthanasia of animals by aortic root transection at the base of the heart. Surrounding tissue was trimmed and the heart washed in PBS. Those destined for immunolabelling were flash frozen whole in liquid nitrogen and stored on site in Revco freezers at -80^0C.

Haematoxylin-phloxine-saffron (HPS) staining

These were kindly stained and photographed by myself (a set of H&E slides also) with help from Ms F Liu. Hearts from a subset of six animals were removed and fixed in 10% formalin and embedded in paraffin for histological evaluation after staining with HPS.

Tissue Handling and Immunolabelling

The following were performed by me having received training from Ms Fanny Liu and Dr Gutstein. At the end of each pacing experiment, hearts were rapidly excised and placed in a container with dry ice and frozen in Tissue Tek OCT compound (Sakura Finetek USA, Inc. Torrance, CA). The OCT mounted hearts were stored and retrieved when needed. 5μm thick sections were cut in an HM 560 cryostat (Microm, Walldorf, Germany) at -20^oC, placed onto microscopy slides (Superfrost/Plus, Fisher Scientific, Pittsburgh, PA) and fixed in acetone. Sections were blocked with bovine serum albumin (BSA) and then double-stained with a custom-made rabbit polyclonal anti-Cx43 antibody at 1:1000 and wheat germ agglutinin (WGA) to visualise myocytes borders. A FITC-conjugated anti-Cx43 antibody was used to visualise Cx43.

For cadherin staining, frozen sections were incubated with rabbit anti-pan-cadherin antibody 1:5000 (Sigma), followed by a Texas Red-conjugated goat anti-rabbit secondary antibody

(Jackson ImmunoResearch Laboratories) and a FITC-conjugated anti-Cx43 antibody for colocalisation studies of these 2 proteins.

Fluorescence microscopy visualised immunostained sections on an Axioskop 2 Plus microscope and I collected images using uniform exposure settings for each staining run on an Axiocam camera with AxioVision 4.30 software (Carl Zeiss, Munchen-Hallbergmoos, Germany).

Quantification of Cx43 and Cadherin Immunosignal

Images of immunostained sections were acquired by me using a set of blinded immunostained slides. The images were digitally archived for offline analysis. Blinded image files were uniformly threshold by eliminating signal free areas above and below the distribution of intensity values using the histogram function on Adobe Photoshop. Digital image processing was then performed according to previously established techniques again in a blinded fashion, with NIH Image J to determine Cx43 and cadherin signal area as a percentage of total tissue area, as well as Cx43 plaque size and the number of Cx43 plaques per 40 x fields.

Statistical analysis of Cx43 and Cadherin Immunosignal

Quantitative immunofluorescence data were compared between groups with ANOVA using StatView (SAS Institute, Inc, Cary, NC) and data were expressed as mean ± SEM. These experiments were performed by me except for the RV analysis which was done by Marc Ponzio.
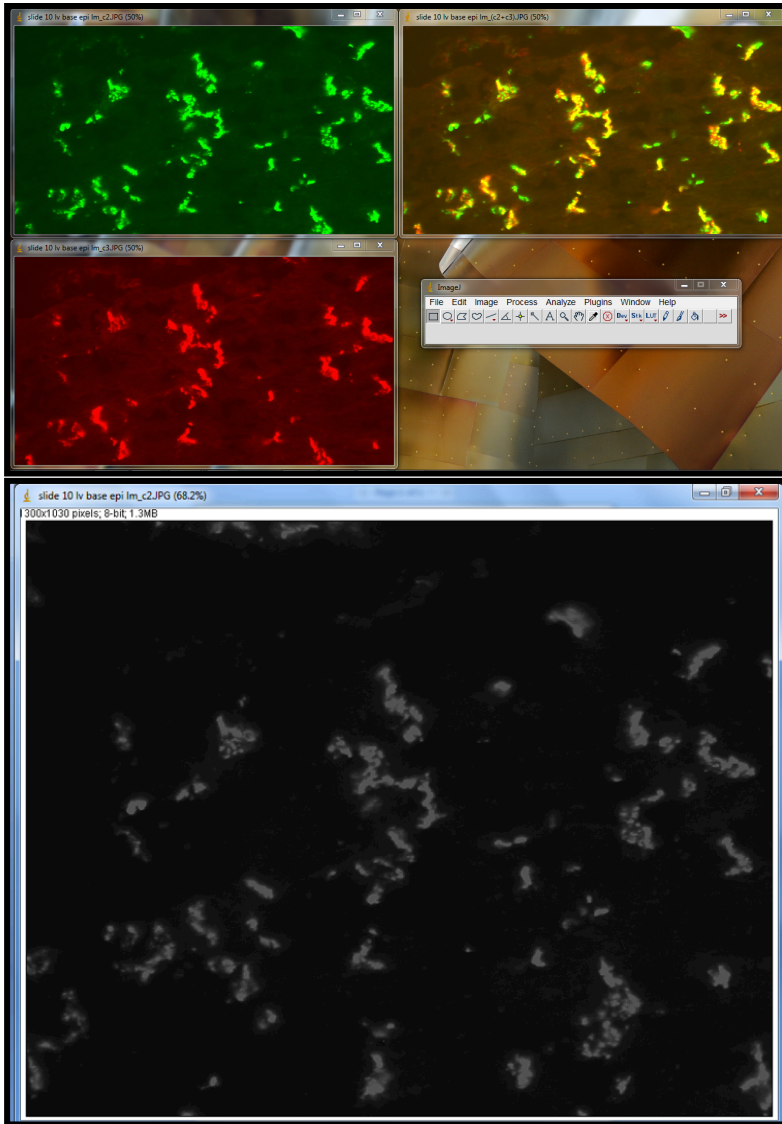
Figure 30. 40x magnification field acquired from the base of the left ventricle.

Images are focused on the epicardial layer of myocardial cells co-stained for Cx43 (in green) and Cadherin (in red) with merged image (in yellow).

Using NIH Image J software, images were converted into 8bit format. Using the *image* menu in Image J, and then *adjust* option, images were threshold to reflect signal area. Raw data were then measured by selecting the *analyze* menu, *measure and analyse particles* tool and exported into Excel for comparison.
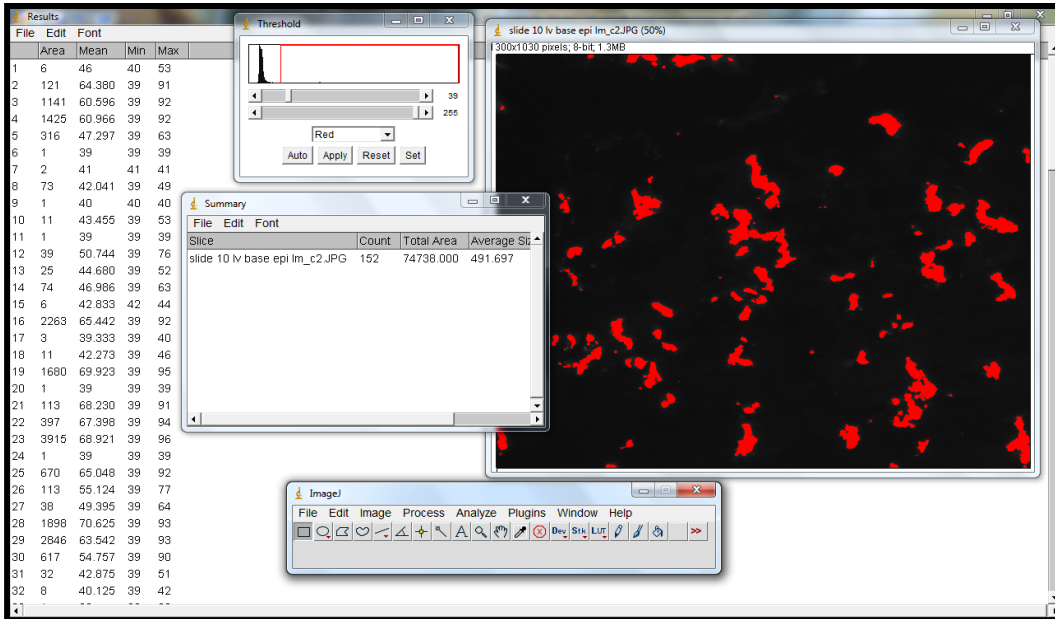
Figure 31-Desktop view of Image J generated raw data measuring Cx43 total signal area, number per field and size of gap junction plaques.

Figure represents blinded slide 10 with auto-threshold applied to remove signal-free areas from the analysis. Data for cadherin were captured in a similar fashion.

Immunoblotting and Densitometry-WT Mice

The following experiments were performed by me with assistance from Marc Ponzio and Dr Gutstein.

Endocardial ventricular tissue from paced and sham-paced hearts was prepared by Dounce homogenisation in lysis buffer supplemented with Complete® protease inhibitor cocktail (Roche, Mannheim, Germany) to assess total protein levels. The endocardial samples were prepared by mounting the excised LV free wall in an OCT block, separating the endocardial, mid-myocardial and epicardial regions by sectioning on an HM 560 cryostat and homogenising. The inner third of the LV free wall was considered the endocardial region, middle third mid-myocardial and outer third, epicardial. Protein concentration (determined by Bradford assay) was performed in triplicate. Equal loading was confirmed with coomassie staining and proteins were electrophoresed on 10% SDS-PAGE gels and transferred onto nitrocellulose blots (Bio-Rad laboratories, Hercules, CA). Immunoblots were blocked with milk followed by incubation with appropriate primary antibodies directed against Cx43, cadherin, Cx45 (Johnson), Cx40 (Alpha Diagnostics, San Antonio, TX) and GAPDH (Chemicon/Millipore, Billerica, MA). Horse radish peroxidise (HRP)-conjugated secondary antibody Santa Cruz Biotechnology, Santa Cruz, CA) was then applied, followed by HyGlo chemiluminescent processing (Denville Scientific, Metuchen, NJ) and autoradiography. At least two separate experiments were quantified by scanning the autoradiograph on a Bio-Rad Gel Doc GS 800 and calculating band intensity using Quantity One Software (Bio Rad, Hercules, CA). Connexin band intensities were normalised to the relative intensity of the corresponding GAPDH band for each sample. Results were expressed as a percentage of matched controls.

Immunoblot Analysis in Cx43$^{+/-}$ murine experiments

A custom manufactured rabbit polyclonal antibody directed against an epitope on the carboxy-terminus of Cx43 was used on ventricular lysates and a monoclonal antibody directed against GAPDH (Chemicon/Millipore, Billerica, MA). HRP-conjugated secondary antibody was then applied to the immunoblots, followed by HyGlo chemiluminescent processing. Cx43 band intensities from 3 separate experiments were quantified by densitometry and normalised to the relative intensity of the corresponding GAPDH band for each sample.

Fraction Preparation and Immunoprecipitation

These experiments were performed by Dr Gutstein and Marc Ponzio with assistance from me.

Heart samples were Dounce homogenised centrifuged at 500g for 10 minutes removing the insolubles. Lysates were then layered over a 45% sucrose cushion. After centrifuging at 7000g for 20 minutes the supernatant (considered the non-sarcolemmal fraction) was separated from the cloudy layer immediately overlying the sucrose (sarcolemmal fraction). Protein concentrations in each fraction (determined by Bradford Assay) were performed in triplicate and equal loading was confirmed with coomassie staining. The resulting fractions were analyzed by SDS-PAGE and Western blotting.

The immunoprecipitation experiments were kindly performed by Pritha Gupta. 50μg of total heart lysate was incubated with polyclonal anti-Cx43 antibody. After addition of protein A agarose-immobilised protein beads (Roche) to the samples, the protein A suspension was centrifuged at 5000xg and the supernatant removed. The protein A beads were washed in IP buffer and resuspended in loading buffer prior to incubation at 100°C and analysis by SDS-

PAGE. Resulting blots were incubated with a monoclonal antibody directed against ubiquitin (FK2, Biomol).

RNA isolation and Quantitative Real-Time PCR (qRT-PCR)

These experiments required the isolation of RNA from the LV free walls of paced and sham-paced hearts excised and mounted in OCT and snap frozen in liquid nitrogen. Endocardial and epicardial thirds were collected by sectioning (performed by me) through the LV free wall as described earlier and then isolating RNA in an RNA free space using Trizol (Invitrogen, Carlsbad, CA) according to the manufacturer's protocol (the isolations were carried out by me).

I assisted Jonathan Feig through the remaining experiment-he kindly created the primer sequences; I aided in the assessment of RNA quality, estimation of RNA concentration and assisted with quantitative PCR to generate the data for the graphs which were created by Jonathan and Dr Gutstein.

RNA quality was verified with an Agilent 2100 Bioanalyzer (Agilent Technologies, Santa Clara, CA). Ribogreen RNA Quantitation Kit (Molecular Probes/ Invitrogen, Carlsbad, CA) allowed assessment of RNA concentration. ABI Prism 7700 Sequence Detection System (Applied Biosystems, Foster City, CA) performed real time quantitative PCR using primer sequences as outlined in Kontogeorgis et al. Data were normalised to Cyclophilin A (primer sequences as outlined in Trogan et al 2002) and expressed as fold change compared to the sham-paced controls. Negative controls were performed for each of the samples, in which reverse transcriptase was not added prior to RNA quantification. Results per animal represent the mean of six measurements of each endocardial and epicardial sample.

Cardiac Myocyte Isolation

Once I had completed pacing mice for 6hours, harvested whole hearts were prepared for cell isolation protocols and this was primarily performed by Marc Ponzio and Dr Gutstein for further experimentation by Dr Xiaodong Li. I assisted Marc and learnt how to generate the solutions for myocyte isolation and aided with hanging the heart on the Langendorff as well as mechanically dissociating hearts after digestion as well as adding solutions to generate healthy cells under microscopy.

Ventricular myocytes were isolated from $Cx43^{+/-}$ and WT littermate hearts immediately following pacing or "sham-pacing" using an enzymatic technique. Mice were first anti-coagulated with 1000U/kg heparin administered intraperitoneally 20min prior to removal of the heart whilst still under general anaesthesia. Under isoflurane anaesthesia hearts were rapidly removed and perfused in a constant-pressure Langendorff system with Minimum Essential Medium Eagle (Joklik modification; Sigma), 0.44mM EGTA, 34.5mM $NaHCO3$, 1mM $MgSO4$ and 10mM 2, 3 Butanedione Monoxime at $37\,^{\circ}C$ for 5 min. Hearts were then perfused with the same solution containing 0.05% (wt/vol) collagenase (Worthington Type 2), 0.1% bovine serum albumin, 12.5μM $CaCl2$, but without EGTA, $37\,^{\circ}C$ for 15min.

The heart was removed from the Langendorff system and dispersed mechanically. The dissociated heart tissue was then incubated in medium containing 10% foetal bovine serum (Atlanta Biologicals, Lawrenceville, GA, USA) and 12.5 μM $CaCl2$ for 10min at room temperature followed by additional 10min incubation in medium containing 5% foetal bovine serum and 12.5 μM $CaCl2$.

Isolated myocytes were then incubated for 30 min at room temperature in Kraftbrűhe (KB) solution, which contained (in mM): 20 taurine, 50 glutamine, 10 glucose, 10 HEPES, 0.5 EGTA, 3 MgSO4, 30 KH2PO4, 30 KCL, 85 KOH, (pH 7.2 adjusted with KOH).KB solution was gradually replaced with modified Tyrode's solution (in mM: 140 NaCl, 4 KCL, 10 HEPES, 1.1 MgCl2, 1.8 CaCL2 and 10 glucose, pH 7.4 adjusted with NaOH). For action potential measurements, ventricular myocytes were isolated from both ventricles. For potassium currents, cells were isolated exclusively from the right ventricle. Cells were used for patch-clamp experiments within 6 hours of isolation by Dr X Li.

Patch clamp

Cellular Electrophysiology

Isolated myocytes were placed in a bath (~500 µl volume) on the stage of an inverted microscope (Nikon Diaphot, Tokyo, Japan) and whole-cell patch clamp recordings (15) were obtained at RT. Experiments were performed using an EPC 9/2 amplifier and Pulse 8.79 software (HEKA Elektrotonik, Lambrecht,Germany). For recording action potential (AP), modified Tyrode's solution was used as the bath solution (components as above). Recording pipettes were fabricated from borosilicate capillary glass (Warner Instruments, Novato, CA, USA) using a Sutter Model P-97 micropipette puller (Novato, CA, USA) and polished using a MF-830 Micro Forge (Narishige, Japan) to resistances of 2-5 M when filled with pipette solution. The pipette solution for recording APs consisted of (in mM): 135 KCl, 4 MgCl2, 5 EGTA, 10 glucose, 10 Hepes, 5 Na2-ATP, 3 Na2-creatine phosphate, pH 7.2 with LiOH. For recording potassium currents, the bath solution contained (in mM): 135 choline chloride, 5.4 KCl, 1.1 MgCl2, 1.8 CaCl2, 0.001 ryanodine, 0.01 atropine sulfate, 0.5 CdCl2, 10 glucose and 10 Hepes; pH 7.4 (with NaOH); pipette solution contained (in mM): 115 potassium aspartate, 5.0 KCl, 7 MgCl2, 5 EGTA, 10 HEPES, 4 Na2-ATP, pH 7.2 (with KOH). After

establishing the whole-cell configuration, membrane capacitances (Cm) were determined by integrating capacitance transients recorded during a brief 5 mV step from a holding potential (HP) of −70 mV. The cell capacitance was calculated as the ratio of the integral of the capacitance transient divided by the voltage step. Series resistance (Rs) was estimated from the decay of the capacitative transients. In each cell, Rs was compensated electronically by 80- 90%. Tip potentials were zeroed before membrane-pipette seals were formed. The liquid junction potential was calculated to be -18 mV (Axoscope, Axon Instruments). Membrane potentials were not corrected for the liquid junction potential. Only data obtained from cells with seal resistances > 1 G were analyzed. Action potential and potassium current recordings were performed in the whole-cell configuration. Action potentials were recorded at RT in the current clamp mode by stimulating with a 3 ms pulse at a frequency of 1 Hz.

Peak outward potassium current (IKpeak) was recorded using 1 sec depolarizing voltage steps at 10 mV increments between -50 and +50 mV from a HP of -60 mV at 0.01 Hz. The interval between voltage steps was set at 10 sec to allow complete recovery of outward potassium current. Steady state inactivation of the outward potassium current was examined with a standard 2-pulse protocol consisting of 1 sec prepulses from -80 to +5 mV in 5 mV increments from a HP of -60 mV followed by a 500 ms test pulse to +40 mV. Recovery of Ito from inactivation was measured by using two depolarizing pulses to +40 mV from a HP of -60 mV separated by sequentially increasing intervals of 5 to 185 ms in 10 ms increments (26). Outward potassium current was recorded before and after application of 2mM 4-Aminopyridine (AP) to separate the 4-AP insensitive current (Iss) from the 4-AP sensitive current (Ito)(176). Inward rectifier potassium current (IK1) was recorded in response to voltage steps to potentials between -20 and -140 mV from a HP of -60 mV. Currents were low-pass filtered at 2.9 kHz, digitized at 10 kHz, and stored for subsequent off-line analysis.

[168]

Electrophysiology Data Analysis

Data were analyzed using PulseFit 8.79 (HEKA). Iss was measured 100 ms from the end of each voltage step after application of 4-AP. The peak Ito was calculated as the maximal current amplitude after subtraction of the 4-AP insensitive current from IKpeak at each depolarizing voltage step. IK1 was measured 100 ms from the end of each voltage step. Potassium current densities were obtained by dividing the measured currents by the whole-cell membrane capacitance, Cm. Inactivation of Ito was fitted using the following equation to current traces after subtraction of the 4-AP insensitive current from IKpeak:

$$y(t) = a0 + a1 \exp(-t/f) + a2 \exp(-t/s),$$

Where t is time; f and s are the time constants of inactivation of Ito; a1 and a2 are the amplitudes of the inactivating current components; and a0 is the residual amplitude of the steady-state, non-inactivating component of the total outward K+ current after subtraction of the 4-AP insensitive component. Steady-state inactivation curves were obtained by using a two-pulse protocol as described above. Curve fitting after normalization of the current was performed using the Boltzmann equation, $1/[1+ \exp(V-V1/2)/k]$, where V is the prepulse potential, V1/2 is half-maximal inactivation potential, and K is slope factor for steady-state inactivation curves. The time course of recovery of Ito was described by a first-order exponential function as follows (177):

$$y = 1 - \exp{-x/},$$

Where y is the normalized current, x is time and is the time constant of recovery from Ito inactivation (recovery).

[169]

Optical mapping

I assisted with these experiments in Dr G Morley's lab. Isolated hearts were given 15minutes to equilibrate and perfused with voltage sensitive dye, di-4-ANEPPS (Molecular Probes) by injecting a 0.3ml bolus containing 125nmol/L into a 10ml compliance chamber within the perfusion line. High resolution optical mapping of voltage dependent fluorescence was performed on an upright Olympus microscope (BX50WI) with a reflected light fluorescene attachment. Images were acquired at 947frames/sec with 12-bit resolution of 40 μm (2x objective,N.A 0.14).No pharmacological e.g. blebbistatin or mechanical manipulations were used to limit motion (178). I assisted his lab staff to generate solutions for perfusing the heart as well as recording raw data and reviewing the data offline as well as generating the graphs for epicardial breakthrough.

Statistics WT Mice:

Data are expressed as mean ± SEM. Quantitative immunofluorescence data were compared between groups with ANOVA using StatView (SAS Institute, Inc., Cary, NC). Data from electrocardiography, echocardiography, programmed electrical stimulation, immunoblot densitometry and qRT-PCR were compared between groups with unpaired two-tailed t-tests (Microsoft Excel). Electrocardiographic indices, echocardiographic measurements and effective refractory period values obtained during or after the pacing protocol were compared to baseline measurements with paired two-tailed t-tests (Microsoft Excel). $P<0.05$ was considered statistically significant.

Statistics Cx43-deficient mice:

Data are expressed as mean ± SEM. Electrocardiographic indices and echocardiographic measurements obtained after the pacing protocol were compared to baseline measurements with paired two-tailed t-tests (Microsoft Excel). Electrocardiography, echocardiography, programmed electrical stimulation and cellular electrophysiology results in the paced and unpaced $Cx43^{+/-}$ mice and their wildtype littermates were compared between groups with ANOVA followed by Fisher's protected least significant difference (PLSD) post-test using StatView 5.0 (SAS Institute, Inc., Cary, NC). A post-hoc analysis was performed to compare IK1 in wildtype versus $Cx43^{+/-}$ myocytes. IK1 in unpaced versus paced subgroups was first compared using ANOVA, followed by pooling and comparison of all data from wildtype versus $Cx43^{+/-}$ myocytes at each voltage using ANOVA. $P < 0.05$ was considered statistically significant.

Results:

Determining the duration necessary to induce GJR; "Cx43 Lateralization" study:

As mentioned in chapter 3, I performed experiments at 1hr, 4hr and the 6hr time point representing approximately 1,2½ and 4 half-lives for Cx43.At each of these time points I determined whether short term pacing induced functional effects in terms of electrocardiography while 1hr and 6hr time points were measured *in vivo* for arrhythmia inducibility using programmed electrical stimulation (i.e. whether pacing resulted in a "pathological arrhythmia prone" phenotype).

Qualitative Microscopy

Immunostaining with 3 blinded observers (Dr Gutstein, Ms Liu and I) was undertaken at each time point 1hr, 4hr and 6hr and examined microscopically for evidence of gross differences in Cx43 immunosignal and distribution. Furthermore, we looked at low power at the whole heart as well as at higher power within regions of the RV, LV, Base, Apex and Epicardium, Mid and Endocardial layers for profound differences in Cx43 immunostaining signal intensity and distribution. It became evident to all that using this approach we were unable to distinguish sham-paced compared to neither paced mice at any of the three stated time points nor identify differences in a particular region.

To further test whether pacing induced dyssynchrony was having any effect at all on gap junction remodelling or lateralisation a set of blinded slides was prepared for analysis by an external examiner. The external blinded observer (Dr Kaba) was to review a set of slides to see if he were able to determine any gap junction changes between the groups utilising a subjective semi-quantitative scoring tool developed in Prof Peter's lab.

I also embarked on a set of immunostaining experiments using a semiquantitative method designed and refined by me to attempt quantifying the immunosignal of gap junctions along lines described in the Yamada/Saffitz lab.

Finally, to further assess structural changes tissue samples were prepared for ultrastructural techniques and electron microscopy.

Electron Microscopy experiment.

Pravina Patel kindly performed the staining for gap junctions and electron microscopy on tissue prepared by me in the USA and sent to the UK.I provided a paced heart after 6hr pacing to assess if any gap junction lateralisation was observed. Pravina's experiment is illustrated in the figure below (see Figure 32).The electron microscopy findings supported the notion that only very subtle remodelling was occurring with evidence of lateralisation seen on EM.
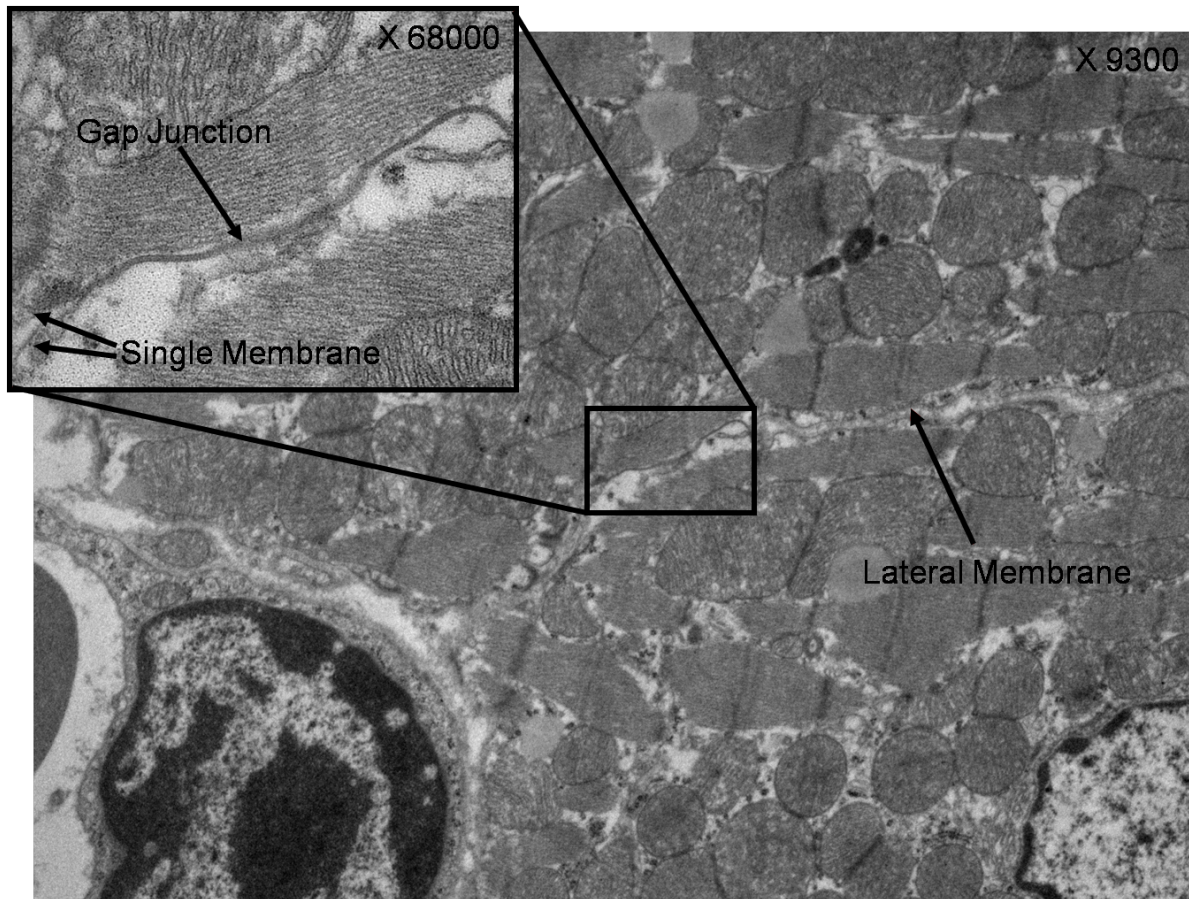
Figure 32. EM staining demonstrating subtle presence of lateralised gap junctions (x 9300 magnification and x 68 000 magnification for inset panel).

Experiment kindly performed by Pravina Patel (unpublished figure).

Lateralisation Scoring Experiment:

Samples were examined by a 4th blinded observer (Dr Kaba) to further assess the effects of short-term pacing on targeting of Cx43 protein along the cardiac myocyte membrane. He used a subjective scoring system developed by Kaba and colleagues. The degree of Cx43 immunosignal at the lateral myocyte borders in sections from paced and sham-paced hearts was compared. Paced and sham paced hearts were assigned scores ranging from 0 (no lateralization) to 3 (extensive lateralization).We found that sham sections demonstrated extensive subjective lateralization of Cx43 signal (2.75 ± 0.25) and that the extent of lateralization did not appear significantly different in the paced hearts (2.40 ± 0.40,p=ns)
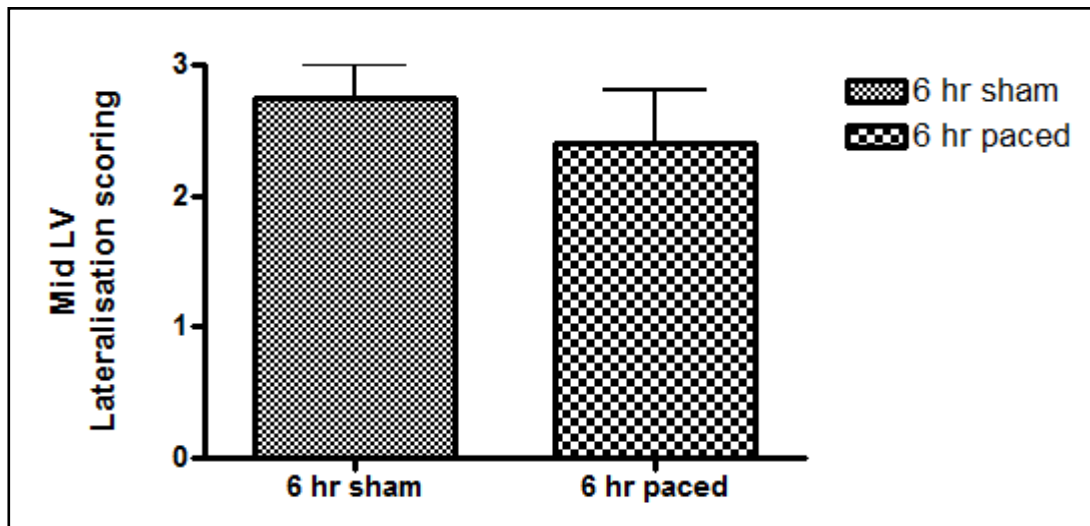
Figure 33 Semi-quantitative scoring of lateralised Cx43 immunosignal.

After 6hour sham pacing (n=4) and 6 hour pacing (n=5) there were no significant differences(p=ns) unpublished figure (179).

Semiquantitative protocol experiments.

Distribution of Cx43 Immunosignal area after 6hr pacing.

I developed a protocol for semi-quantitatively measuring the degree of fluorescence on a regional basis and applied this to blinded images taken from immunostained samples. The methodology of this approach was stated earlier in the chapter. I proceeded to examine prepared tissue for evidence of Cx43 lateralisation or differences in immunosignal on a regional basis by measuring the Cx43 signal as a ratio to tissue area and also the size and number of gap junction plaques in the groups that were paced or sham paced. This was initially commenced with pilot data at low magnification 10x tissue field but no differences were observed and I proceeded to a 40x high power regional analysis of wildtype mice at 1hr and 6hr pacing duration. No differences were observed after 1 hour pacing.

Cx43 signal area/total tissue area % after 6hr pacing

LV immunosignal

I performed all the quantification experiments for the LV. Initially I utilised a 10x wide field for the analysis but could detect no differences and so I chose a higher field of view at 40x as I considered the possibility that the differences may be more subtle and region specific e.g. Base vs. Apex; Epicardium vs. Midmyocardium vs. Endocardium; Septum vs. LV free wall.

Cx43 immunosignal was distributed heterogeneously only in gap junction plaques in the LV free wall with a gradient noted from epicardium to endocardium. Sham-paced hearts demonstrated a greater Cx43 signal area as a percentage of total tissue area in the LV free wall endocardium compared to the epicardium (9.12 ±1.2% and 6.82 ± 0.4% respectively; $p<0.05$). This transmural gradient of Cx43 has also been observed by the Yamada group. The

effect of six hours of pacing was to reduce the Cx43 immunosignal area at the LV free wall endocardium (6.76 ± 0.6%) compared to sham-paced controls(p<0.05) yet no change occurred in the epicardium (6.41 ± 0.3%). These changes in the Cx43 signal area appeared significantly reduced only at basal LV segments in paced hearts compared to sham-paced hearts (6.38% ± 0.5% in paced vs 9.36 ± 1.28% in sham-paced hearts, p<0.01).The apex and mid ventricle endocardial and epicardial regions were not significantly reduced with respect to Cx43 signal area (6.76 ± 0.89% in paced vs 7.97 ± 0.96% in sham at the apex and 7.15% ±0.69% in paced vs 9.10 ± 1.59% in sham at the mid-ventricle).

RV quantification of immunosignal

Also, no differences in Cx43 signal area were observed in right ventricular sections between paced and sham-paced mice (3.40 ± 0.25% and 3.91 ± 0.45% respectively). A specific analysis was made of the RV apex where the pacing electrode was sited with Cx43 signal area in paced (4.16 ± 0.53%) and sham-paced (3.51 ± 0.46%) hearts showing no significant difference.

Gap Junction Plaque Size and Number of Gap Junction Plaques

No significant differences were noted between the groups in terms of plaque size. There was no significant difference in the number of gap junction plaques per 40x field in sham-paced and paced endocardial and epicardial regions.

	Sham Epi	Sham Endo	Paced Epi	Paced Endo
Cx43	A.	B.	C.	D.
Cadherin	E.	F.	G.	H.
Merge	I.	J.	K.	L.

50 μm

M. Cx43 Signal Area (% of tissue area)

N. Ave. Cx43 GJ Plaque Size (μm²)

O. Cx43 GJ Plaques/ 40X Field

P. Sham RV   Cx43

Q. Paced RV   Cx43

100 μm
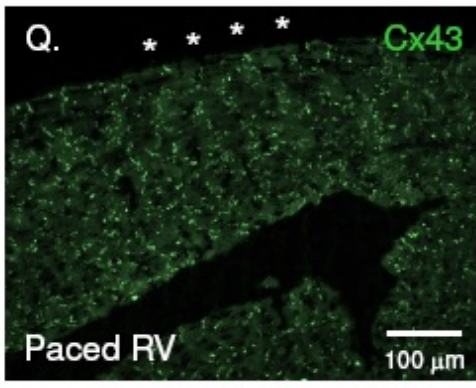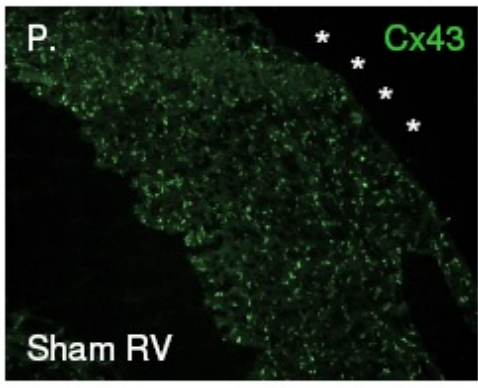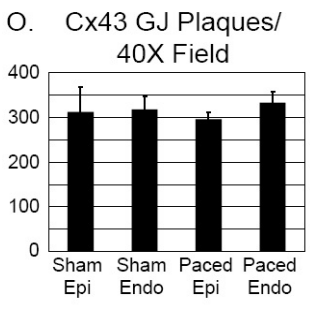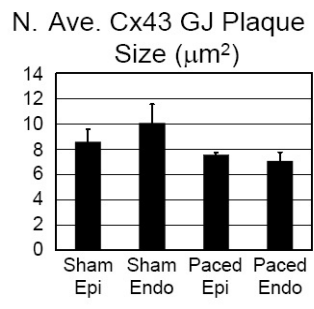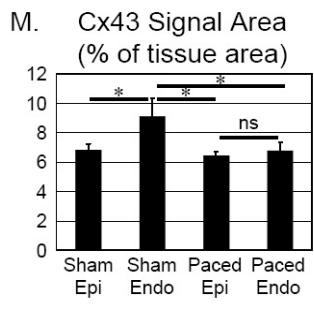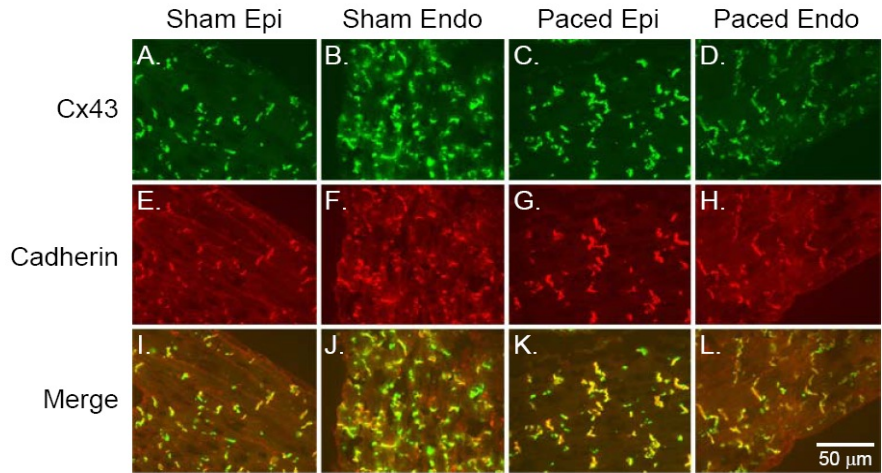
Figure 34 Immunofluorescene Images of Cx43 and Cadherin Staining in the Epicardial and Endocardial Regions of Sham-Paced and Paced Hearts.

Cx43 immuno-signal area is higher in the endocardium than the epicardium in sham-paced hearts (Panels A and B). In the paced hearts, Cx43 immuno-signal area is decreased specifically at the endocardium, thereby eliminating the gradient of endocardial to epicardial Cx43 immuno-signal area seen in the sham paced hearts (Panels C and D). Cadherin staining pattern and area is unchanged in the paced hearts (Panels E-H). Co-localization of Cx43 and cadherin immuno-signal, as demonstrated by the merged images, is statistically unchanged in the paced hearts compared to sham-paced controls (Panels I-L). Quantification of Cx43 immuno-signal area shows an increasing epicardial-to-endocardial gradient in the sham but not in the paced mice, due to decreased signal area specifically in the endocardial region of the paced mice (Panel M). Average Cx43 gap junction (GJ) plaque size appears to increase from epicardium to endocardium in sham but not paced mice, although these differences were not statistically significant (Panel N). There were no significant differences in the number of Cx43 GJ plaques per high power field in epicardial vs. endocardial segments of sham and paced mice (Panel O). Cx43 immunostaining pattern appeared similar at the RV apex of sham (Panel P) and paced hearts (Panel Q). RV epicardial surface is denoted by asterisks. Epi, epicardial region; Endo, endocardial region. Reproduced with permission from Kontogeorgis et al (179)

[179]

Impact of short-term pacing on the relationship of Cx43 to its binding partner cardiac adherens junctions(AJ)

Adherens junctions like gap junctions are concentrated at the intercalated discs of adult cardiac myocytes. Cadherin is a critical component of the adherens junction and co-localises with Cx43.There was no epicardial-to-endocardial gradient of cadherin immunosignal in control hearts and after 6 hours of pacing. This suggests that the reduction in Cx43 immunosignal occurs in the absence of changes in the distribution of the adherens junctions.

Quantifying expression of Cx43 mRNA in the LV free wall after 6hr pacing

Since Cx43 immunosignal was reduced at the LV endocardium after 6hours of pacing we determined to test the transcription levels of Cx43 mRNA. qRT-PCR of paced samples demonstrated a 2.5 ± 0.1 fold down-regulation in expression of Cx43 mRNA at the endocardial region of the paced hearts compared to controls (p=0.001;n=3 sham and 3 paced).
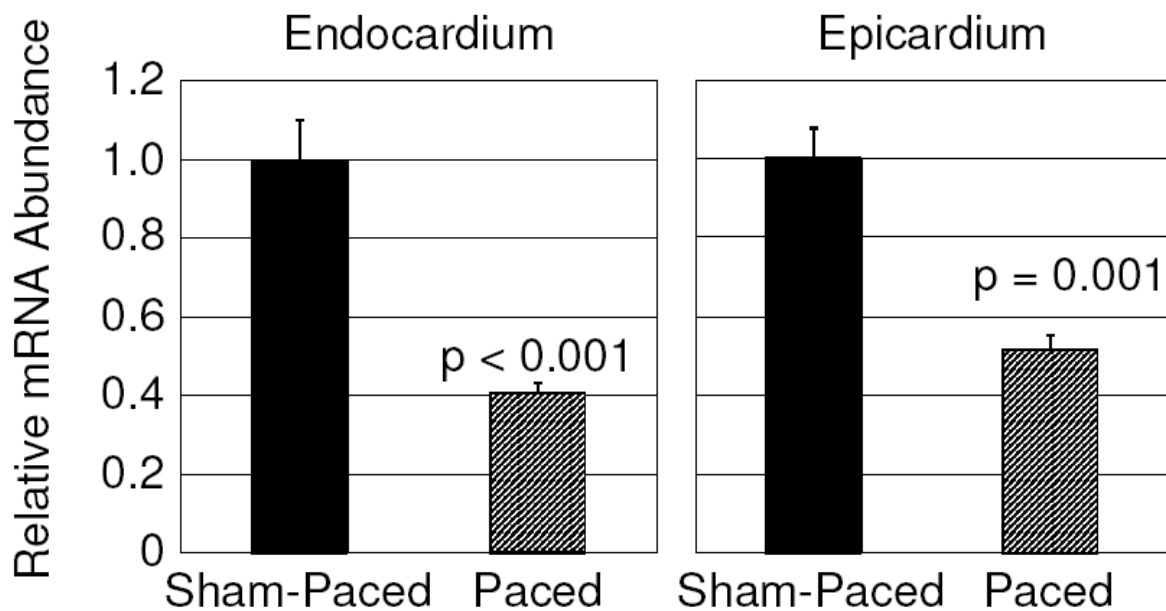
Figure 35 Quantitative Real-Time PCR(qRT-PCR) of LV free wall endocardium and epicardium.

This demonstrates reduced Cx43 mRNA levels in paced hearts. Both the endocardium and the epicardium of the LV free wall demonstrated significantly reduced Cx43 mRNA levels after the short-term pacing protocol(179). With permission from Kontogeorgis et al.

Cx43 Protein levels in the LV endocardial region after short-term pacing.

There was no significant change in Cx43 protein expression in the paced LV endocardial region compared to sham-paced controls (n=11 sham and 11 paced). Quantitative densitometry confirmed no significant difference in mean Cx43/GAPDH 0.92 vs 0.84 arbitrary units (a.u.) .Furthermore densitometry comparing slower migrating Cx43 bands as a ratio of lower most bands to assess differences in phosphorylation state were also not significantly different.
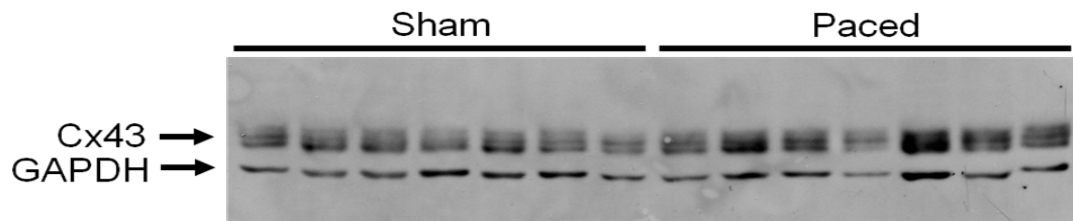
Figure 36. Cx43 Protein levels after 6hours of pacing.

Cx43 protein levels remain unchanged compared to sham-paced controls normalized to GAPDH (endocardial lysates). Note that there are 3 bands within Cx43 and represent various states of phosphorylation from top to bottom P2,P1,P0 respectively(179). With permission from Kontogeorgis et al (179).
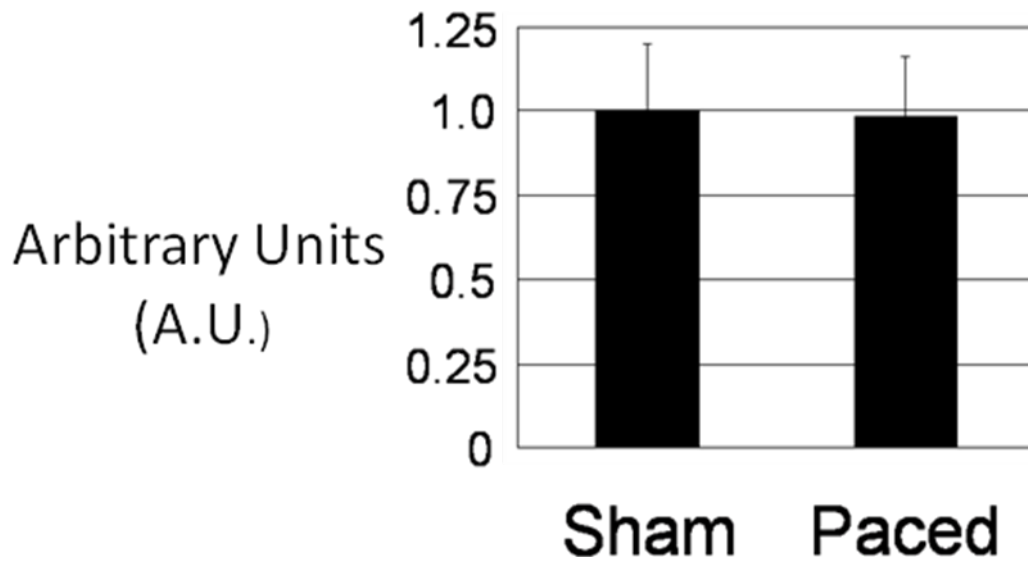
Figure 37. Cx43 densitometry relative to GAPDH loading expressed as arbitrary units(A.U.).

There is no significant difference in Cx43 immunoblotting after 6hours of pacing and sham-pacing(179). With permission from Kontogeorgis et al(179).
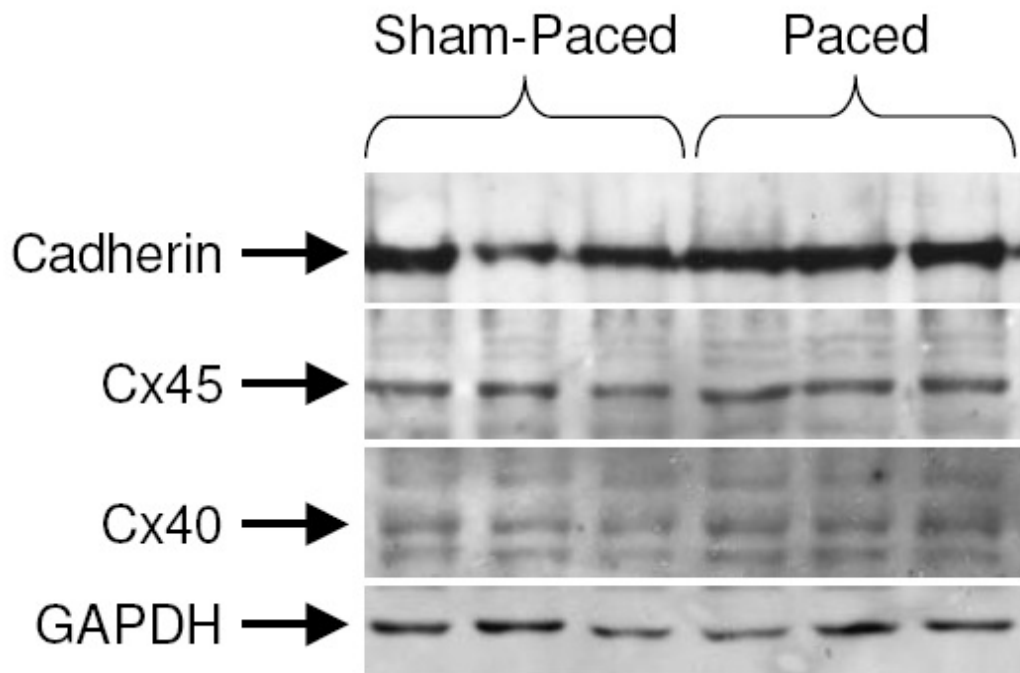
Figure 38. Cx45, Cx40 and Cadherin protein levels after 6 hours of pacing.

Cx45, Cx40 and Cadherin protein levels are unchanged after 6 hours of pacing without significant difference in the mean band densities normalized to GAPDH (endocardial lysates).(179) With permission from Kontogeorgis et al (179).

Cadherin,Cx40 and Cx45 protein expression.

Cadherin, Cx40 and Cx45 levels were statistically unchanged after pacing in the endocardium of the LV free wall.

Fractionation study

Heart samples demonstrated significantly reduced Cx43 abundance in the membrane-enriched fraction isolated from paced hearts compared with controls (40.4 ± 8.7% decrease in the paced hearts; p<0.05; n=11 sham and 12 paced hearts). In contrast, Cx43 levels in the supernatant (non-membrane fraction) increased by 104.0 ± 35.5% (p<0.05). These findings suggest intracellular redistribution of Cx43 protein.
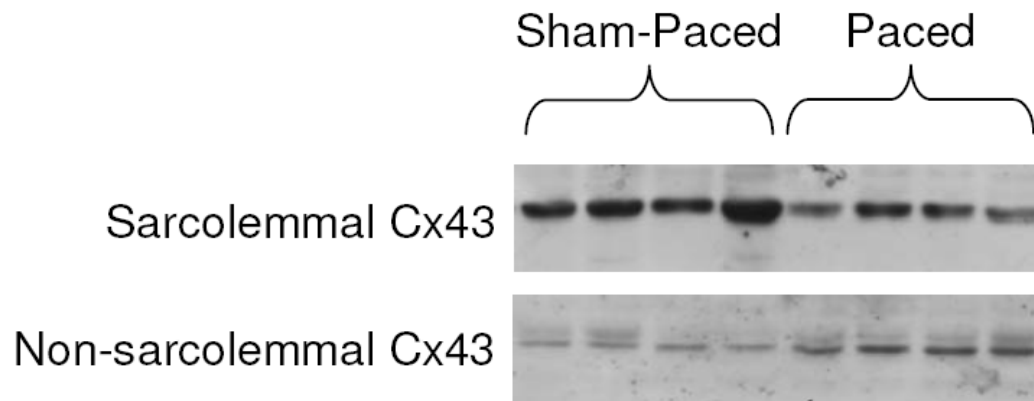
Figure 39 Cx43 levels in membrane and cytosolic pools after 6hr pacing and sham-pacing.

Cx43 levels in membrane (sarcolemmal) fraction n=4 after 6hr paced and sham-paced showing a significant reduction. There is a significant increase post pacing as compared to cytosolic (non-sarcolemmal) pool of Cx43 (p<0.05). Cx43 mean band densities 0.73 in paced and 1A.U. in unpaced Cx43membrane bound fraction(179). With permission from Kontogeorgis et al.

Immunoprecipitation study- Cx43 gap junction degradation.

To test whether degradation of gap junctions appear to be disrupted Dr Gutstein and Ms Gupta kindly performed an immunoprecipitation study of Cx43 from lysates generated (5 sham and 5 paced hearts) and these were immunoblotted with ubiquitin. Immunoblotting for ubiquitin revealed a substantial increase in expression of ubiquitinated forms in the paced hearts.
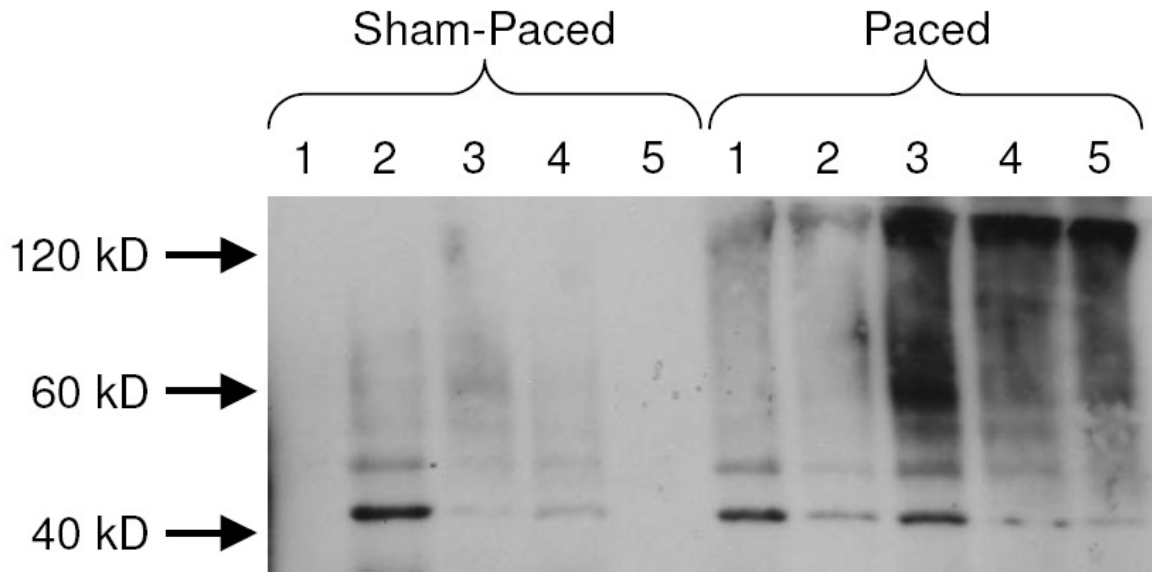
Figure 40. Cx43 distribution and ubiquitination with pacing and Ubiquitin Quantification at baseline and after 6hr pacing.

Immunoblot demonstrating increased accumulation of ubiquitinated Cx43 in paced hearts. In this image, monoubiquitinated Cx43 is seen just above the 40kD size marker and polyubiquitinated forms of Cx43 appear as a slower migrating smear(179). With permission from Kontogeorgis et al.
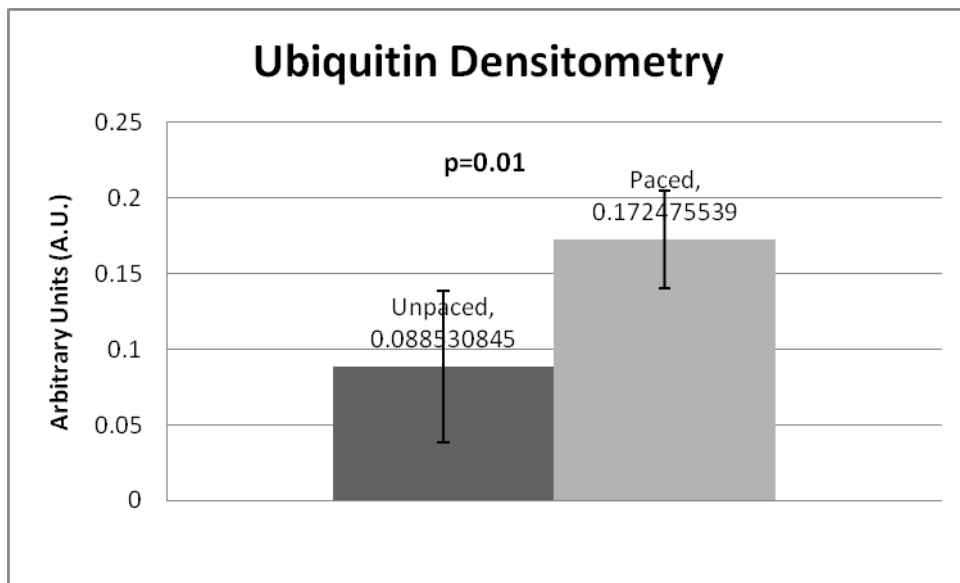
Figure 41 Significant increase in mean ubiquitinated Cx43 after 6hr pacing normalised to GAPDH (p=0.01).

Ubiquitin mean densitometry expressed as a ratio to GAPDH loading in arbitrary units and

 error bars indicating standard deviation.

Electroanatomical correlation in Cx43$^{+/-}$ mice.

Cellular electrophysiologic properties post myocyte isolation using whole cell patch clamp.

To investigate how pacing in the setting of reduced Cx43 expression (Cx43$^{+/-}$) influences electrophysiologic properties, I designed and undertook a set of experiments that would investigate the repolarisation properties of these hearts at a cellular level. Dr Li executed experiments using whole cell patch clamp techniques to record action potentials in ventricular myocytes obtained from unpaced and paced wildtype and Cx43$^{+/-}$ mice respectively (Figure 41 and Table 13). Findings are presented over the next section and I present the following parameters:

1. Resting membrane potential, action potential maximal amplitude and morphology and Action Potential Duration at 50 and 90ms (see figure 41 and Table 13)

2. I assisted Marc Ponzio and executed the immunostaining of Cx43$^{+/-}$ hearts; sections were costained with cadherin for qualitative microscopy (see fig 42) to assess the pattern of distribution of Cx43. Furthermore western blots were undertaken of samples from Cx43$^{+/-}$ paced and unpaced hearts to compare levels of Cx43 (fig 43). Findings confirmed that the transgenic hearts express 66% reduced levels of Cx43 on quantitative immunoblotting (see fig 43 panel A).

3. I assisted Mr Feig who kindly tested the effects of pacing on levels of mRNA in Cx43$^{+/-}$ hearts in order to assess any potential transcriptional effects.

4. I worked with Dr Morley's lab and optically mapped the Cx43$^{+/-}$ hearts after 6hr pacing to determine the sinus rhythm breakthrough activation pattern.
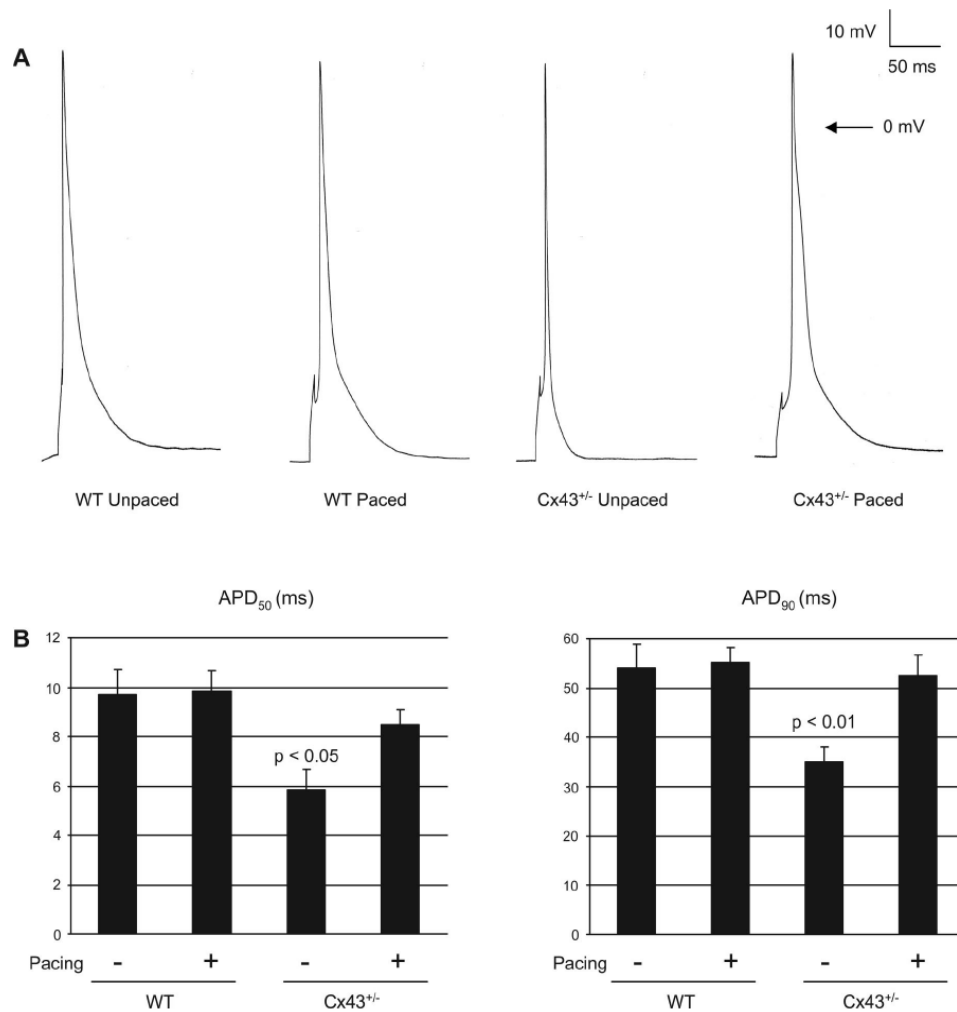
Figure 42. Action Potentials in Unpaced and Paced Wildtype and Cx43$^{+/-}$ Cardiac Myocytes.

A) Representative action potentials from unpaced and paced wildtype and Cx43$^{+/-}$ cardiac myocytes. Action potentials were recorded from adult ventricular myocytes in current-clamp mode, with cells stimulated by 3ms, 3 – 5 mV pulses at a frequency of 1 Hz. B) Summary data of action potential duration at 50 percent (APD50) and at 90 percent (APD90) of repolarization. Unpaced Cx43$^{+/-}$ cells had shorter APD50 and APD90 values compared with the unpaced wildtype cells. APD increased significantly in the Cx43$^{+/-}$ cells with pacing, whereas there was no significant change with pacing in the wildtype cells(161). Reproduced from Kontogeorgis et al.

[192]

Action Potential Duration in Unpaced Cx43$^{+/-}$ Myocytes and WT Myocytes

Myocytes isolated from unpaced Cx43$^{+/-}$ hearts had significantly shorter action potentials than unpaced wildtype cells. In wildtype myocytes, pacing had no effect on APD. Myocytes isolated from unpaced wildtype hearts demonstrated APD measurements that were no different from paced wildtype myocytes (APD50 = 9.7 ± 1.0 ms in unpaced wildtype vs. 9.9 ± 0.8 ms in paced wildtype; APD90 = 54.1 ± 4.8 ms in unpaced wildtype vs. 55.3 ± 3.0 ms in paced wildtype; p = NS for both comparisons) (figure 41 and table 13).

Action Potential Duration in Paced Cx43$^{+/-}$ Myocytes and WT Myocytes:

Cx43$^{+/-}$ myocytes demonstrated significant prolongation of APD after pacing compared to unpaced Cx43$^{+/-}$ myocytes (APD50 = 5.8 ± 0.9 ms in unpaced Cx43$^{+/-}$ vs. 8.5 ± 0.6 ms in paced Cx43$^{+/-}$, p < 0.05; APD90 = 35.0 ± 3.2 ms in unpaced Cx43$^{+/-}$ vs. 52.7 ± 4.1 ms in paced Cx43$^{+/-}$; p <0.01). While pacing resulted in no significant change in APD in wildtype cardiac myocytes, the imposition of pacing on Cx43-deficient cells resulted in a significant lengthening of APD compared to its unpaced baseline (figure 41 and table 13).

Action Potential Amplitude and Resting Membrane Potential:

Action potential amplitude and resting membrane potential were no different among the unpaced and paced wildtype and Cx43$^{+/-}$ subgroups (figure 41 and table 13)..

Table 13. Comparison of Action Potential Parameters in Wildtype and

Cx43$^{+/-}$ Unpaced and Paced Mice

	WT unpaced (n=6)	WT paced (n=11)	Cx43$^{+/-}$ unpaced (n=7)	Cx43$^{+/-}$ paced (n=10)
Amplitude, mV	101.8 ± 3.8	97.2 ± 1.7	97.6 ± 4.0	97.8 ± 2.0
RMP, mV	-72.0 ± 0.5	-72.5 ± 1.0	-71.5 ± 1.0	-72.0 ± 1.0
APD20, ms	2.7 ± 0.3	2.6 ± 0.2	2.0 ± 0.2	2.3 ± 0.2
APD50, ms	9.7 ± 1.0	9.9 ± 0.8	5.8 ± 0.9*	8.5 ± 0.6
APD90, ms	54.1 ± 4.8	55.3 ± 3.0	35.0 ± 3.2†	52.3 ± 4.1

Data are presented as group means ± SEM. Comparisons between groups were performed with ANOVA. *, $p < 0.05$ compared to all other groups; †, $p < 0.01$ compared to all other groups. RMP, resting membrane potential; APD, action potential duration (161). With permission from Kontogeorgis et al (161).

[194]

Assessment of Cx43 protein expression at basal levels and after 6hr pacing:

Immunosignal assessment: Cx43 and cadherin in unpaced Cx43$^{+/-}$ hearts compared to 6hr paced hearts was not significantly altered (figure 42).
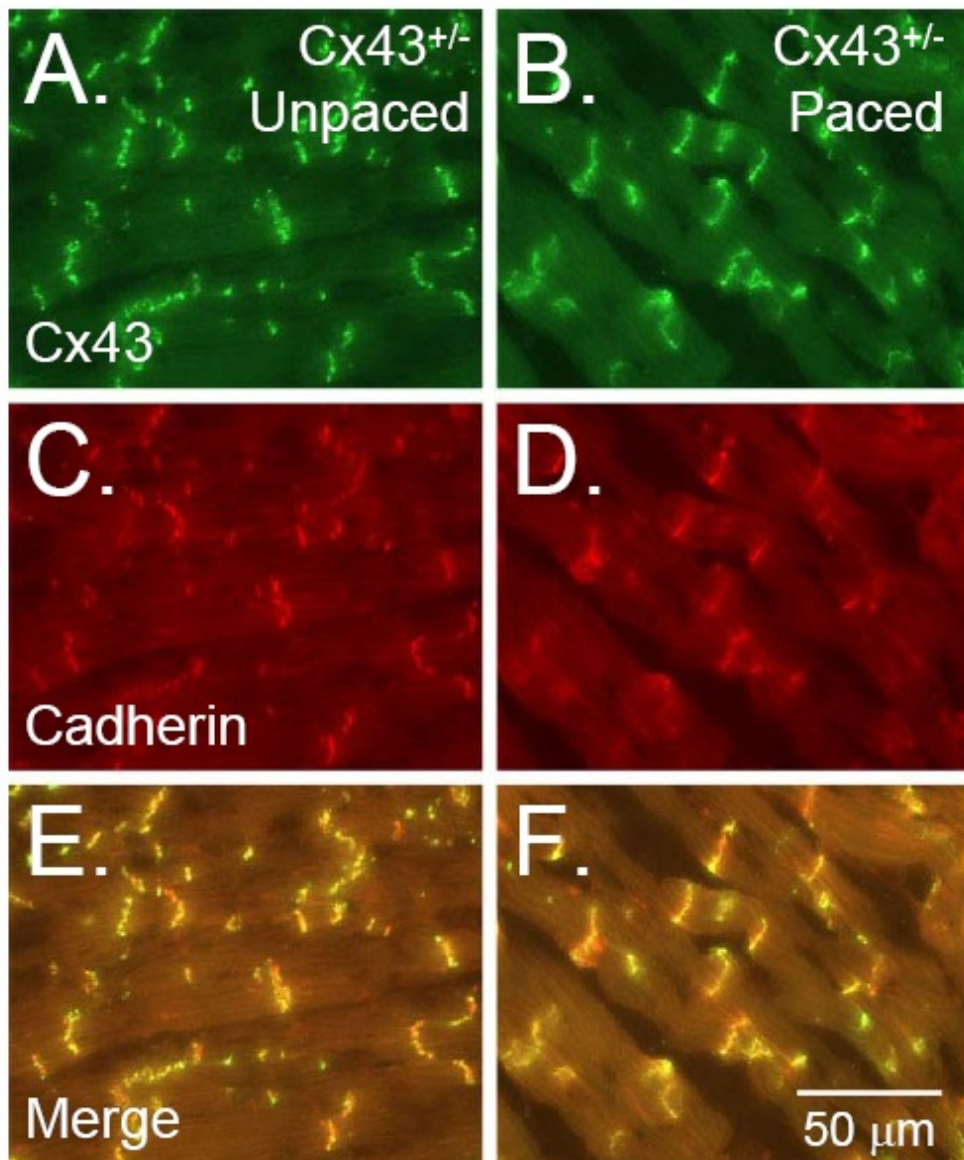
Figure 43. **Cx43 (green) and Cadherin (red) immunostaining in Cx43$^{+/-}$ mice.**

Courtesy of Dr Gutstein; Cx43 and Cadherin immunosignal in paced and unpaced mice showed no significant differences.

[195]

Immunoblotting:

Cx43$^{+/-}$ hearts had reduced Cx43 protein levels compared to matched samples from littermate WT (34.3 ± 4.4%; p <0.01). Pacing for 6hr did not significantly affect overall Cx43 protein levels in Cx43$^{+/-}$ mice.
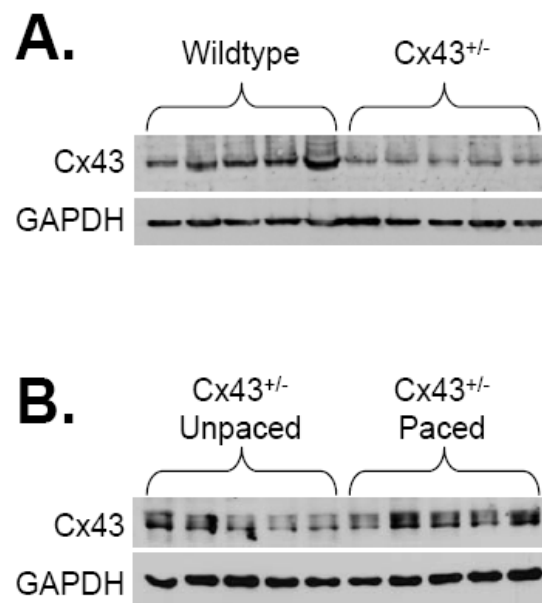
Figure 44. **Cx43 expression in Cx43$^{+/-}$ hearts:**

Western blot showing reduced Cx43$^{+/-}$ (A)compared to wildtype (66% reduction on quantitative densitometry normalised to GAPDH , data not shown). The effect of pacing on Cx43 protein levels (B) in Cx43$^{+/-}$ mice was not significantly altered (161). Reproduced from Kontogeorgis et al.

Relative Cx43 mRNA abundance in Cx43$^{+/-}$ mice after 6hr pacing:

No significant differences were found in Cx43 mRNA abundance in Cx43$^{+/-}$ hearts relative to

their baseline levels after 6hour pacing (figure 44).
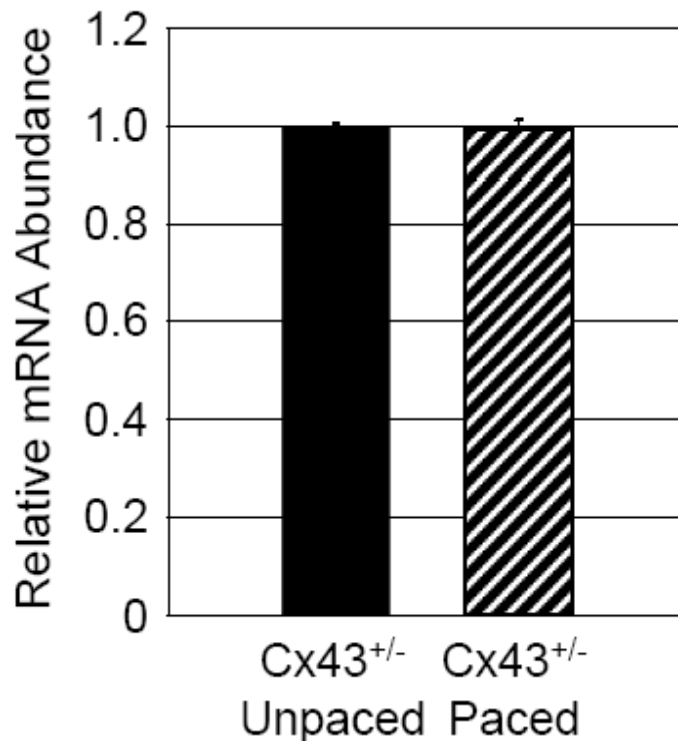
Figure 45. **Relative Cx43 mRNA abundance**

Relative Cx43 mRNA abundance in Cx43$^{+/-}$ hearts after 6hour pacing were not significantly

changed(161). Reproduced from Kontogeorgis et al

Epicardial sinus activation breakthrough after 6hr pacing.

Using optical mapping we tested for altered epicardial activation or breakthrough between the right and left ventricle (normally earliest activation occurs on the right followed by the left) and found no significant evidence to suggest Bundle branch block as a mechanism for mechanical dyssynchrony.
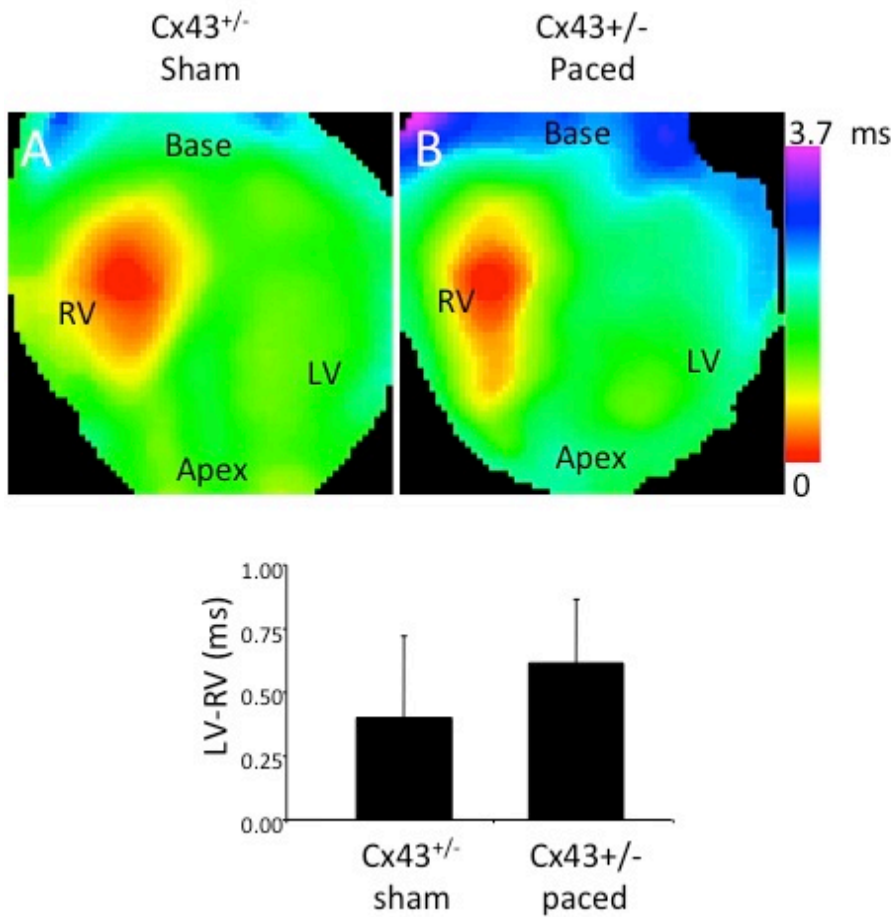
Figure 46 Epicardial activation breakthrough patterns in Cx43$^{+/-}$ unpaced and Cx43$^{+/-}$ paced hearts.

Epicardial breakthrough patterns and time difference between LV and RV breakthrough were not significantly altered.

Investigating repolarization properties as potential determinant of altered action potential duration in cardiac myocytes:

Since action potential duration in cardiac cells is largely determined by voltage-dependent potassium channels (160), a set of experiments were undertaken to determine whether changes in repolarization in unpaced and paced $Cx43^{+/-}$ myocytes might result from altered potassium current properties of:

1. Inward rectifier K+ current (IK1)

2. Total Outward K+ current (IKpeak) comprised of :

i) Steady state K+ current (Iss)-this is the 4-AP insensitive component of the outward current

ii) The 4-AP sensitive component of the outward K+ current, (Ito).

Assessing the Inward Rectifier Potassium Current (IK1) in RV Cx43$^{+/-}$ Myocytes:

IK1 was measured in the whole-cell configuration, in which calculated cell capacitances are 144.6 ± 7.6 pF in wild type RV myocytes (n=28) and 145.9 ± 5.5 pF in Cx43$^{+/-}$ RV myocytes (n=29; p = NS).

The background inward rectifier potassium current, IK1, which is responsible for maintaining the resting membrane potential and influences the late phase of repolarization was investigated first(180). Initially, no significant differences were observed in a 4-way comparison of IK1 in unpaced wildtype (peak current = -14.3 ± 1.4 pA/pF), paced wildtype (-13.7 ± 1.3 pA/pF), unpaced Cx43$^{+/-}$ (-17.7 ± 1.2 pA/pF) and paced Cx43$^{+/-}$ myocytes (-16.3 ± 1.3 pA/pF; Figure 46 A-E). Because IK1 was not statistically different in unpaced versus paced wildtype myocytes across all of the tested voltages, the data from these two groups was pooled at each voltage to increase statistical power. IK1 values in unpaced and paced Cx43$^{+/-}$ myocytes were also pooled at each voltage, since they were not significantly different (except at -30 mV, p = 0.028). A post-hoc analysis of the pooled values from wildtype versus Cx43$^{+/-}$ myocytes revealed significantly increased IK1 in the Cx43$^{+/-}$ myocytes compared to wild types (Figure 46 F). Thus, increased IK1 in Cx43$^{+/-}$ myocytes may contribute to APD shortening. However, there was no significant effect of pacing on IK1 in either wildtype or Cx43$^{+/-}$ myocytes.
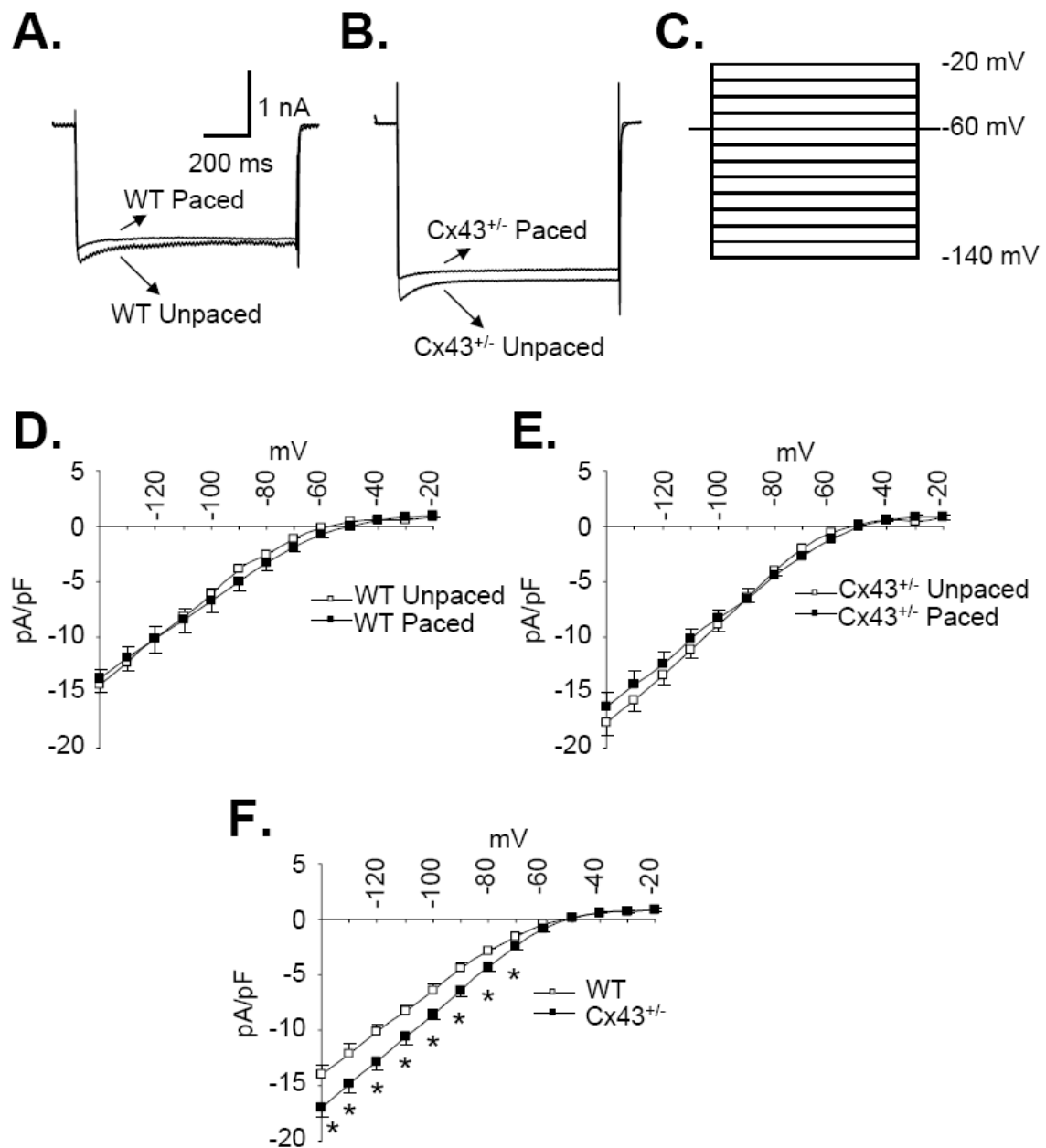
Figure 47**. Effect of Pacing on the Inward Rectifier Potassium Current, IK1, in Wildtype and Cx43^{+/−} Right Ventricular Cardiac Myocytes.**

A and B) Representative recordings of IK1 from wildtype (panel A) and Cx43^{+/−} (panel B) unpaced and paced right ventricular myocytes at a potential of −140mV. C) Voltage-clamp protocol consisted of steps of 10mV increments between -140mV and -20mV (1s duration, 0.01Hz) from a holding potential of −60mV. D and E) IK1 amplitude, measured at the end of

a 1s pulse, was plotted as a function of applied voltage for wildtype unpaced (n=5) and paced (n=5) right ventricular myocytes (panel D) and Cx43$^{+/-}$ unpaced (n=5) and paced (n=6) myocytes (panel E). Results indicate that there are no significant differences between any of the four subgroups. F) Post-hoc analysis of pooled IK1 values comparing results from all wildtype versus Cx43$^{+/-}$ cells at each voltage showed significantly increased IK1 in the Cx43$^{+/-}$ myocytes compared to wild types at voltages of $\leq$ -70mV. *, $p < 0.05$. (From Kontogeorgis et al (161).

Table 14. Comparison of Ito Inactivation, Steady-State Inactivation and Recovery from Inactivation in Wildtype and Cx43$^{+/-}$ Unpaced and Paced Mice

	WT unpaced	WT paced	Cx43$^{+/-}$unpaced	Cx43$^{+/-}$paced
	Ito Inactivation Kinetics			
τf, ms	47.4 ± 6.7	49.2 ± 5.5	45.9 ± 3.8	43.6 ± 1.3
τs, ms	1138 ± 188	1161 ± 182	1104 ± 126	1190 ± 144
a0, nA	0.4 ± 0.06	0.4 ± 0.05	0.4 ± 0.04	0.4 ± 0.04
a1, nA	1226 ± 304	1176 ± 305	1295 ± 275	1450 ± 309
a2, nA	1.7 ± 0.4	1.6 ± 0.3	1.5 ± 0.4	1.6 ± 0.4
	Steady-State Inactivation			
Vh, mV	-26.3 ± 2.0	-27.9 ± 2.4	-30.5 ± 3.5	-26.8 ± 2.3
K, mV	11.3 ± 1.2	11.0 ± 1.3	9.5 ± 1.0	8.3 ± 1.2
	Recovery from Inactivation			
τrecovery, ms	31.5 ± 4.6	30.3 ± 4.9	44.3 ± 5.5	36.6 ± 3.7

Data are presented as group means ± SEM (n = 8 per group). f, time constant of the fast component of inactivation; s, time constant of the slow component of inactivation; a1 and a2, amplitudes of the inactivating current components; a0, residual amplitude of the steady-state, non-inactivating component of the total outward K+ current after subtraction of the 4-AP insensitive component; Vh, half maximal inactivation potential; K, slope factor for steady-state inactivation curves at the half-maximal inactivation potential; recovery, time constant of recovery from inactivation. Comparisons between groups were performed with ANOVA. P = NS for all comparisons. With permission from Kontogeorgis et al (161).

[204]

Changes in Steady-State Potassium Current (Iss) in Unpaced and Paced RV WT and Cx43$^{+/-}$ Myocytes

The two components of the total voltage-dependent outward potassium current are also critical in determining APD (Figure 47A); they are distinguished by sensitivity to 4-aminopyridine (4-AP). Outward potassium current in cardiac myocytes is comprised of a 4-AP insensitive component (Iss; Figure 47B) and a 4-AP sensitive component (Ito; Figure 47C) (177;181;182). Figure 47 recordings from an adult murine RV myocyte.
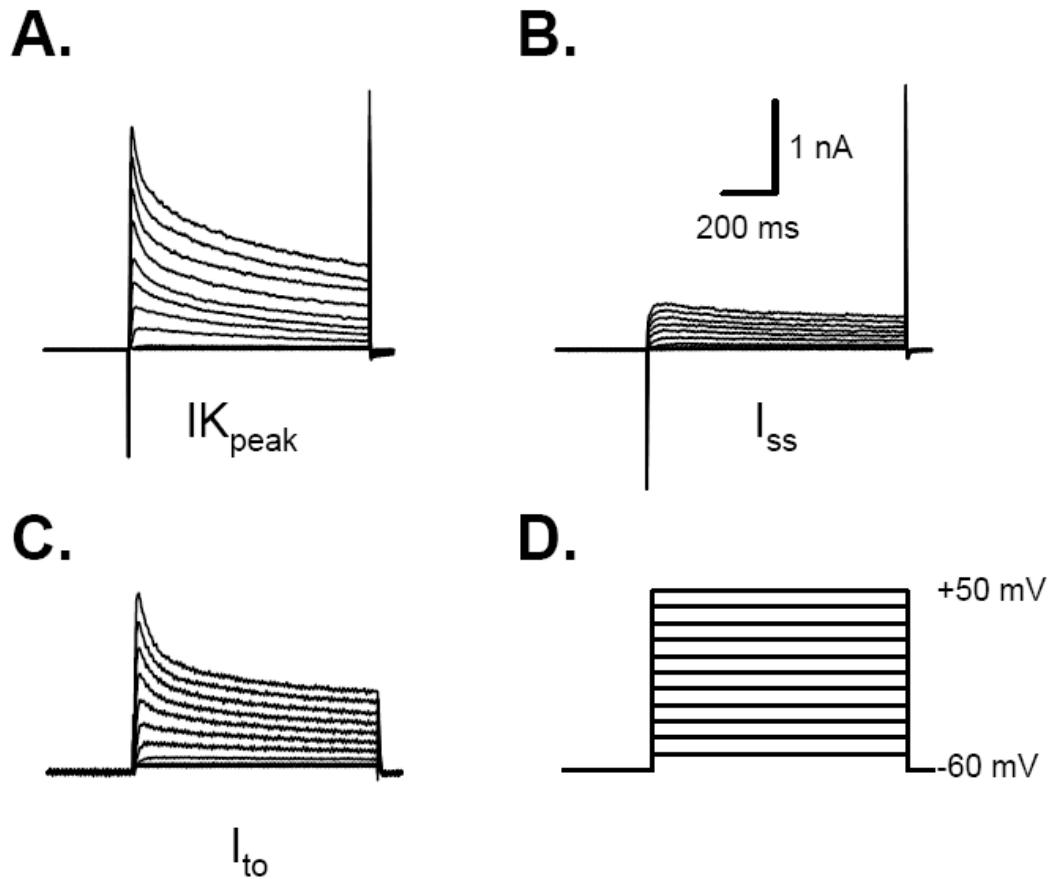
Figure 48. Outward Potassium Current in Adult Murine Right Ventricular Cardiac Myocytes.

A) Total outward potassium current, as shown, is termed IKpeak. B) A 4-AP insensitive steady-state current, Iss, was obtained after 2mM 4-AP was applied. C) The transient outward potassium current, Ito, was obtained offline by subtracting Iss from IKpeak. D) Voltage-clamp protocol consisted of steps of 10mV increments between –50mV and +50mV (1s duration, 0.01Hz) from a holding potential of –60mV (161).Reproduced from Kontogeorgis et al.

Changes in 4-AP-sensitive current (Ito) in unpaced and paced WT and Cx43$^{+/-}$ Myocytes:

There was no difference in amplitude among the unpaced wildtype, paced wildtype, unpaced Cx43$^{+/-}$ or paced Cx43$^{+/-}$ mice in the 4-AP-sensitive current, Ito (Figure 48).

Inactivation kinetics of Ito and recovery indices:

There were no differences in the inactivation kinetics of Ito and indices of recovery of Ito from inactivation in any of the groups (Figure 49 and Table 14).
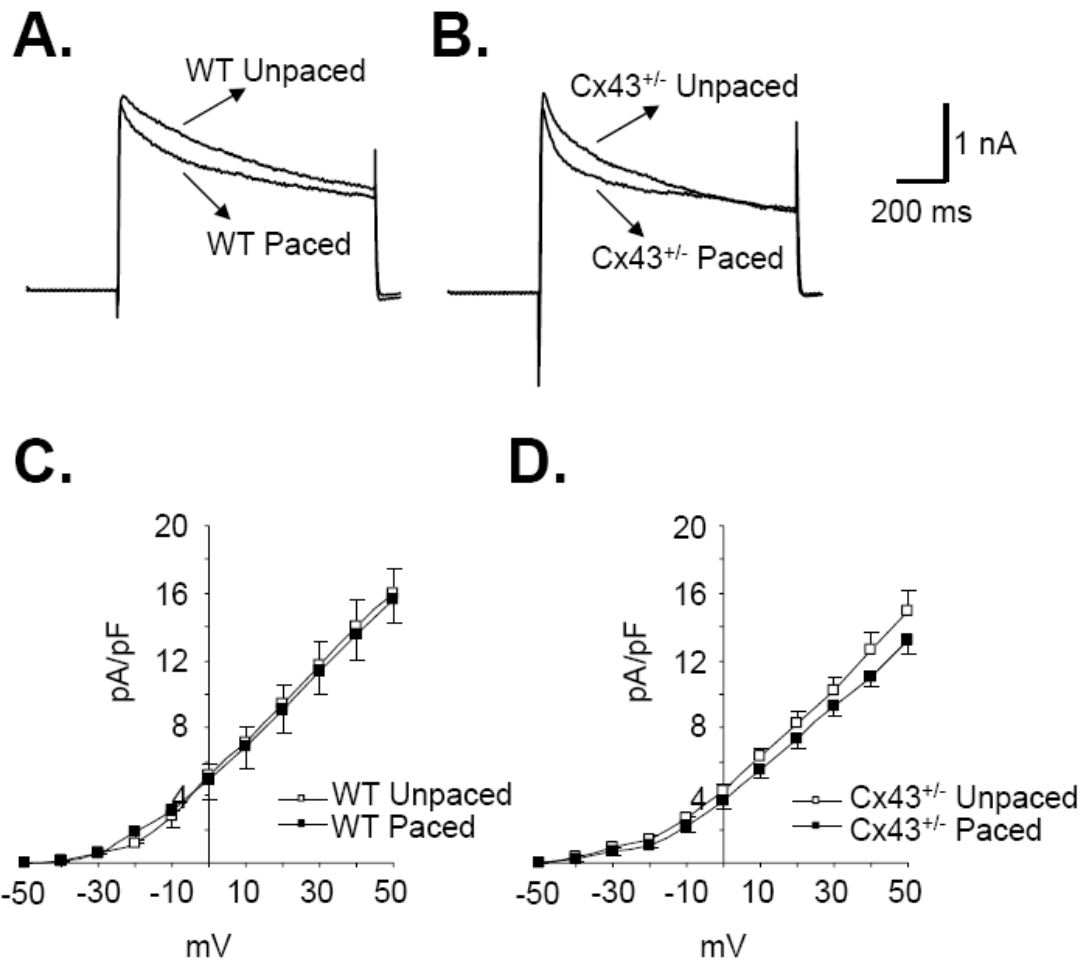
Figure 49**. Effect of Pacing on the Transient Outward Current, Ito, in Wildtype and Cx43$^{+/-}$ Right Ventricular Cardiac Myocytes.**

A and B) Representative Ito traces from wildtype (panel A) and Cx43$^{+/-}$ (panel B) unpaced and paced right ventricular myocytes at +52mV. C and D) Ito peak amplitude was measured and plotted as a function of applied voltage for WT unpaced and paced (n = 6 and 5, respectively; panel C) and Cx43$^{+/-}$ unpaced and paced myocytes (n = 6 and 7, respectively; panel D). There were no significant differences between any of the subgroups(161). Reproduced from Kontogeorgis et al.
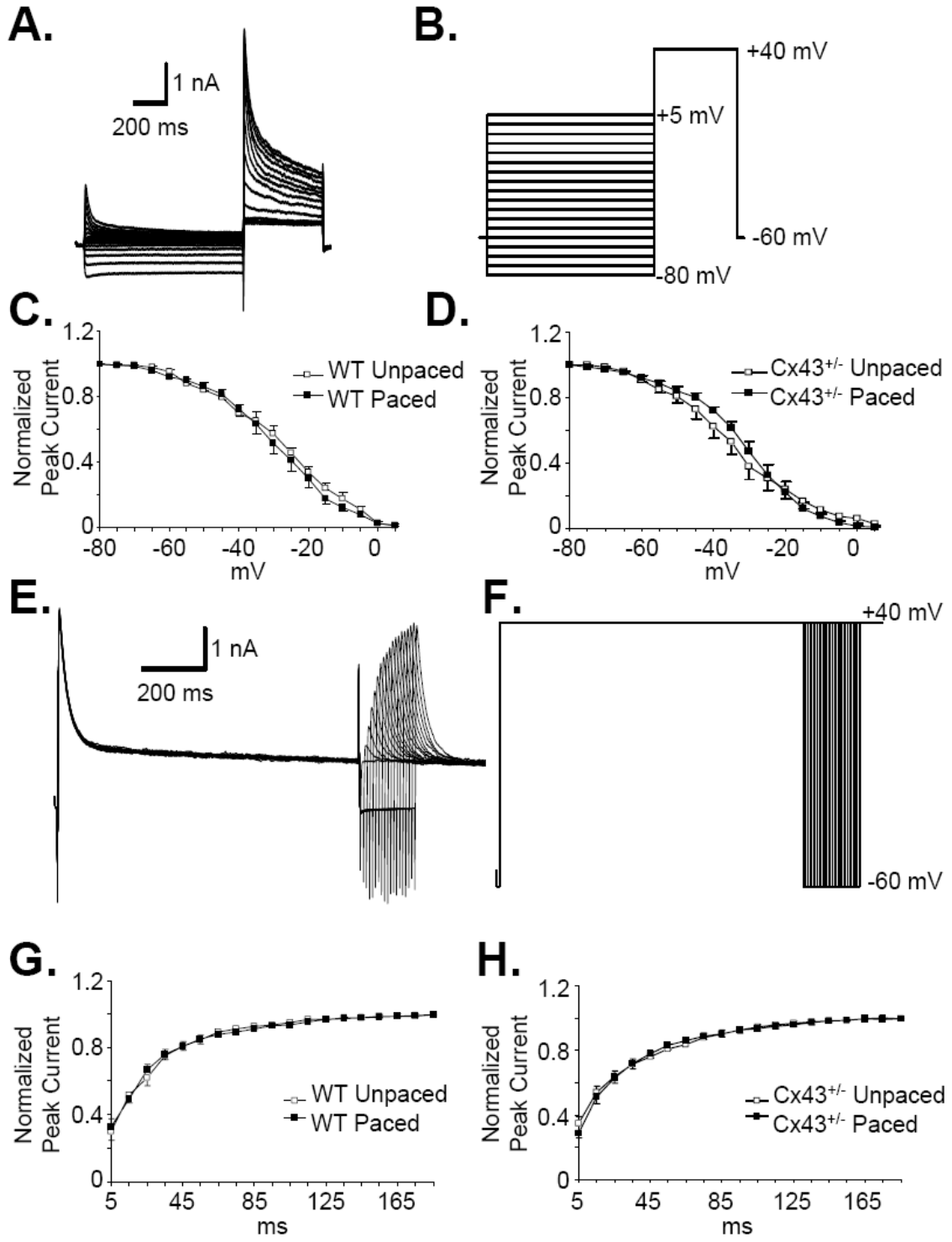
Figure 50 **. Effect of Pacing on Kinetics of Ito Inactivation Properties and Recovery of Ito from Inactivation in WT and Cx43$^{+/-}$ Myocytes.**

A) Representative Ito recording made during a 2-pulse voltage-clamp protocol to assess voltage dependence of steady-state inactivation. B) The 2-pulse protocol consisted of a 1 s prepulse delivered from a holding potential of –60mV in 5 mV increments from –80mV to +5mV, followed by a 500ms test pulse to +40mV. C and D) Steady-state inactivation curves obtained from peak current obtained during second pulse in wildtype unpaced and paced (n = 6 each; panel C) and Cx43$^{+/-}$ unpaced and paced myocytes (n = 6 and 5, respectively; panel D). Data were normalized to peak current amplitude at a prepulse of –80mV, plotted as a function of prepulse potentials and fitted with the best nonlinear least-squares fit of a Boltzmann function. E) Representative tracings of recovery of Ito from inactivation. F) Recovery of Ito from inactivation was measured by using 2 depolarizing pulses to +40mV, from a holding potential of -60mV, separated by intervals of increasing duration from 5ms to 185ms in 10ms increments. G and H) Recovery of Ito current was obtained from WT unpaced and paced (n = 8 and 7, respectively; panel G) and Cx43$^{+/-}$ unpaced and paced cells (n = 8 each; panel H). Data were normalized to maximum current value, plotted as a function of recovery time and fitted with a first-order exponential function. No significant differences among the subgroups were identified in inactivation properties or recovery kinetics of Ito. Reproduced from Kontogeorgis et al(161).

Steady-State Potassium Current (Iss) in Unpaced and Paced RV WT and Cx43$^{+/-}$ Myocytes

Mice with conditional loss of Cx43 expression in the heart demonstrate significant elevations in the 4-AP insensitive current, Iss, in right ventricular myocytes(13) . In this study, Iss was significantly increased in unpaced Cx43+/− myocytes (peak current = 4.2 ± 0.5 pA/pF) compared to unpaced wildtype myocytes (2.4 ± 0.2 pA/pF; $p < 0.01$). Pacing did not affect a significant change in Iss current density in wildtype myocytes (2.7 ± 0.1 pA/pF after pacing; Figure 50 A and C). Pacing was associated with a significant reduction of Iss current density in the Cx43+/− myocytes (2.9 ± 0.2 pA/pF; $p < 0.01$ compared to unpaced Cx43$^{+/-}$ myocytes; Figure50 B and D).At these levels they were not statistically different from those of the wildtype myocytes. Changes in the Iss density most likely represent a major mechanism underlying corresponding alterations in APD in unpaced and paced Cx43$^{+/-}$ myocytes.
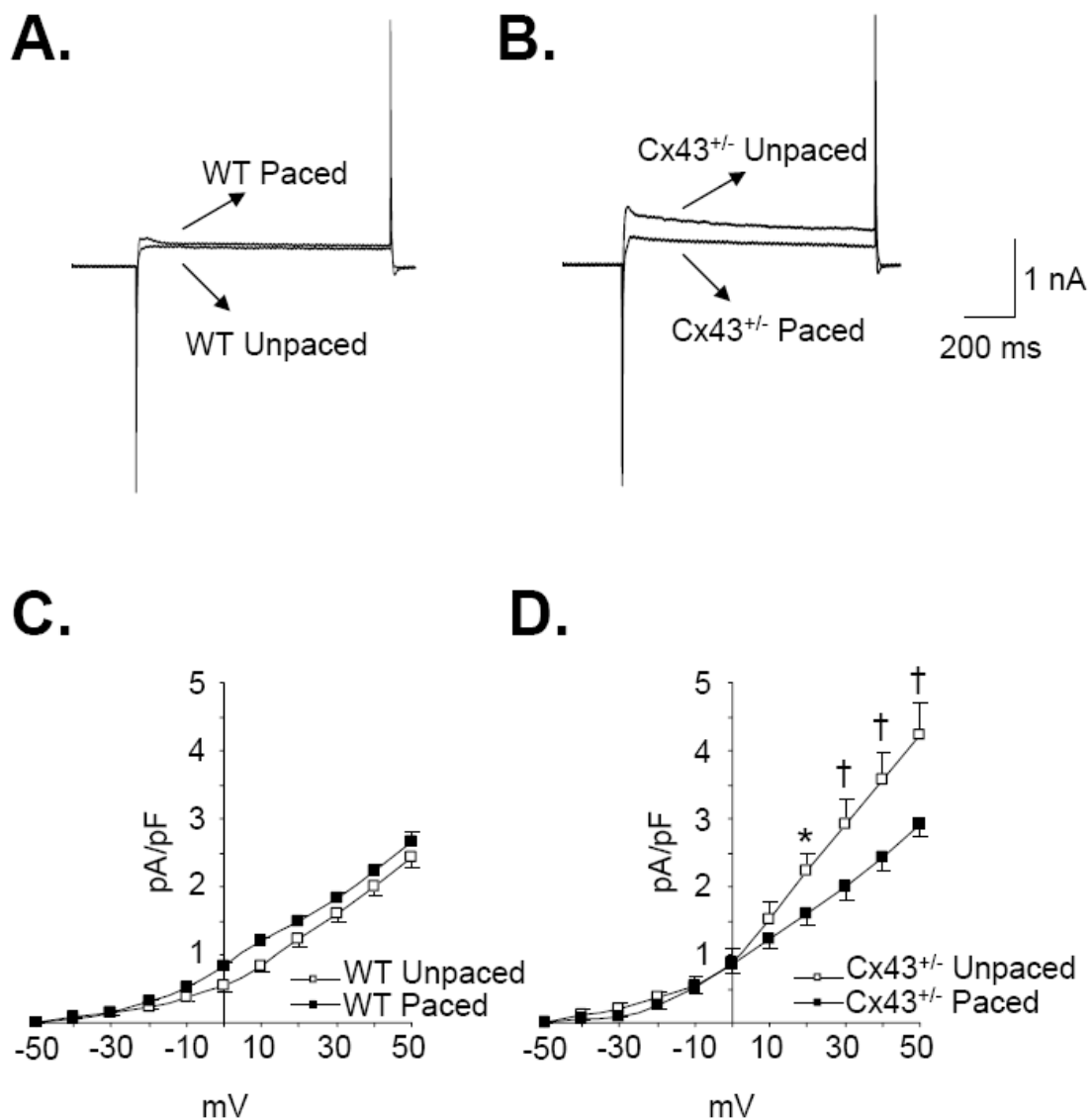
Figure 51. Effect of Pacing on Steady-State Outward Potassium Current, Iss.

A and B) Representative recordings of Iss from wildtype unpaced and paced (n = 6 each; panel A) and Cx43^{+/−} unpaced and paced myocytes (n = 5 and 6, respectively; panel B) at +50mV. C and D) Iss amplitude was measured at the end of the depolarization pulse, and plotted as a function of applied voltage for wildtype (panel C) and Cx43^{+/−} cells (panel D). The results indicated that Iss was not altered by pacing in the wildtype cells. However, Iss was elevated in the Cx43^{+/−} unpaced cells in comparison to all other groups, and was

diminished significantly by pacing in the Cx43$^{+/-}$ myocytes. *, $p < 0.05$; †, $p <$

0.01.Reproduced from Kontogeorgis et al (161).

Electroanatomical correlation in Cx40$^{+/+}$, Cx40$^{+/-}$ and Cx40$^{-/-}$ mice, age dependence and regional analysis.

Dr Morley and Leaf requested practical help with immunostaining and quantification of gap junctions along similar lines to that described earlier in the pacing model. To explore further electroanatomical correlation between gap junction remodelling and altered electrophysiologic functional effects a transgenic Cx40 knockout mouse was studied. Utilising quantitative immunohistochemistry and immunoblotting, characterisation of anatomical data for a cohort of Cx40$^{+/+}$, Cx40$^{+/-}$ and Cx40$^{-/-}$ mice was performed.

These were correlated with functional data obtained from optical mapping experiments in collaboration with Dr Leaf.

Assessing Cx40 and Cx43 Expression

The blinded Mean Cx43 Fluorescent Index study

Expression of Connexin 43 (Cx43) immunosignal in Wild type mice and Cx40$^{-/-}$ mice was evaluated and compared (n=4+4) to assess for compensatory changes. A small age-dependent sub-group analysis was performed; 2 mice were less than 8 weeks old and 2 older than 8 weeks in each sub-group.

Quantification of the mean fluorescent signal of Cx43 involved standardised image processing in Adobe Photoshop 7.0.1(San Jose, California, USA).Utilising Image J (NIH available online) , raw data measurements included total pixel count area and total tissue area. The mean fluorescent Cx43 signal was calculated and comparison made of the Right and Left Atrium in each heart.

The blinded Mean (Cx43/Cx40) colocalisation Index study-regional analysis-RAA vs. LAA and effects of ageing.

The age-dependent colocalised Cx43 and Cx40 signal in wild type Cx40$^{+/+}$ mice was compared . Fluorescent measurements were assessed in mice aged less than 8 weeks and those older than 8 weeks (n=6+6). Prior to fluorescent staining standard H&E staining was undertaken to identify suitable blinded regions representing the right atrial appendage (RAA) , right atrium (RA), left atrial appendage (LAA) and left atrium (LA).Quantification of the mean colocalisation index of Cx43 and Cx 40 required multiple 8-bit images for a colocalised measurement of each region RA, RAA, LA, LAA (Figure 52).

Statistical analysis.

Data are presented as means ± SEM for the RA, LA, RAA, LAA as well as old and young mice for each heart respectively. Comparison between these groups was performed with a 2-tailed *t* test using Microsoft Excel software. *P*, < 0.05 was considered statistically significant. Changes in colocalisation data between young and old mice per region were compared using one-way ANOVA in Prism and Statview.

Results

Analysis of Cx40 protein levels to assess atrial differences

Cx40 immunostaining to assess protein levels was performed to determine whether gradients in Cx40 expression were present in the mouse atria (Figure 51). Comparing samples of Cx40$^{+/+}$ mice revealed no overt regional right–left differences.
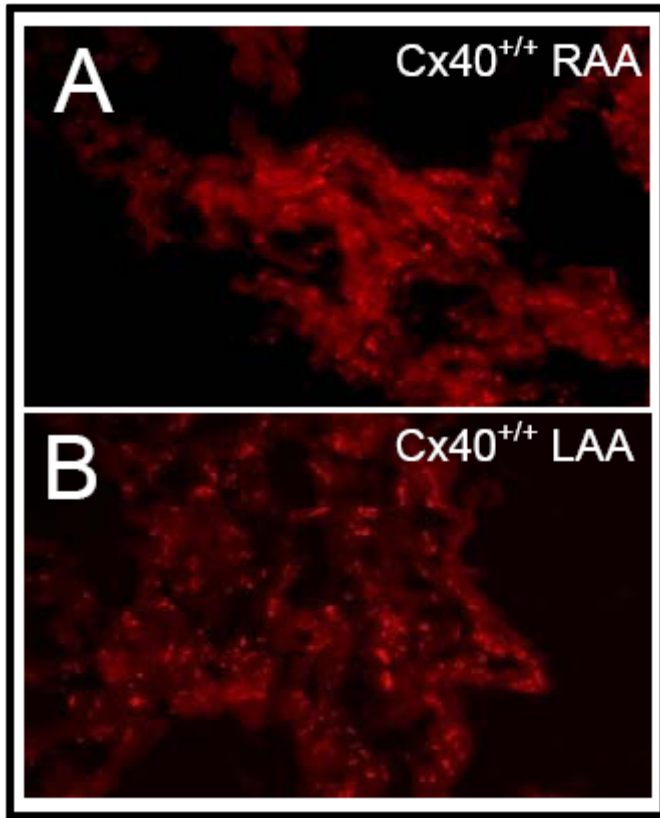
Figure 52 **Regional comparison of Cx 40 immunostaining in wild type mice.**

No significant difference in Cx40 immunosignal in RAA and LAA tissue of wildtype mice.

Reproduced with permission from Leaf et al(183)

The mean Cx43 fluorescent index

Cx43 immunostaining in both Cx40$^{+/+}$ and Cx40$^{-/-}$ mice was performed to exclude the possibility of compensatory changes in Cx43 (Figure 52). Cx43 expression did not appear altered in the Cx40$^{-/-}$ compared with the Cx40$^{+/+}$ mice nor were right–left differences detected in mice of either genotype suggesting that there was no apparent upregulation of Cx43.In addition, there was no significant quantitative difference comparing younger to older mice for Cx43 immunosignal heterogeneity +/ upregulation.

The mean colocalisation index

Mean colocalisation of young and old Cx40$^{+/+}$ hearts comparing the RA to RAA as well as LA to LAA were not significant (figure 53). The ANOVA analysis was not significant (figure 54).
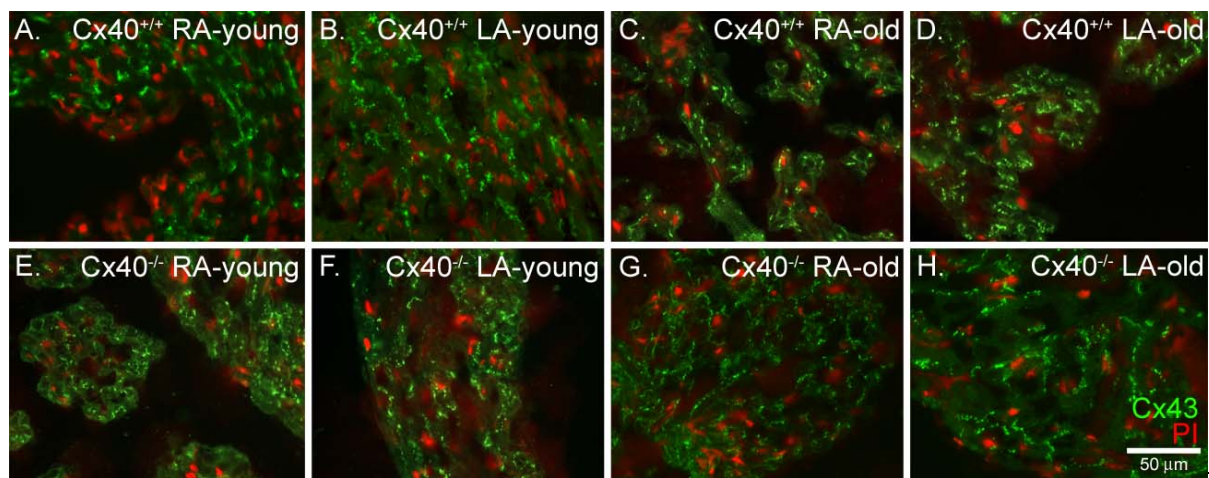
Figure 53 Cx43 immunostaining in Cx40$^{+/+}$ and Cx40$^{-/-}$ mice.

Regional as well as age comparison of colocalised Cx40 and Cx43 immunosignal without significant differences. With permission from Leaf et al (183).
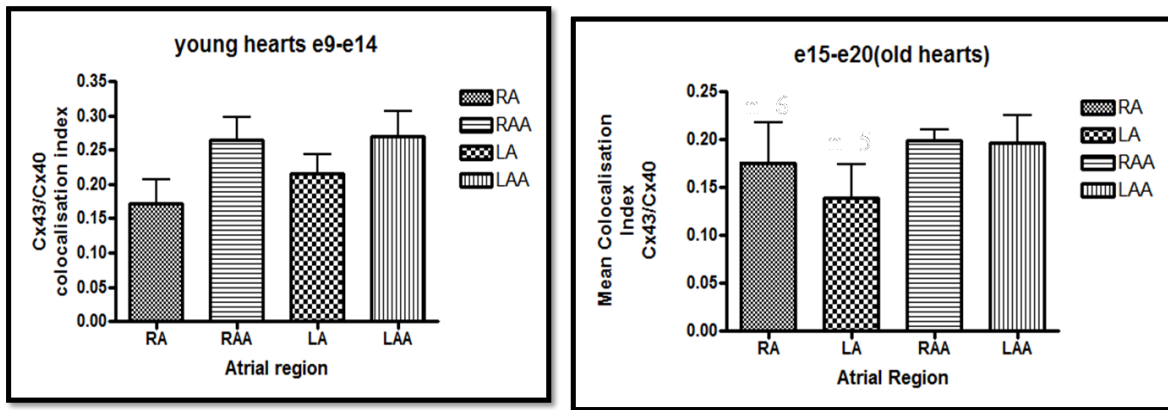
N=6 in all groups and p=ns

p RA vs RAA=ns
p LA vs LAA=ns

Figure 54. Cx43/Cx40 Colocalisation index, regional comparison in young and old hearts.

Comparison of regional Cx43/Cx40 colocalisation showed no significant difference in young and old hearts.
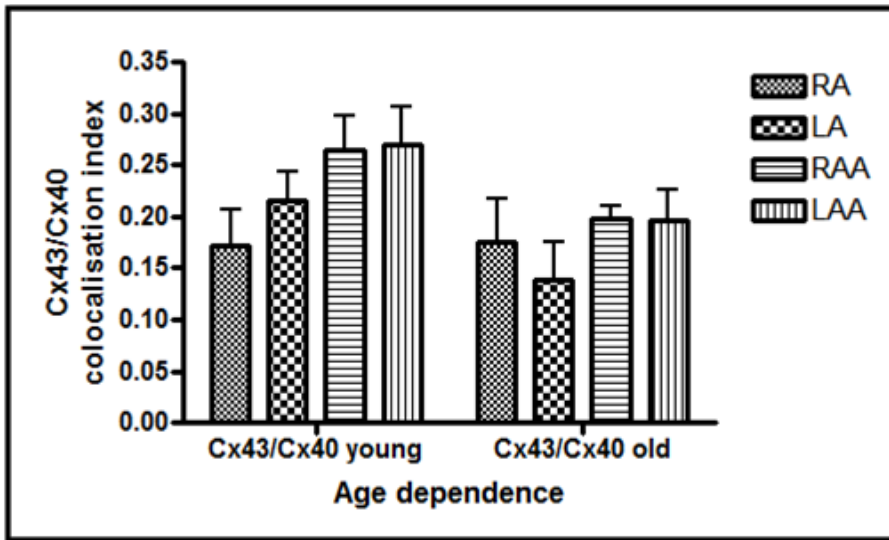
Figure 55. Comparison of Cx43/Cx40 colocalisation between young and old hearts.

No significant difference of Cx43/Cx40 colocalisation when comparing young vs old hearts

on a regional basis.

Discussion:

Pacing in wild type Cx43$^{+/+}$ mice seems to have a significant effect on mRNA transcription and or stability at the LV free wall epicardium and endocardium suggesting that early regulatory changes are being implemented to reduce overall gap junction levels.

These in turn likely reduce the amount of Cx43 available at the cardiac membrane and alter the degree of electrical coupling. Models of arrhythmia strongly associate with reduced levels of Cx43 as seen in animal models of infarction (canine and rat models) as well as the conditional Cx43 knockout mouse model which succumbs to lethal arrhythmias.

However, in this study the overall magnitude of Cx43 reduction may be insufficient to precipitate arrhythmia on inducibility testing in the wildtype mouse. It is possible that additional insults such as infarction or pre existing heart failure might alter this risk of arrhythmia.

Altering the duration of the pacing protocol to a longer period of time, i.e. 6hours did not result in extensive gap junction remodelling as might have been predicted. This also did not result in a significant change in ECG, ECHO or PES measures.

Cx43 is degraded along the ubiquitin proteasome pathway via a highly regulated process that includes but is not limited to epidermal growth factor (EGF) which hyperphosphorylates gap junction protein. However, I did not find a difference in the ratio of Cx43 upper bands/lower bands in the paced endocardium to suggest a difference with pacing suggesting that a non-EGF pathway may be targeting the gap junctions towards degradation.

Altered degradation may represent a regulatory step in altering the distribution and levels of Cx43 expression at the cardiac membrane in order to modulate the degree of electrical coupling in response to pacing but without significant functional effect.

Prolonging the pacing duration to even longer time point e.g. 12 or 24 hours may have revealed such an effect. I did not undertake such an experimental direction due to practical time constraints and additional concerns regarding fluid balance within the preparation.

Regional heterogeneities exist within the normal heart and Cx43 expression at a regional level may have important effects on cardiac electrophysiology. Pacing reduced the level of Cx43 signal area/total tissue area at the LV endocardium. It is possible that a normal heart may tolerate such subtle changes better than hearts where pre-existing disease or additional insults may be far more deleterious from an electrophysiology perspective.

To test this further I embarked on a trial to pace mice with heterozygous loss of Cx43 (Cx43$^{+/-}$) at baseline and compared them to wildtype mice and found an association with prolonged ventricular refractoriness that sustained itself despite a 2hr rest period. To investigate the prolonged refractoriness further a set of experiments to study action potentials and potassium currents were performed.

Cx43 deficient murine hearts have shorter action potential duration without differences in resting membrane potential or action potential amplitude when compared to wildtype mice. These are likely due to increased Iss and IK1 density. Pacing lengthens the duration of the action potential with a corresponding reduction in Iss but not IK1 Cx43$^{+/-}$ myocytes.

Chapter 7

Conclusions

Introduction

The work in this thesis set out to explore the effects of pacing induced cardiac dyssynchrony on gap junction remodelling in a mouse model. The effects of cardiac dyssynchrony (and the resulting aberrant ventricular activation) were studied by adapting a novel model previously used for programmed stimulation for subdiaphragmatic pacing. The functional effects of dyssynchrony were characterised in this model utilising electrocardiography, echocardiography and programmed electrical stimulation (for VERP and arrhythmia inducibility) *in vivo* in mice expressing wild type levels of Cx43, Cx43$^{+/+}$. To model clinical and animal arrhythmia disease models, where gap junction remodelling and reduced levels are observed, a group of Cx43$^{+/-}$ mice expressing 66% reduced Cx43 levels were also paced transdiaphragmatically to determine the effects of dyssynchrony.

Summary of Key Findings in this Thesis.

The key findings are listed below and address the aims and objectives set at the outset of this thesis in Chapter 1.To aid the reader they are included in this section.

Development of the pacing model:

The following findings fulfilled objectives 1,2 and 3 which were outlined in Chapter 1 and are repeated briefly here for reference:

1.To develop and refine an in vivo subdiaphragmatic murine pacing induced dyssynchrony model that allows short term pacing, with 100% stable capture, is well tolerated and reproducible without thoracic, abdominal, vascular or cardiac injury, without need for intubation and in the absence of ischaemia or hypothermia.

2. To demonstrate feasibility of the pacing protocol, undertake a set of experiments designed to test the duration of pacing tolerated in wildtype mice:

        Over the short term i.e. 15, 30, 45 and 60 mins.

        Over the longer term i.e. 4hr and 6hr.

3. To demonstrate survival of animals after 1hr pacing experiments in wildtype mice

        immediate survival experiment- 4.5hr survival study (3 half-lives)

        Long-term survival experiment-2 week survival study.

Findings

1.I have shown that murine pacing induced dyssynchrony, is feasible using the subdiaphragmatic approach, and can be safely undertaken for 1- 6hours.

2. It successfully induces electrical and mechanical dyssynchrony as evidenced by altered ECG morphology during pacing as well as late activation of the posterior LV wall on echocardiography.

3. The model has no overt disease process i.e. tachycardia induced heart failure ischaemia/infarction or direct traumatic injury.

4. It appears well tolerated as mice are able to survive their procedures for up to two weeks.

5. The macroscopic appearance of the heart and the stable thresholds, further support the absence of an overt disease process.

In Wild type Cx43$^{+/+}$ mice:

The following findings relate specifically to wildtype Cx43$^{+/+}$ mice, the objectives outlined in Chapter 1 and they are reminded here:

Objective 4. To establish whether there is any effect of subdiaphragmatic pacing on cardiac function, assess the following measurable parameters in wildtype Cx43+/+ mice

> 4.1 Characterise ECG parameters, at baseline, and after pacing at 15, 30, 45 mins, 1hr, 4hr and 6hr.

> 4.2 Characterise ECHO parameters, at baseline, during pacing and after 1hr and 6hr pacing.

> 4.3 Characterise arrhythmia inducibility testing using PES and determine the VERP, at baseline and after 1hr and 6hr pacing.

> 4.4 Characterise the pacing threshold at baseline and after 1hr, 4hr and 6hr pacing.

Objective 7. Characterise cellular electrophysiology (using patch clamp) in Cx43+/+ wildtype mice at baseline and after pacing and look at the following measurable parameters:

> 7.1 Resting membrane potential,

> 7.2 Action potential duration at 50ms and 90ms.

> 7.3 Activation and repolarisation kinetics

> 7.4 At baseline and post 6hr pacing in the Cx43$^{+/+}$ mice.

Objective 8.To determine the effects of subdiaphragmatic pacing on cardiac architecture/structure.

8.1 Macroscopic study of whole heart and cellular architecture:

After 1 hour of pacing (using HPS staining to determine macroscopically whether there are features of cellular injury due to the electrode or pacing).

8.2 Establish a semiquantitative method (using immunohistochemistry) for assessing Cx43 cellular and tissue immunofluorescence in wildtype Cx43$^{+/+}$ mice

8.2.1 Assess measurables at baseline and after 1hr, 4hr and 6hr pacing.

8.2.2 Mean Cx43 Immunofluorescence Index

8.2.3 Assess Cx43 Distribution using Cx43 immunosignal/tissue area as well as Cx43 lateralisation study

8.2.4 Cx43 plaque numbers

8.2.5 Size of Cx43 plaques.

Objective 9. Assess these parameters outlined in 8.2 in whole heart and on a regional basis to determine if there is local or spatial Cx43 heterogeneity post sham-pacing and pacing in Cx43$^{+/+}$ and Cx43$^{+/-}$ mice.

9.1 LV vs. RV

9.2 LV Base vs. Mid vs. Apex

9.3 LV septum vs. LV free wall

9.4 Epicardium vs. Mid-myocardium vs. Endocardium.

Objective 11.Characterise changes in Cx43 protein expression levels (using immunoblotting) after sham-pacing and after pacing in wildtype Cx43$^{+/+}$ mice:

11.1 At baseline and after 6hr pacing and sham-pacing

11.2. Determine Cx43 expression using immunoblotting

11.2.1. at baseline and after 6hr pacing.

11.2.2 on a regional basis

LV epicardium and endocardium.

LV free wall and LV septum

LV Base and Apex

Objective 12.Assess rates of Translation at baseline and after 6hr pacing in whole heart lysates from Cx43$^{+/+}$ mice and assess Cx43 mRNA on a regional basis (using qRT-PCR) in

12.1.   LV free wall epicardium

12.2.   LV free wall endocardium

Objective 13 Assess Cx43 distribution at baseline and after 6hr pacing using Cell fractionation techniques to assess Cx43 trafficking between membrane associated and cytosolic pools.

Objective 14 Assess degradation of Cx43 in Cx43$^{+/+}$ mice after 6hour sham-pacing and 6hr pacing using immunoblotting for ubiquitin (with Cx43 coimmunoprecipitation).

Objective 15. Examine the relationship of Cx43 with other connexin isoforms (Cx40, Cx45) and its binding partners e.g. cadherin (using immunofluorescence colocalisation methods) after 6hr sham-pacing and 6hr pacing

15.1 In wildtype mice

15.2 In Cx43$^{+/-}$ mice

Cx43$^{+/+}$ Findings:

1. Dyssynchrony alters ECG and ECHO during pacing in WT mice but there are no persistent changes after 1hr or 6hr pacing; programmed electrical stimulation demonstrates no change in VERP or inducibility into arrhythmia after 1hr or 6hr pacing. The pacing threshold remains stable after 1hr, 4hr and 6hr pacing. This addresses objectives 4 of this thesis.

2. Altered ventricular activation using pacing results in redistribution of Cx43 immunosignal at the LV endocardium with loss of the baseline transmural Cx43 gradient across the LV free wall. Regional and whole heart analysis demonstrated no differences in immunostaining when comparing the following regions in objective 9.

9.1 LV vs. RV

9.2 LV Base vs. Mid vs. Apex

9.3 LV septum vs. LV free wall.

The changes were consistent with observed Cx plaque size, numbers and distribution but no evidence of overt lateralisation was seen on immunostaining; though electron microscopy suggested that very subtle remodelling may be taking place .

3. Dysynchrony does not result in differences in Cx43 protein expression at the whole heart level after 6hr pacing and sham-pacing and when comparing regional segments. This addresses objective 11.

4. Pacing induced dyssynchrony results in reduced membrane bound Cx43 gap junctions and higher cytosolic component of Cx43 gap junctions on fractionation study. This supports objective 13.

5. Dyssynchrony does not alter the distribution of gap junction associated proteins such as cadherin, an important and critical component of the adherens junction.

6. Dyssynchrony results in significant reductions in Cx43 mRNA transcription and or stability at the epicardium and endocardium of the LV free wall.

7. Dyssynchrony appears to disrupt the process of degradation of Cx43 along the ubiquitin proteasome pathway without a discernible difference in the phosphorylation state of Cx43 suggesting this may be via an EGF independent pathway.

8. Dyssynchrony does not alter APD in wild type isolated cells after 6hr pacing or sham-pacing. There are no significant differences in the resting membrane potential or repolarisation properties in Cx43$^{+/+}$ isolated cells after 6hr pacing and sham-pacing thus addressing the aims of objective 7.

In Cx43$^{+/-}$ mice:

The following findings relate specifically to Cx43$^{+/-}$ mice and to the objectives outlined in Chapter 1 and are briefly repeated:

Objective 5.Repeat all of the measured parameters and determine functional effects in transgenic Cx43$^{+/-}$ mice:

>5.1 Characterise ECG, parameters at baseline and after 6hr pacing.

>5.2 Characterise ECHO parameters at baseline and after 6hr pacing

>5.3 Characterise arrhythmia inducibility and VERP at baseline and after 6hr pacing.

>5.4 Characterise the pacing threshold at baseline and after 6hr pacing

>5.5 Characterise functional effects, if any, and whether sustained after a period of recovery (2hr).

Objective 6.To determine the epicardial breakthrough activation pattern and conduction velocity post pacing using optical mapping in Cx43$^{+/+}$ and Cx43$^{+/-}$ mice

Objective 7.This has already been outlined above for wildtype Cx43$^{+/+}$ mice in terms of characterising cellular electrophysiology (using patch clamp) in Cx43$^{+/-}$ mice at baseline and after pacing and looking at specific measurable parameters (see objective 7 above).

Objective 8. This has already been outlined earlier for wildtype Cx43$^{+/+}$ mice and here we look at Cx43$^{+/-}$ mice in terms of determining the effects of subdiaphragmatic pacing on cardiac architecture/structure (see objective 8 above).

[231]

Objective 9. Refer to earlier on pg 232 where this is outlined in detail for Cx43$^{+/+}$ and Cx43$^{+/-}$ mice..

Objective 11.This has already been outlined earlier (refer to objective 11 above).

Objective 12.Also outlined in objective 12 earlier (see objective 12).

Objective 15.This has been outlined earlier (refer to objective 15).

Cx43$^{+/-}$ Findings:

1. There were no significant changes in ECG and ECHO data, however, dyssynchrony induces prolonged and sustained (after a 2hr rest period) refractoriness (VERP) and mechanical dyssynchrony (SPWMD) after 6hours of pacing in Cx43$^{+/-}$ hearts.

2. Dyssynchrony does not alter the epicardial sinus activation breakthrough pattern between the right and left ventricle.

3. Dyssynchrony in Cx43$^{+/-}$ mice does not alter Cx43 protein levels on immunoblotting nor Cx43 immunostaining patterns and colocalisation with its binding partner cadherin.

4. Dyssynchrony does not induce any difference in relative mRNA abundance between paced and unpaced Cx43$^{+/-}$ hearts.

5.Cx43$^{+/-}$ myocytes have shortened APD compared to paced WT isolated cells due to an increased Iss and IK1 density at baseline.

6. Dyssynchrony in Cx43$^{+/-}$ mice induces APD prolongation with reduction in Iss but not IK1 after pacing.

Mice expressing Cx40$^{+/+}$, Cx40$^{+/-}$ and Cx40 $^{-/-}$:

The role of Cx40 in cardiac arrhythmogenesis is not fully understood.

The principal structural findings from the immunosignal and colocalization study are outlined here and address objective 14 laid out in Chapter 1.

1.) No difference is observed in Cx43 expression in Cx40$^{-/-}$ mice and Cx40$^{+/+}$ mice.

2.) No significant difference is observed in Cx40 expression between LA and RA in Cx40$^{+/+}$ mice.

3.) Cx43 and Cx40 colocalise in wild type Cx40$^{+/+}$ mice with no age dependent differences

4.) Cx43 and Cx40 colocalise in wild type Cx40$^{+/+}$ mice with no RA/LA/RAA/LAA regional differences.

Clinical relevance of cardiac dyssynchrony and utility of murine model of pacing induced dyssynchrony:

This study furthers what we know in terms of small animal model pacing induced dyssynchrony and induction of gap junction remodelling with differences in the response to pacing seen in wildtype mice as compared to $Cx43^{+/-}$ mice.

In Chapter 1 I outlined the factors that modulate gap junctions both in terms of their distribution, trafficking and degradation and it is likely that there are layers of regulation and changes taking place in response to pacing with Cx43 playing a permissive role to electrical heterogeneity and changes in action potential duration.

The association of Cx43 with other proteins at the intercalated disc affects the trafficking of Connexins and there appears to be feedback to alter these proteins too. The role of altered phosphorylation state and also enzyme interactions responsible for unhooking connexin from its binding partners has been postulated as a molecular mechanism of remodelling. However, in my study there appeared to be no change in the colocalisation of Cx43 with its other isoforms and importantly the cadherin protein at the intercalated disc(51;117).

ECG,ECHO and PES ; effects of pacing induced dyssynchrony in Cx43$^{+/+}$ mice:

Interestingly, the measured data from ECG parameters and ECHO were not altered after 1hr, 4hr or 6hr asynchronous pacing in wild type mice suggesting that wild type mice did not develop any significant electrical remodelling. Nonetheless, subtle morphological changes at 1hr and 6hr suggested that prolonged pacing may have resulted in a more significant effect of long term cardiac memory as has been described in the canine pacing model (21 days of pacing were utilised). A further limitation of the study is that I was not able to measure the contribution of any functional mitral regurgitation that may have developed as a consequence of the pacing induced dyssynchrony. In addition, no haemodynamic measurements were made to invasively correlate pacing effect on cardiac pump function during pacing but Dr Gutstein and I agreed that the invasive requirement would have compromised the stability of the animal for a 6hr period. The non invasive nature of echo made it our preferred choice. Despite the gap junction remodelling that occurs in this model with redistribution of gap junctions to the intracellular pool I did not observe any sustained mechanical dyssynchrony on ECHO or ECG change with cessation of pacing. It is possible that the magnitude of change with asynchronous pacing in wild type mice is insufficient to result in significant change especially since the experiment lasted no longer than six hours in this project. This may also account for the non inducibility to arrhythmia with programmed electrical stimulation. However, in the setting of reduced levels of Cx43 as in some disease states, the effects of dyssynchrony may be far more pronounced and may work together with disease processes such as ischaemia and scarring to promote arrhythmia.

Structural remodelling

The significant reductions in Cx43 transcription and/or mRNA stability suggest that in wild type mice there is an effect on transcription that may represent a negative feedback loop mediated through Cx43 during dyssynchrony to downregulate the gap junctions at the surface and limit their expression in the longer term. This suggests that sustained pacing induced dyssynchrony may modulate gap junction intercellular communication by regulating transcription. This underscores the possibility that a longer period of pacing may have resulted in more dramatic effects to gap junction remodelling. That gap junctions should also be targeted to the ubiquitin proteasome pathway with accumulation of ubiquitinated Cx43 forms as a consequence of asynchronous pacing suggests that other regulatory steps in the degradation pathway of biotrafficking are also thrown into play in order to reduce the available gap junctions at the cell surface and presumably alter cellular coupling. Whether the observed effects in murine wild type hearts translate to human clinical studies is uncertain but this study adds to the current level of understanding dyssynchrony and its effects on gap junction remodelling and raises hypotheses that can potentially be pursued in human studies of pacing induced dyssynchrony.

Limitations

A limitation of this study is that the role of Ca2+ has not been characterised in pacing induced dyssynchrony. Alterations in the canine model of pacing induced dyssynchrony described by Spragg included a 30% reduction in sarcoplasmic Ca2+ (2). Furthermore the ischaemic (post MI) rabbit heart has been shown to demonstrate a reduction in Ca2+ transients with marked inhomogeneities(184;185). Work by Kohlhaas et al has highlighted the importance of CaMKII in sensitising the ryanodine receptor to Ca2+ by hyperphosphorylation in rabbit hearts, supporting work previously done in mice(186). The macromolecular complex of the Ryanodine Receptor and its associated proteins has been characterised by Marks et al and there is a clear relationship with phosphorylation proteins including PKA(187-190). It is unclear from the study in wild type mice whether there are changes in the Ca2+ subcellular pools or changes in the phosphoproteins activity. However, there appeared to be no difference in the level of Cx43 phosphorylation between the sham paced and paced groups suggesting that gap junctions were unaffected in terms of their phsoporylation state. Of course, we did not assess any potential differences in Ca2+ gating of gap junctions in this model as a possible mechanism for reducing coupling.

This concept in gap junction biology has become accepted though considerable debate remains regarding the electro-anatomical correlation. When connexons are visualised in tissue there exists an assumption as to their functionality (i.e. whether they are in the "open" or "closed" configuration of a pore-like channel) and this is a key limitation in the field(65).

Furthermore,there are other cell based techniques to study coupling or gap junction function using dye transfer techniques or gap junction specific patch clamp but these were not available or used to test the model in this thesis (27;58;191).

ECG,ECHO and PES; Dyssynchrony in mice expressing 66% reduced levels of Cx43.

Down-regulation of Cx43 is a common finding in a multitude of cardiac diseases and potentially contributes to the arrhythmogenic substrate. To study the effects of dyssynchrony I used a cohort of mice expressing lower levels of Cx43 at baseline.

Structural remodelling

Dyssynchrony in $Cx43^{+/-}$ mice did not alter Cx43 protein levels on immunoblotting and there is neither discernible redistribution of Cx43 on immunostaining nor disruption of colocalisation with its binding partner cadherin. This confirms that despite reduced levels of Cx43 the cadherin component of the intercalated disc structure is not remodelled and colocalises with the available Cx43. In the context of reduced levels of Cx43 it appears that there is no discernible redistribution of the available gap junctions on immunostaining and immunoblotting. However, a potential limitation of this study is that I did not perform any fractionation experiments to look for subtle redistribution as occurred in the wild type mice. However, the qRT-PCR data support the notion that Cx43 may not be altered in these animals

In terms of regulation at the protein level or transcription level since dyssynchrony did not induce any difference in relative mRNA abundance between paced and unpaced $Cx43^{+/-}$ hearts. Though speculative, it may be that in this context there is a hierarchy of regulation; once gap junction levels have been reduced there is targeting of the ion channels to reduce the coupling properties of the myocardium with dyssynchrony.

ECG,ECHO and PES

Since there was evidence of sustained mechanical dyssynchrony without ECG evidence of a bundle branch block pattern I asked Dr Morley's lab to investigate the pattern of epicardial breakthrough activation in sinus rhythm. Optical mapping experiments have been useful in characterising the local conduction patterns in mouse models including the Cx40$^{-/-}$ mouse which was shown by the Jalife group to demonstrate conduction slowing in the right bundle (178;192). Subsequent characterisation by Dr Morley looking of the Cx43$^{+/-}$ mouse did not shown any evidence of local conduction slowing (178). What isn't known is how pacing might modulate the local conduction properties in the latter group and since there was evidence of APD prolongation, sustained refractoriness and mechanical dyssynchrony a re-evaluation of this group of mice was undertaken. Dyssynchrony however does not alter the epicardial sinus activation breakthrough pattern between the right and left ventricle.

 It was particularly interesting that these animals should have prolonged refractoriness and sustained dyssynchrony even after a 2hour rest period. They demonstrated shortened APD at baseline which prolonged with asynchronous pacing. Shortened APD90 has been observed in NRVM cultured strands isolated from Cx43$^{+/-}$ hearts (193;194). The cardiac specific conditional knockout Cx43 mouse also shows a reduced APD with corresponding increased outward K currents (13). At the time of this project this was the first study to demonstrate that pacing Cx43$^{+/-}$ deficient mice alters indices of repolarisation and refractoriness and this resembles cardiac memory. Cardiac memory has been described in larger mammals such as canines and in humans but has not previously been reported in mice. However, as mentioned earlier, the mouse is not an ideal species for studying cardiac memory due to species differences in repolarising currents. However, Cx43 appears to play a role in pacing induced dyssynchrony altering repolarisation currents as these were only seen in the Cx43$^{+/-}$ hearts.

Recent work from Yoram Rudy's group on humans subjected to right ventricular pacing has also shed light on the mechanism of cardiac memory and observed increased dispersion of repolarisation gradients nearest to the pacing site(195).

In the context of dyssynchrony, the interaction between gap junctions and ion channels appears to be dynamic with Cx43 playing a permissive role in the remodelling of repolarising currents which in the context of disease can potentially create a substrate for re-entrant arrhythmias. This concept of gap junction and ion channel interactions is supported by the finding of altered repolarisation as a mechanism for arrhythmia in the Cx43 knockout mouse as well as a recent publication in 2012 from the Delmar group demonstrating Cx43 regulating Nav1.5(13).

Future directions:

Animal Studies

In animal models of infarction, pacing induced gap junction remodelling could be utilised subdiaphragmatically as a Gap junction modulator, prior to ligation of the coronary artery to assess the prevalence of acute, reperfusion and chronic MI arrhythmia burden.

Concluding remark:

The data in this thesis suggests that short-term cardiac pacing at rates just fast enough to ensure capture alters myocardial activation and induces electrical and mechanical dyssynchrony of the left ventricle in the murine heart. Limited exposure to dyssynchronous activation in wildtype Cx43 hearts, results in remodelling of the cardiac gap junctions in the absence of sustained measurable effects on contractility or arrhythmic inducibility.

Myocardial tissue with reduced baseline expression of Cx43 responds quite differently to pacing than does myocardium with wild-type levels of Cx43. This may be especially relevant in the clinical setting of cardiac disease where abundance of Cx43 is shown to be focally reduced in zones of ischaemia and hibernation. The imposition of pacing in such a clinical scenario could lead to the remodelling of repolarisation currents in regions of reduced Cx43, thus greatly enhancing dispersion of refractoriness around hibernating or ischaemic zones, potentially creating a substrate for arrhythmia reentry.

References

Reference List

(1) Patel PM, Plotnikov A, Kanagaratnam P, Shvilkin A, Sheehan CT, Xiong W, et al. Altering ventricular activation remodels gap junction distribution in canine heart. J Cardiovasc Electrophysiol 2001 May;12(5):570-7.

(2) Spragg DD, Akar FG, Helm RH, Tunin RS, Tomaselli GF, Kass DA. Abnormal conduction and repolarization in late-activated myocardium of dyssynchronously contracting hearts. Cardiovasc Res 2005 Jul 1;67(1):77-86.

(3) Kass DA. Pathobiology of cardiac dyssynchrony and resynchronization. Heart Rhythm 2009 Nov;6(11):1660-5.

(4) Spragg DD, Kass DA. Pathobiology of left ventricular dyssynchrony and resynchronization. Prog Cardiovasc Dis 2006 Jul;49(1):26-41.

(5) Severs NJ, Bruce AF, Dupont E, Rothery S. Remodelling of gap junctions and connexin expression in diseased myocardium. Cardiovasc Res 2008 Oct 1;80(1):9-19.

(6) Gutstein DE, Morley GE, Tamaddon H, Vaidya D, Schneider MD, Chen J, et al. Conduction slowing and sudden arrhythmic death in mice with cardiac-restricted inactivation of connexin43. Circ Res 2001 Feb 16;88(3):333-9.

(7) Gutstein DE, Morley GE, Vaidya D, Liu F, Chen FL, Stuhlmann H, et al. Heterogeneous expression of Gap junction channels in the heart leads to conduction defects and ventricular dysfunction. Circulation 2001 Sep 4;104(10):1194-9.

(8) Peters NS, Coromilas J, Severs NJ, Wit AL. Disturbed connexin43 gap junction distribution correlates with the location of reentrant circuits in the epicardial border zone of healing canine infarcts that cause ventricular tachycardia. Circulation 1997 Feb 18;95(4):988-96.

(9) Peters NS. New insights into myocardial arrhythmogenesis: distribution of gap-junctional coupling in normal, ischaemic and hypertrophied human hearts. Clin Sci (Lond) 1996 Jun;90(6):447-52.

(10) Beardslee MA, Laing JG, Beyer EC, Saffitz JE. Rapid turnover of connexin43 in the adult rat heart. Circ Res 1998 Sep 21;83(6):629-35.

(11) Severs NJ. Gap junction remodeling and cardiac arrhythmogenesis: cause or coincidence? J Cell Mol Med 2001 Oct;5(4):355-66.

(12) Cabo C, Yao J, Boyden PA, Chen S, Hussain W, Duffy HS, et al. Heterogeneous gap junction remodeling in reentrant circuits in the epicardial border zone of the healing canine infarct. Cardiovasc Res 2006 Nov 1;72(2):241-9.

(13) Danik SB, Rosner G, Lader J, Gutstein DE, Fishman GI, Morley GE. Electrical remodeling contributes to complex tachyarrhythmias in connexin43-deficient mouse hearts. FASEB J 2008 Apr;22(4):1204-12.

(14) Kaprielian RR, Gunning M, Dupont E, Sheppard MN, Rothery SM, Underwood R, et al. Downregulation of immunodetectable connexin43 and decreased gap junction size in the pathogenesis of chronic hibernation in the human left ventricle. Circulation 1998 Feb 24;97(7):651-60.

(15) Kitamura H, Ohnishi Y, Yoshida A, Okajima K, Azumi H, Ishida A, et al. Heterogeneous loss of connexin43 protein in nonischemic dilated cardiomyopathy with ventricular tachycardia. J Cardiovasc Electrophysiol 2002 Sep;13(9):865-70.

(16) Matsushita T, Oyamada M, Fujimoto K, Yasuda Y, Masuda S, Wada Y, et al. Remodeling of cell-cell and cell-extracellular matrix interactions at the border zone of rat myocardial infarcts. Circ Res 1999 Nov 26;85(11):1046-55.

(17) Sambelashvili AT, Nikolski VP, Efimov IR. Virtual electrode theory explains pacing threshold increase caused by cardiac tissue damage. Am J Physiol Heart Circ Physiol 2004 Jun;286(6):H2183-H2194.

(18) Angst BD, Khan LU, Severs NJ, Whitely K, Rothery S, Thompson RP, et al. Dissociated spatial patterning of gap junctions and cell adhesion junctions during postnatal differentiation of ventricular myocardium. Circ Res 1997 Jan;80(1):88-94.

(19) Coppen SR, Kaba RA, Halliday D, Dupont E, Skepper JN, Elneil S, et al. Comparison of connexin expression patterns in the developing mouse heart and human foetal heart. Mol Cell Biochem 2003 Jan;242(1-2):121-7.

(20) Strik M, van Middendorp LB, Vernooy K. Animal models of dyssynchrony. J Cardiovasc Transl Res 2012 Apr;5(2):135-45.

(21) Auricchio A, Regoli F. Past, present, and future of CRT. Heart Fail Rev 2011 May;16(3):205-14.

(22) Spragg DD, Kass DA. Pathobiology of left ventricular dyssynchrony and resynchronization. Prog Cardiovasc Dis 2006 Jul;49(1):26-41.

(23) Strik M, van Middendorp LB, Vernooy K. Animal models of dyssynchrony. J Cardiovasc Transl Res 2012 Apr;5(2):135-45.

(24) Freudenberger RS, Wilson AC, Lawrence-Nelson J, Hare JM, Kostis JB. Permanent pacing is a risk factor for the development of heart failure. Am J Cardiol 2005 Mar 1;95(5):671-4.

(25) Kapa S, Bruce CJ, Friedman PA, Asirvatham SJ. Advances in Cardiac Pacing: Beyond the Transvenous Right Ventricular Apical Lead. Cardiovasc Ther 2010 Jun 11.

(26) van Deursen CJ, Strik M, Rademakers LM, van HA, Kuiper M, Wecke L, et al. Vectorcardiography as a tool for easy optimization of cardiac resynchronization therapy in canine left bundle branch block hearts. Circ Arrhythm Electrophysiol 2012 Jun 1;5(3):544-52.

[245]

(27) Saez JC, Berthoud VM, Branes MC, Martinez AD, Beyer EC. Plasma membrane channels formed by connexins: their regulation and functions. Physiol Rev 2003 Oct;83(4):1359-400.

(28) Kumar NM, Gilula NB. The gap junction communication channel. Cell 1996 Feb 9;84(3):381-8.

(29) Buehler LK, Stauffer KA, Gilula NB, Kumar NM. Single channel behavior of recombinant beta 2 gap junction connexons reconstituted into planar lipid bilayers. Biophys J 1995 May;68(5):1767-75.

(30) Yeager M, Gilula NB. Membrane topology and quaternary structure of cardiac gap junction ion channels. J Mol Biol 1992 Feb 20;223(4):929-48.

(31) Milks LC, Kumar NM, Houghten R, Unwin N, Gilula NB. Topology of the 32-kd liver gap junction protein determined by site-directed antibody localizations. EMBO J 1988 Oct;7(10):2967-75.

(32) Benedetti EL, Emmelot P. Electron microscopic observations on negatively stained plasma membranes isolated from rat liver. J Cell Biol 1965 Jul;26(1):299-305.

(33) Robertson JD. The occurrence of a subunit pattern in the unit membranes of club endings in Mauthner cell synapses in goldfish brains.. J Cell Biol 1963 Oct;19:201-21.

(34) Revel JP, Karnovsky MJ. Hexagonal array of subunits in intercellular junctions of the mouse heart and liver. J Cell Biol 1967 Jun;33(3):C7-C12.

(35) Beyer EC, Paul DL, Goodenough DA. Connexin43: a protein from rat heart homologous to a gap junction protein from liver. J Cell Biol 1987 Dec;105(6 Pt 1):2621-9.

(36) Beyer EC, Paul DL, Goodenough DA. Connexin family of gap junction proteins. J Membr Biol 1990 Jul;116(3):187-94.

(37) Weidmann S. The electrical constants of Purkinje fibres. J Physiol 1952 Nov;118(3):348-60.

(38) Barr L, Dewey MM, Berger W. Propagation of Action potentials and the structure of the nexus in cardiac muscle. J Gen Physiol 1965 May;48:797-823.

(39) Paul DL. Molecular cloning of cDNA for rat liver gap junction protein. J Cell Biol 1986 Jul;103(1):123-34.

(40) Zhang JT, Nicholson BJ. Sequence and tissue distribution of a second protein of hepatic gap junctions, Cx26, as deduced from its cDNA. J Cell Biol 1989 Dec;109(6 Pt 2):3391-401.

(41) Zhang JT, Nicholson BJ. The topological structure of connexin 26 and its distribution compared to connexin 32 in hepatic gap junctions. J Membr Biol 1994 Apr;139(1):15-29.

(42) Beyer EC, Davis LM, Saffitz JE, Veenstra RD. Cardiac intercellular communication: consequences of connexin distribution and diversity. Braz J Med Biol Res 1995 Apr;28(4):415-25.

(43) Moreno AP. Biophysical properties of homomeric and heteromultimeric channels formed by cardiac connexins. Cardiovasc Res 2004 May 1;62(2):276-86.

(44) Severs NJ, Rothery S, Dupont E, Coppen SR, Yeh HI, Ko YS, et al. Immunocytochemical analysis of connexin expression in the healthy and diseased cardiovascular system. Microsc Res Tech 2001 Feb 1;52(3):301-22.

(45) Severs NJ. Gap junction remodeling and cardiac arrhythmogenesis: cause or coincidence? J Cell Mol Med 2001 Oct;5(4):355-66.

(46) Hombach S, Janssen-Bienhold U, Sohl G, Schubert T, Bussow H, Ott T, et al. Functional expression of connexin57 in horizontal cells of the mouse retina. Eur J Neurosci 2004 May;19(10):2633-40.

(47) Kelsell DP, Dunlop J, Stevens HP, Lench NJ, Liang JN, Parry G, et al. Connexin 26 mutations in hereditary non-syndromic sensorineural deafness. Nature 1997 May 1;387(6628):80-3.

(48) Carrasquillo MM, Zlotogora J, Barges S, Chakravarti A. Two different connexin 26 mutations in an inbred kindred segregating non-syndromic recessive deafness: implications for genetic studies in isolated populations. Hum Mol Genet 1997 Nov;6(12):2163-72.

(49) Gerido DA, White TW. Connexin disorders of the ear, skin, and lens. Biochim Biophys Acta 2004 Mar 23;1662(1-2):159-70.

(50) White TW. Nonredundant gap junction functions. News Physiol Sci 2003 Jun;18:95-9.

(51) Laird DW. Life cycle of connexins in health and disease. Biochem J 2006 Mar 15;394(Pt 3):527-43.

(52) Heynkes R, Kozjek G, Traub O, Willecke K. Identification of a rat liver cDNA and mRNA coding for the 28 kDa gap junction protein. FEBS Lett 1986 Sep 1;205(1):56-60.

(53) Paul DL. Molecular cloning of cDNA for rat liver gap junction protein. J Cell Biol 1986 Jul;103(1):123-34.

(54) Hertzberg EL, Disher RM, Tiller AA, Zhou Y, Cook RG. Topology of the Mr 27,000 liver gap junction protein. Cytoplasmic localization of amino- and carboxyl termini and a hydrophilic domain which is protease-hypersensitive. J Biol Chem 1988 Dec 15;263(35):19105-11.

(55) Quist AP, Rhee SK, Lin H, Lal R. Physiological role of gap-junctional hemichannels. Extracellular calcium-dependent isosmotic volume regulation. J Cell Biol 2000 Mar 6;148(5):1063-74.

(56) Yancey SB, John SA, Lal R, Austin BJ, Revel JP. The 43-kD polypeptide of heart gap junctions: immunolocalization, topology, and functional domains. J Cell Biol 1989 Jun;108(6):2241-54.

(57) Zimmer DB, Green CR, Evans WH, Gilula NB. Topological analysis of the major protein in isolated intact rat liver gap junctions and gap junction-derived single membrane structures. J Biol Chem 1987 Jun 5;262(16):7751-63.

(58) Desplantez T, Dupont E, Severs NJ, Weingart R. Gap junction channels and cardiac impulse propagation. J Membr Biol 2007 Aug;218(1-3):13-28.

(59) Desplantez T, Dupont E, Severs NJ, Weingart R. Gap junction channels and cardiac impulse propagation. J Membr Biol 2007 Aug;218(1-3):13-28.

(60) Severs NJ, Coppen SR, Dupont E, Yeh HI, Ko YS, Matsushita T. Gap junction alterations in human cardiac disease. Cardiovasc Res 2004 May 1;62(2):368-77.

(61) Beyer EC, Gemel J, Martinez A, Berthoud VM, Valiunas V, Moreno AP, et al. Heteromeric mixing of connexins: compatibility of partners and functional consequences. Cell Commun Adhes 2001;8(4-6):199-204.

(62) Martinez AD, Hayrapetyan V, Moreno AP, Beyer EC. Connexin43 and connexin45 form heteromeric gap junction channels in which individual components determine permeability and regulation. Circ Res 2002 May 31;90(10):1100-7.

(63) Beyer EC, Gemel J, Seul KH, Larson DM, Banach K, Brink PR. Modulation of intercellular communication by differential regulation and heteromeric mixing of co-expressed connexins. Braz J Med Biol Res 2000 Apr;33(4):391-7.

(64) Loewenstein WR. Junctional intercellular communication: the cell-to-cell membrane channel. Physiol Rev 1981 Oct;61(4):829-913.

(65) Severs NJ, Bruce AF, Dupont E, Rothery S. Remodelling of gap junctions and connexin expression in diseased myocardium. Cardiovasc Res 2008 Oct 1;80(1):9-19.

(66) Laird DW. The life cycle of a connexin: gap junction formation, removal, and degradation. J Bioenerg Biomembr 1996 Aug;28(4):311-8.

(67) Crow DS, Beyer EC, Paul DL, Kobe SS, Lau AF. Phosphorylation of connexin43 gap junction protein in uninfected and Rous sarcoma virus-transformed mammalian fibroblasts. Mol Cell Biol 1990 Apr;10(4):1754-63.

(68) Filson AJ, Azarnia R, Beyer EC, Loewenstein WR, Brugge JS. Tyrosine phosphorylation of a gap junction protein correlates with inhibition of cell-to-cell communication. Cell Growth Differ 1990 Dec;1(12):661-8.

(69) Musil LS, Beyer EC, Goodenough DA. Expression of the gap junction protein connexin43 in embryonic chick lens: molecular cloning, ultrastructural localization, and post-translational phosphorylation. J Membr Biol 1990 Jun;116(2):163-75.

(70) Musil LS, Cunningham BA, Edelman GM, Goodenough DA. Differential phosphorylation of the gap junction protein connexin43 in junctional communication-competent and -deficient cell lines. J Cell Biol 1990 Nov;111(5 Pt 1):2077-88.

(71) Laird DW, Castillo M, Kasprzak L. Gap junction turnover, intracellular trafficking, and phosphorylation of connexin43 in brefeldin A-treated rat mammary tumor cells. J Cell Biol 1995 Dec;131(5):1193-203.

(72) Puranam KL, Laird DW, Revel JP. Trapping an intermediate form of connexin43 in the Golgi. Exp Cell Res 1993 May;206(1):85-92.

(73) Das SJ, Wang F, Koval M. Targeted gap junction protein constructs reveal connexin-specific differences in oligomerization. J Biol Chem 2002 Jun 7;277(23):20911-8.

(74) Diez JA, Ahmad S, Evans WH. Assembly of heteromeric connexons in guinea-pig liver en route to the Golgi apparatus, plasma membrane and gap junctions. Eur J Biochem 1999 May;262(1):142-8.

(75) Martin PE, Blundell G, Ahmad S, Errington RJ, Evans WH. Multiple pathways in the trafficking and assembly of connexin 26, 32 and 43 into gap junction intercellular communication channels. J Cell Sci 2001 Nov;114(Pt 21):3845-55.

(76) Musil LS, Goodenough DA. Multisubunit assembly of an integral plasma membrane channel protein, gap junction connexin43, occurs after exit from the ER. Cell 1993 Sep 24;74(6):1065-77.

(77) Rahman S, Carlile G, Evans WH. Assembly of hepatic gap junctions. Topography and distribution of connexin 32 in intracellular and plasma membranes determined using sequence-specific antibodies. J Biol Chem 1993 Jan 15;268(2):1260-5.

(78) Ahmad S, Evans WH. Post-translational integration and oligomerization of connexin 26 in plasma membranes and evidence of formation of membrane pores: implications for the assembly of gap junctions. Biochem J 2002 Aug 1;365(Pt 3):693-9.

(79) Smyth JW, Vogan JM, Buch PJ, Zhang SS, Fong TS, Hong TT, et al. Actin cytoskeleton rest stops regulate anterograde traffic of connexin 43 vesicles to the plasma membrane. Circ Res 2012 Mar 30;110(7):978-89.

(80) George CH, Kendall JM, Evans WH. Intracellular trafficking pathways in the assembly of connexins into gap junctions. J Biol Chem 1999 Mar 26;274(13):8678-85.

(81) Martin PE, Blundell G, Ahmad S, Errington RJ, Evans WH. Multiple pathways in the trafficking and assembly of connexin 26, 32 and 43 into gap junction intercellular communication channels. J Cell Sci 2001 Nov;114(Pt 21):3845-55.

(82) Smyth JW, Shaw RM. The gap junction life cycle. Heart Rhythm 2012 Jan;9(1):151-3.

(83) Shaw RM, Fay AJ, Puthenveedu MA, von ZM, Jan YN, Jan LY. Microtubule plus-end-tracking proteins target gap junctions directly from the cell interior to adherens junctions. Cell 2007 Feb 9;128(3):547-60.

(84) Smyth JW, Shaw RM. Forward trafficking of ion channels: what the clinician needs to know. Heart Rhythm 2010 Aug;7(8):1135-40.

(85) Smyth JW, Hong TT, Gao D, Vogan JM, Jensen BC, Fong TS, et al. Limited forward trafficking of connexin 43 reduces cell-cell coupling in stressed human and mouse myocardium. J Clin Invest 2010 Jan;120(1):266-79.

(86) Lauf U, Giepmans BN, Lopez P, Braconnot S, Chen SC, Falk MM. Dynamic trafficking and delivery of connexons to the plasma membrane and accretion to gap junctions in living cells. Proc Natl Acad Sci U S A 2002 Aug 6;99(16):10446-51.

(87) Fujimoto K, Nagafuchi A, Tsukita S, Kuraoka A, Ohokuma A, Shibata Y. Dynamics of connexins, E-cadherin and alpha-catenin on cell membranes during gap junction formation. J Cell Sci 1997 Feb;110 (Pt 3):311-22.

[249]

(88)	Jongen WM, Fitzgerald DJ, Asamoto M, Piccoli C, Slaga TJ, Gros D, et al. Regulation of connexin 43-mediated gap junctional intercellular communication by Ca2+ in mouse epidermal cells is controlled by E-cadherin. J Cell Biol 1991 Aug;114(3):545-55.

(89)	Saez JC, Berthoud VM, Branes MC, Martinez AD, Beyer EC. Plasma membrane channels formed by connexins: their regulation and functions. Physiol Rev 2003 Oct;83(4):1359-400.

(90)	Meyer RA, Laird DW, Revel JP, Johnson RG. Inhibition of gap junction and adherens junction assembly by connexin and A-CAM antibodies. J Cell Biol 1992 Oct;119(1):179-89.

(91)	Flores CE, Nannapaneni S, Davidson KG, Yasumura T, Bennett MV, Rash JE, et al. Trafficking of gap junction channels at a vertebrate electrical synapse in vivo. Proc Natl Acad Sci U S A 2012 Feb 28;109(9):E573-E582.

(92)	Simek J, Churko J, Shao Q, Laird DW. Cx43 has distinct mobility within plasma-membrane domains, indicative of progressive formation of gap-junction plaques. J Cell Sci 2009 Feb 15;122(Pt 4):554-62.

(93)	Laird DW, Puranam KL, Revel JP. Turnover and phosphorylation dynamics of connexin43 gap junction protein in cultured cardiac myocytes. Biochem J 1991 Jan 1;273(Pt 1):67-72.

(94)	Fallon RF, Goodenough DA. Five-hour half-life of mouse liver gap-junction protein. J Cell Biol 1981 Aug;90(2):521-6.

(95)	Musil LS, Le AC, VanSlyke JK, Roberts LM. Regulation of connexin degradation as a mechanism to increase gap junction assembly and function. J Biol Chem 2000 Aug 18;275(33):25207-15.

(96)	Beyer EC, Berthoud VM. Gap junction synthesis and degradation as therapeutic targets. Curr Drug Targets 2002 Dec;3(6):409-16.

(97)	Jordan K, Chodock R, Hand AR, Laird DW. The origin of annular junctions: a mechanism of gap junction internalization. J Cell Sci 2001 Feb;114(Pt 4):763-73.

(98)	Larsen WJ. Biological implications of gap junction structure, distribution and composition: a review. Tissue Cell 1983;15(5):645-71.

(99)	Mazet F, Wittenberg BA, Spray DC. Fate of intercellular junctions in isolated adult rat cardiac cells. Circ Res 1985 Feb;56(2):195-204.

(100)	Murray SA, Larsen WJ, Trout J, Donta ST. Gap junction assembly and endocytosis correlated with patterns of growth in a cultured adrenocortical tumor cell (SW-13). Cancer Res 1981 Oct;41(10):4063-74.

(101)	Catarino S, Ramalho JS, Marques C, Pereira P, Girao H. Ubiquitin-mediated internalization of connexin43 is independent of the canonical endocytic tyrosine-sorting signal. Biochem J 2011 Jul 15;437(2):255-67.

(102)	Kelly SM, VanSlyke JK, Musil LS. Regulation of ubiquitin-proteasome system mediated degradation by cytosolic stress. Mol Biol Cell 2007 Nov;18(11):4279-91.

(103) Kjenseth A, Fykerud T, Rivedal E, Leithe E. Regulation of gap junction intercellular communication by the ubiquitin system. Cell Signal 2010 Sep;22(9):1267-73.

(104) Laing JG, Beyer EC. The gap junction protein connexin43 is degraded via the ubiquitin proteasome pathway. J Biol Chem 1995 Nov 3;270(44):26399-403.

(105) Leithe E, Kjenseth A, Sirnes S, Stenmark H, Brech A, Rivedal E. Ubiquitylation of the gap junction protein connexin-43 signals its trafficking from early endosomes to lysosomes in a process mediated by Hrs and Tsg101. J Cell Sci 2009 Nov 1;122(Pt 21):3883-93.

(106) Leithe E, Rivedal E. Ubiquitination of gap junction proteins. J Membr Biol 2007 Jun;217(1-3):43-51.

(107) Leithe E, Rivedal E. Ubiquitination and down-regulation of gap junction protein connexin-43 in response to 12-O-tetradecanoylphorbol 13-acetate treatment. J Biol Chem 2004 Nov 26;279(48):50089-96.

(108) Leithe E, Rivedal E. Epidermal growth factor regulates ubiquitination, internalization and proteasome-dependent degradation of connexin43. J Cell Sci 2004 Mar 1;117(Pt 7):1211-20.

(109) Saez JC, Nairn AC, Czernik AJ, Fishman GI, Spray DC, Hertzberg EL. Phosphorylation of connexin43 and the regulation of neonatal rat cardiac myocyte gap junctions. J Mol Cell Cardiol 1997 Aug;29(8):2131-45.

(110) Saez JC, Martinez AD, Branes MC, Gonzalez HE. Regulation of gap junctions by protein phosphorylation. Braz J Med Biol Res 1998 May;31(5):593-600.

(111) Dhein S. Pharmacology of gap junctions in the cardiovascular system. Cardiovasc Res 2004 May 1;62(2):287-98.

(112) Lampe PD, Lau AF. The effects of connexin phosphorylation on gap junctional communication. Int J Biochem Cell Biol 2004 Jul;36(7):1171-86.

(113) Ingebritsen TS, Cohen P. The protein phosphatases involved in cellular regulation. 1. Classification and substrate specificities. Eur J Biochem 1983 May 2;132(2):255-61.

(114) Cohen PT. Novel protein serine/threonine phosphatases: variety is the spice of life. Trends Biochem Sci 1997 Jul;22(7):245-51.

(115) Saez JC, Nairn AC, Czernik AJ, Spray DC, Hertzberg EL, Greengard P, et al. Phosphorylation of connexin 32, a hepatocyte gap-junction protein, by cAMP-dependent protein kinase, protein kinase C and Ca2+/calmodulin-dependent protein kinase II. Eur J Biochem 1990 Sep 11;192(2):263-73.

(116) Saez JC, Spray DC, Nairn AC, Hertzberg E, Greengard P, Bennett MV. cAMP increases junctional conductance and stimulates phosphorylation of the 27-kDa principal gap junction polypeptide. Proc Natl Acad Sci U S A 1986 Apr;83(8):2473-7.

(117) Laird DW. The gap junction proteome and its relationship to disease. Trends Cell Biol 2010 Feb;20(2):92-101.

(118) Britz-Cunningham SH, Shah MM, Zuppan CW, Fletcher WH. Mutations of the Connexin43 gap-junction gene in patients with heart malformations and defects of laterality. N Engl J Med 1995 May 18;332(20):1323-9.

(119) Dasgupta C, Martinez AM, Zuppan CW, Shah MM, Bailey LL, Fletcher WH. Identification of connexin43 (alpha1) gap junction gene mutations in patients with hypoplastic left heart syndrome by denaturing gradient gel electrophoresis (DGGE). Mutat Res 2001 Aug 8;479(1-2):173-86.

(120) Paznekas WA, Boyadjiev SA, Shapiro RE, Daniels O, Wollnik B, Keegan CE, et al. Connexin 43 (GJA1) mutations cause the pleiotropic phenotype of oculodentodigital dysplasia. Am J Hum Genet 2003 Feb;72(2):408-18.

(121) Dobrowolski R, Sasse P, Schrickel JW, Watkins M, Kim JS, Rackauskas M, et al. The conditional connexin43G138R mouse mutant represents a new model of hereditary oculodentodigital dysplasia in humans. Hum Mol Genet 2008 Feb 15;17(4):539-54.

(122) Kalcheva N, Qu J, Sandeep N, Garcia L, Zhang J, Wang Z, et al. Gap junction remodeling and cardiac arrhythmogenesis in a murine model of oculodentodigital dysplasia. Proc Natl Acad Sci U S A 2007 Dec 18;104(51):20512-6.

(123) Christiansen J, Dyck JD, Elyas BG, Lilley M, Bamforth JS, Hicks M, et al. Chromosome 1q21.1 contiguous gene deletion is associated with congenital heart disease. Circ Res 2004 Jun 11;94(11):1429-35.

(124) Hauer RN, Groenewegen WA, Firouzi M, Ramanna H, Jongsma HJ. Cx40 polymorphism in human atrial fibrillation. Adv Cardiol 2006;42:284-91.

(125) Gollob MH, Jones DL, Krahn AD, Danis L, Gong XQ, Shao Q, et al. Somatic mutations in the connexin 40 gene (GJA5) in atrial fibrillation. N Engl J Med 2006 Jun 22;354(25):2677-88.

(126) Matsushita T, Oyamada M, Fujimoto K, Yasuda Y, Masuda S, Wada Y, et al. Remodeling of cell-cell and cell-extracellular matrix interactions at the border zone of rat myocardial infarcts. Circ Res 1999 Nov 26;85(11):1046-55.

(127) Lampe PD, Cooper CD, King TJ, Burt JM. Analysis of Connexin43 phosphorylated at S325, S328 and S330 in normoxic and ischemic heart. J Cell Sci 2006 Aug 15;119(Pt 16):3435-42.

(128) Li F, Sugishita K, Su Z, Ueda I, Barry WH. Activation of connexin-43 hemichannels can elevate [Ca(2+)]i and [Na(+)]i in rabbit ventricular myocytes during metabolic inhibition. J Mol Cell Cardiol 2001 Dec;33(12):2145-55.

(129) Evans WH, De VE, Leybaert L. The gap junction cellular internet: connexin hemichannels enter the signalling limelight. Biochem J 2006 Jul 1;397(1):1-14.

(130) Spray DC, Ye ZC, Ransom BR. Functional connexin "hemichannels": a critical appraisal. Glia 2006 Nov 15;54(7):758-73.

(131) Garcia-Dorado D, Rodriguez-Sinovas A, Ruiz-Meana M. Gap junction-mediated spread of cell injury and death during myocardial ischemia-reperfusion. Cardiovasc Res 2004 Feb 15;61(3):386-401.

(132)   Garcia-Dorado D, Inserte J, Ruiz-Meana M, Gonzalez MA, Solares J, Julia M, et al. Gap junction uncoupler heptanol prevents cell-to-cell progression of hypercontracture and limits necrosis during myocardial reperfusion. Circulation 1997 Nov 18;96(10):3579-86.

(133)   Ruiz-Meana M, Rodriguez-Sinovas A, Cabestrero A, Boengler K, Heusch G, Garcia-Dorado D. Mitochondrial connexin43 as a new player in the pathophysiology of myocardial ischaemia-reperfusion injury. Cardiovasc Res 2008 Jan 15;77(2):325-33.

(134)   Haugan K, Marcussen N, Kjolbye AL, Nielsen MS, Hennan JK, Petersen JS. Treatment with the gap junction modifier rotigaptide (ZP123) reduces infarct size in rats with chronic myocardial infarction. J Cardiovasc Pharmacol 2006 Feb;47(2):236-42.

(135)   Hennan JK, Swillo RE, Morgan GA, Keith JC, Jr., Schaub RG, Smith RP, et al. Rotigaptide (ZP123) prevents spontaneous ventricular arrhythmias and reduces infarct size during myocardial ischemia/reperfusion injury in open-chest dogs. J Pharmacol Exp Ther 2006 Apr;317(1):236-43.

(136)   Kjolbye AL, Haugan K, Hennan JK, Petersen JS. Pharmacological modulation of gap junction function with the novel compound rotigaptide: a promising new principle for prevention of arrhythmias. Basic Clin Pharmacol Toxicol 2007 Oct;101(4):215-30.

(137)   Allessie M, Ausma J, Schotten U. Electrical, contractile and structural remodeling during atrial fibrillation. Cardiovasc Res 2002 May;54(2):230-46.

(138)   Dhein S. Role of connexins in atrial fibrillation. Adv Cardiol 2006;42:161-74.

(139)   Ohara T, Qu Z, Lee MH, Ohara K, Omichi C, Mandel WJ, et al. Increased vulnerability to inducible atrial fibrillation caused by partial cellular uncoupling with heptanol. Am J Physiol Heart Circ Physiol 2002 Sep;283(3):H1116-H1122.

(140)   Ryu K, Li L, Khrestian CM, Matsumoto N, Sahadevan J, Ruehr ML, et al. Effects of sterile pericarditis on connexins 40 and 43 in the atria: correlation with abnormal conduction and atrial arrhythmias. Am J Physiol Heart Circ Physiol 2007 Aug;293(2):H1231-H1241.

(141)   Dupont E, Ko Y, Rothery S, Coppen SR, Baghai M, Haw M, et al. The gap-junctional protein connexin40 is elevated in patients susceptible to postoperative atrial fibrillation. Circulation 2001 Feb 13;103(6):842-9.

(142)   Juang JM, Chern YR, Tsai CT, Chiang FT, Lin JL, Hwang JJ, et al. The association of human connexin 40 genetic polymorphisms with atrial fibrillation. Int J Cardiol 2007 Mar 2;116(1):107-12.

(143)   Sawaya SE, Rajawat YS, Rami TG, Szalai G, Price RL, Sivasubramanian N, et al. Downregulation of connexin40 and increased prevalence of atrial arrhythmias in transgenic mice with cardiac-restricted overexpression of tumor necrosis factor. Am J Physiol Heart Circ Physiol 2007 Mar;292(3):H1561-H1567.

(144)   Andersen HR, Nielsen JC, Thomsen PE, Thuesen L, Mortensen PT, Vesterlund T, et al. Long-term follow-up of patients from a randomised trial of atrial versus ventricular pacing for sick-sinus syndrome. Lancet 1997 Oct 25;350(9086):1210-6.

(145)   Connolly SJ, Kerr CR, Gent M, Roberts RS, Yusuf S, Gillis AM, et al. Effects of physiologic pacing versus ventricular pacing on the risk of stroke and death due to cardiovascular causes. Canadian Trial of Physiologic Pacing Investigators. N Engl J Med 2000 May 11;342(19):1385-91.

(146)   Lamas GA, Lee KL, Sweeney MO, Silverman R, Leon A, Yee R, et al. Ventricular pacing or dual-chamber pacing for sinus-node dysfunction. N Engl J Med 2002 Jun 13;346(24):1854-62.

(147)   Baba S, Dun W, Cabo C, Boyden PA. Remodeling in cells from different regions of the reentrant circuit during ventricular tachycardia. Circulation 2005 Oct 18;112(16):2386-96.

(148)   Danik SB, Liu F, Zhang J, Suk HJ, Morley GE, Fishman GI, et al. Modulation of cardiac gap junction expression and arrhythmic susceptibility. Circ Res 2004 Nov 12;95(10):1035-41.

(149)   Wit AL. Remodeling of cardiac gap junctions: the relationship to the genesis of ventricular tachycardia. J Electrocardiol 2001;34 Suppl:77-83.

(150)   Laird DW. Life cycle of connexins in health and disease. Biochem J 2006 Mar 15;394(Pt 3):527-43.

(151)   Gutstein DE, Danik SB, Sereysky JB, Morley GE, Fishman GI. Subdiaphragmatic murine electrophysiological studies: sequential determination of ventricular refractoriness and arrhythmia induction. Am J Physiol Heart Circ Physiol 2003 Sep;285(3):H1091-H1096.

(152)   Kontogeorgis A, Kaba RA, Kang E, Feig JE, Gupta PP, Ponzio M, et al. Short-term pacing in the mouse alters cardiac expression of connexin43. BMC Physiol 2008;8:8.

(153)   Waller AD. A demonstration of man of electromotive changes accompanying the heart's beat. Ann Noninvasive Electrocardiol 2004 Apr;9(2):189-91.

(154)   Lewis T. The time relations of heart sounds and murmurs with special reference to the acoustic signs in mitral stenosis. Heart 4, 241. 1-1-1912.

(155)   Bazett H. An analysis of the time relations of electrocardiograms. Annals of Noninvasive Electrocardiology 2[2], 177-194. 1-4-1997.

(156)   Wiggers CJ. Circulation in Health and Disease. Philadelphia: Lea and Febiger; 1923.

(157)   Berul CI. In Vivo Cardiac Electrophysiology Studies in the Mouse. Circulation [94], 2641-2648. 19-8-1996.

(158)   Gutstein DE, Danik SB, Lewitton S, France D, Liu F, Chen FL, et al. Focal gap junction uncoupling and spontaneous ventricular ectopy. Am J Physiol Heart Circ Physiol 2005 Sep;289(3):H1091-H1098.

(159)   Danik SB, Cabo C, Chiello C, Kang S, Wit AL, Coromilas J. Correlation of repolarization of ventricular monophasic action potential with ECG in the murine heart. Am J Physiol Heart Circ Physiol 283[1], 372-381. 1-7-2002.

[254]

(160)   Nerbonne JM, Kass RS. Molecular physiology of cardiac repolarization. Physiol Rev 2005 Oct;85(4):1205-53.

(161)   Kontogeorgis A, Li X, Kang EY, Feig JE, Ponzio M, Kang G, et al. Decreased connexin43 expression in the mouse heart potentiates pacing-induced remodeling of repolarizing currents. Am J Physiol Heart Circ Physiol 2008 Nov;295(5):H1905-H1916.

(162)   Feigenbaum H. Evolution of Echocardiography. Circulation 93, 1321-1327. 1996.

(163)   Abraham WT, Fisher WG, Smith AL, DeLurgio DB, Leon AR, Loh E, et al. Cardiac resynchronization in chronic heart failure. N Engl J Med 2002 Jun 13;346(24):1845-53.

(164)   Cleland JG, Daubert JC, Erdmann E, Freemantle N, Gras D, Kappenberger L, et al. The effect of cardiac resynchronization on morbidity and mortality in heart failure. N Engl J Med 2005 Apr 14;352(15):1539-49.

(165)   Higgins SL, Hummel JD, Niazi IK, Giudici MC, Worley SJ, Saxon LA, et al. Cardiac resynchronization therapy for the treatment of heart failure in patients with intraventricular conduction delay and malignant ventricular tachyarrhythmias. J Am Coll Cardiol 2003 Oct 15;42(8):1454-9.

(166)   Kostin S, Dammer S, Hein S, Klovekorn WP, Bauer EP, Schaper J. Connexin 43 expression and distribution in compensated and decompensated cardiac hypertrophy in patients with aortic stenosis. Cardiovasc Res 2004 May 1;62(2):426-36.

(167)   Pitzalis MV, Iacoviello M, Romito R, Massari F, Rizzon B, Luzzi G, et al. Cardiac resynchronization therapy tailored by echocardiographic evaluation of ventricular asynchrony. J Am Coll Cardiol 2002 Nov 6;40(9):1615-22.

(168)   Liu L, Tockman B, Girouard S, Pastore J, Walcott G, KenKnight B, et al. Left ventricular resynchronization therapy in a canine model of left bundle branch block. Am J Physiol Heart Circ Physiol 2002 Jun;282(6):H2238-H2244.

(169)   Prinzen FW, Hunter WC, Wyman BT, McVeigh ER. Mapping of regional myocardial strain and work during ventricular pacing: experimental study using magnetic resonance imaging tagging. J Am Coll Cardiol 1999 May;33(6):1735-42.

(170)   Siu CW, Wang M, Zhang XH, Lau CP, Tse HF. Analysis of ventricular performance as a function of pacing site and mode. Prog Cardiovasc Dis 2008 Sep;51(2):171-82.

(171)   Wellens H J. Value and limitations of programmed electrical stimulation of the heart in the study and treatment of tachycardias. Circulation 57, 845-853. 1978.

(172)   Nerheim P, Birger-Botkin S, Piracha L, Olshansky B. Heart failure and sudden death in patients with tachycardia-induced cardiomyopathy and recurrent tachycardia. Circulation 2004 Jul 20;110(3):247-52.

(173)   O'Rourke B, Kass DA, Tomaselli GF, Kaab S, Tunin R, Marban E. Mechanisms of altered excitation-contraction coupling in canine tachycardia-induced heart failure, I: experimental studies. Circ Res 1999 Mar 19;84(5):562-70.

[255]

(174) Pak PH, Nuss HB, Tunin RS, Kaab S, Tomaselli GF, Marban E, et al. Repolarization abnormalities, arrhythmia and sudden death in canine tachycardia-induced cardiomyopathy. J Am Coll Cardiol 1997 Aug;30(2):576-84.

(175) Shinbane JS, Wood MA, Jensen DN, Ellenbogen KA, Fitzpatrick AP, Scheinman MM. Tachycardia-induced cardiomyopathy: a review of animal models and clinical studies. J Am Coll Cardiol 1997 Mar 15;29(4):709-15.

(176) Apkon M, Nerbonne JM. Characterization of two distinct depolarization-activated K+ currents in isolated adult rat ventricular myocytes. J Gen Physiol 1991 May;97(5):973-1011.

(177) Nakamura TY, Coetzee WA, Vega-Saenz De ME, Artman M, Rudy B. Modulation of Kv4 channels, key components of rat ventricular transient outward K+ current, by PKC. Am J Physiol 1997 Oct;273(4 Pt 2):H1775-H1786.

(178) Morley GE, Vaidya D, Samie FH, Lo C, Delmar M, Jalife J. Characterization of conduction in the ventricles of normal and heterozygous Cx43 knockout mice using optical mapping. J Cardiovasc Electrophysiol 1999 Oct;10(10):1361-75.

(179) Kontogeorgis A, Kaba RA, Kang E, Feig JE, Gupta PP, Ponzio M, et al. Short-term pacing in the mouse alters cardiac expression of connexin43. BMC Physiol 2008;8:8.

(180) Ibarra J, Morley GE, Delmar M. Dynamics of the inward rectifier K+ current during the action potential of guinea pig ventricular myocytes. Biophys J 1991 Dec;60(6):1534-9.

(181) Apkon M, Nerbonne JM. Characterization of two distinct depolarization-activated K+ currents in isolated adult rat ventricular myocytes. J Gen Physiol 1991 May;97(5):973-1011.

(182) Wang L, Duff HJ. Developmental changes in transient outward current in mouse ventricle. Circ Res 1997 Jul;81(1):120-7.

(183) Leaf DE, Feig JE, Vasquez C, Riva PL, Yu C, Lader JM, et al. Connexin40 imparts conduction heterogeneity to atrial tissue. Circ Res 2008 Oct 24;103(9):1001-8.

(184) Dekker LR, Rademaker H, Vermeulen JT, Opthof T, Coronel R, Spaan JA, et al. Cellular uncoupling during ischemia in hypertrophied and failing rabbit ventricular myocardium: effects of preconditioning. Circulation 1998 May 5;97(17):1724-30.

(185) Dekker LR, Coronel R, VanBavel E, Spaan JA, Opthof T. Intracellular Ca2+ and delay of ischemia-induced electrical uncoupling in preconditioned rabbit ventricular myocardium Cardiovasc Res 1999 Oct;44(1):101-12.

(186) Kohlhaas M, Zhang T, Seidler T, Zibrova D, Dybkova N, Steen A, et al. Increased sarcoplasmic reticulum calcium leak but unaltered contractility by acute CaMKII overexpression in isolated rabbit cardiac myocytes. Circ Res 2006 Feb 3;98(2):235-44.

(187) Fitzgerald M, Neylon CB, Marks AR, Woodcock EA. Reduced ryanodine receptor content in isolated neonatal cardiomyocytes compared with the intact tissue. J Mol Cell Cardiol 1994 Oct;26(10):1261-5.

(188) Go LO, Moschella MC, Watras J, Handa KK, Fyfe BS, Marks AR. Differential regulation of two types of intracellular calcium release channels during end-stage heart failure. J Clin Invest 1995 Feb;95(2):888-94.

(189) Kaftan E, Marks AR, Ehrlich BE. Effects of rapamycin on ryanodine receptor/Ca(2+)-release channels from cardiac muscle. Circ Res 1996 Jun;78(6):990-7.

(190) Marx SO, Gaburjakova J, Gaburjakova M, Henrikson C, Ondrias K, Marks AR. Coupled gating between cardiac calcium release channels (ryanodine receptors). Circ Res 2001 Jun 8;88(11):1151-8.

(191) Kizana E, Chang CY, Cingolani E, Ramirez-Correa GA, Sekar RB, Abraham MR, et al. Gene transfer of connexin43 mutants attenuates coupling in cardiomyocytes: novel basis for modulation of cardiac conduction by gene therapy. Circ Res 2007 Jun 8;100(11):1597-604.

(192) Bagwe S, Berenfeld O, Vaidya D, Morley GE, Jalife J. Altered right atrial excitation and propagation in connexin40 knockout mice. Circulation 2005 Oct 11;112(15):2245-53.

(193) Darrow BJ, Laing JG, Lampe PD, Saffitz JE, Beyer EC. Expression of multiple connexins in cultured neonatal rat ventricular myocytes. Circ Res 1995 Mar;76(3):381-7.

(194) Reaume AG, De Sousa PA, Kulkarni S, Langille BL, Zhu D, Davies TC, et al. Cardiac malformation in neonatal mice lacking connexin43. Science 1995 Mar 24;267(5205):1831-4.

(195) Kleber AG, Rudy Y. Basic mechanisms of cardiac impulse propagation and associated arrhythmias. Physiol Rev 2004 Apr;84(2):431-88.

Appendix: summary of permission for third party copyright works

Please read the e-theses advice and guidance web pages, especially the section on clearing third party copyright works and complete the table below for all third party copyright works not covered by the fair dealing exception of criticism and review.

Where you have ticked:

- Permission to reuse - make sure you include proof of permission in this appendix
- Permission requested - make sure you include a copy of the request letter or email
- Orphan work - you include evidence that you have tried to locate the author

Page Number	Type of work: text, figure, map, etc.	Source work	Copyright holder & year	Work out of copyright	Permission to re-use	Permission requested	permission refused	Orphan work
Page 45	Figure 1	Dr Rasheda Chowdhury	Dr Rasheda Chowdhury		✓			
Page 48	Figure 2	Cell 1996 Feb 9;84(3):381-8.	© 1996 Cell Press		✓			
Page 50	Figure 3	Cardiovasc Res 2008 Oct 1;80(1):9-19.	© 2008, Oxford University Press		✓			
Page 51	Figure 4	Cardiovasc Res 2004 May 1;62(2):368-77.	© 2004, Oxford University Press		✓			

Page Number	Type of work: text, figure, map, etc.	Source work	Copyright holder & year	Work out of copyright	Permission to re-use	Permission requested	permission refused	Orphan work
Page 52	Figure 5	Cardiovasc Res 2008 Oct 1;80(1):9-19.	© 2008, Oxford University Press		✓			
Page 54	Figure 6	Cardiovasc Res 2004 May 1;62(2):368-77.	© 2004, Oxford University Press		✓			
Page 61	Figure 7	Physiol Rev 2003 Oct;83(4):1359-400	© 2003, The American Physiological Society		✓			
Page 64	Figure 8	Biochem J 2006 Mar 15;394(Pt 3):527-43.	© 2006, Portland Press com		✓			
Page 67	Figure 9	Biochem J 2006 Mar 15;394(Pt 3):527-43.	© 2006, Portland Press com		✓			
Page 78	Figure 10	Circulation 1997 Feb 18;95(4):988-96.	© 1997, Wolters Kluwer Health		✓			

Page Number	Type of work: text, figure, map, etc.	Source work	Copyright holder & year	Work out of copyright	Permission to re-use	Permission requested	permission refused	Orphan work
Page 91	Figure 11	Vetequip	© Vetequip		✓			
Page 94	Figure 12	Biopac	© Biopac		✓			
Page 96	Figure 13	Am J Physiol Heart Circ Physiol 2003 Sep;285(3):H1091-H1096.	© 2003, The American Physiological Society		✓			
Page 97	Figure 14	Am J Physiol Heart Circ Physiol 2003 Sep;285(3):H1091-H1096.	© 2003, The American Physiological Society		✓			
Page 99	Figure 15	Am J Physiol Heart Circ Physiol 2003 Sep;285(3):H1091-H1096.	© 2003, The American Physiological Society		✓			
Page 102	Figure 16	BMC Physiol 2008;8:8.	Creative commons licence deed		✓			

Page Number	Type of work: text, figure, map, etc.	Source work	Copyright holder & year	Work out of copyright	Permission to re-use	Permission requested	permission refused	Orphan work
Page 103	Figure 17	BMC Physiol 2008;8:8.	Creative commons licence deed		✓			
Page 105	Figure 18	Personal not published			✓			
Page 106	Figure 19	Personal not published			✓			
Page 111	Figure 20	Physiol Rev 2005 Oct;85(4):1205-53.	© 2005, The American Physiological Society		✓			
Page 112	Figure 21	Physiol Rev 2005 Oct;85(4):1205-53.	© 2005, The American Physiological Society		✓			
Page 113	Figure 22	Am J Physiol Heart Circ Physiol 283[1], 372-381. 1-7-2002.	2002, The American Physiological Society		✓			
Page 115	Figure 23	Biopac	© Biopac		✓			
Page 116	Figure 24	Data Science	© Data Science		✓			
Page 118	Figure 25	Personal unpublished work			✓			

Page Number	Type of work: text, figure, map, etc.	Source work	Copyright holder & year	Work out of copyright	Permission to re-use	Permission requested	permission refused	Orphan work
Page 126	Figure 26	Am J Physiol Heart Circ Physiol 2008 Nov;295(5):H1905-H1916.	© 2008, The American Physiological Society		✓			
Page 147	Figure 27	Am J Physiol Heart Circ Physiol 2003 Sep;285(3):H1091-H1096.	© 2003, The American Physiological Society		✓			
Page 149	Figure 28	Personal unpublished work	personal		✓			
Page 150	Figure 29	Personal unpublished work	personal		✓			
Page 161	Figure 30	Personal unpublished work	personal		✓			
Page 162	Figure 31	Personal unpublished work	personal		✓			
Page 174	Figure 32	unpublished work	Ms P Patel			✓		
Page 175	Figure 33	Unpublished figure own work	personal		✓			

Page Number	Type of work: text, figure, map, etc.	Source work	Copyright holder & year	Work out of copyright	Permission to re-use	Permission requested	permission refused	Orphan work
Page 179	Figure 34	BMC Physiol 2008;8:8.	Creative Commons Licence Deed		✓			
Page 181	Figure 35	BMC Physiol 2008;8:8.	Creative Commons Licence Deed		✓			
Page 183	Figure 36	BMC Physiol 2008;8:8.	Creative Commons Licence Deed		✓			
Page 184	Figure 37	BMC Physiol 2008;8:8.	Creative Commons Licence Deed		✓			
Page 185	Figure 38	BMC Physiol 2008;8:8.	Creative Commons Licence Deed		✓			
Page 187	Figure 39	BMC Physiol 2008;8:8.	Creative Commons Licence Deed		✓			

Page Number	Type of work: text, figure, map, etc.	Source work	Copyright holder & year	Work out of copyright	Permission to re-use	Permission requested	permission refused	Orphan work
Page 189	Figure 40	BMC Physiol 2008;8:8.	Creative Commons Licence Deed		✓			
Page 190	Figure 41	Unpublished figure			✓			
Page 192	Figure 42	Am J Physiol Heart Circ Physiol 2008 Nov;295(5):H1905-H1916.	© 2008, The American Physiological Society		✓			
Page 195	Figure 43	Am J Physiol Heart Circ Physiol 2008 Nov;295(5):H1905-H1916.	© 2008, The American Physiological Society		✓			
Page 196	Figure 44	Am J Physiol Heart Circ Physiol 2008 Nov;295(5):H1905-H1916.	© 2008, The American Physiological Society		✓			
Page 197	Figure 45	unpublished work			✓			

Page Number	Type of work: text, figure, map, etc.	Source work	Copyright holder & year	Work out of copyright	Permission to re-use	Permission requested	permission refused	Orphan work
Page 199	Figure 46	Unpublished work	Unpublished work		✓			
Page 202	Figure 47	Am J Physiol Heart Circ Physiol 2008 Nov;295(5):H1905-H1916.	© 2008, The American Physiological Society		✓			
Page 206	Figure 48	Am J Physiol Heart Circ Physiol 2008 Nov;295(5):H1905-H1916.	© 2008, The American Physiological Society		✓			
Page 208	Figure 49	Am J Physiol Heart Circ Physiol 2008 Nov;295(5):H1905-H1916.	© 2008, The American Physiological Society		✓			
Page 210	Figure 50	Am J Physiol Heart Circ Physiol 2008 Nov;295(5):H1905-H1916.	© 2008, The American Physiological Society		✓			

Page Number	Type of work: text, figure, map, etc.	Source work	Copyright holder & year	Work out of copyright	Permission to re-use	Permission requested	permission refused	Orphan work
Page 212	Figure 51	Am J Physiol Heart Circ Physiol 2008 Nov;295(5):H1905-H1916.	© 2008, The American Physiological Society		✓			
Page 216	Figure 52	Circ Res 2008 Oct 24;103(9):1001-8.	© 2008, Wolters Kluwer Health		✓			
Page 217	Figure 53	Circ Res 2008 Oct 24;103(9):1001-8.	© 2008, Wolters Kluwer Health		✓			
Page 218	Figure 54	Personal unpublished work			✓			
Page 219	Figure 55	Personal unpublished work			✓			

Page Number	Type of work: text, figure, map, etc.	Source work	Copyright holder & year	Work out of copyright	Permission to re-use	Permission requested	permission refused	Orphan work
Page 46	Table 1	Biochem J 2006 Mar 15;394(Pt 3):527-43.	© 2006, Portland Press com		✓			
Page 87	Table 2	Personal unpublished work			✓			
Page 101	Table 3	Personal unpublished work			✓			
Page 120	Table 4	Personal unpublished work			✓			
Page 121	Table 5	BMC Physiol 2008;8:8.	Creative Commons Licence Deed		✓			
Page 122	Table 6	Personal unpublished work			✓			
Page 123	Table 7	BMC Physiol 2008;8:8.	Creative Commons Licence Deed		✓			
Page 124	Table 8	Personal unpublished work			✓			
Page 135	Table 9	BMC Physiol 2008;8:8.	Creative Commons Licence Deed		✓			
Page 137	Table 10	BMC Physiol 2008;8:8.	Creative Commons Licence Deed		✓			

Page Number	Type of work: text, figure, map, etc.	Source work	Copyright holder & year	Work out of copyright	Permission to re-use	Permission requested	permission refused	Orphan work
Page 138	Table 11	Am J Physiol Heart Circ Physiol 2008 Nov;295(5):H1905-H1916.	© 2008, The American Physiological Society			✓		
Page 152	Table 12	Am J Physiol Heart Circ Physiol 2008 Nov;295(5):H1905-H1916.	© 2008, The American Physiological Society		✓	✓		
Page 194	Table 13	Am J Physiol Heart Circ Physiol 2008 Nov;295(5):H1905-H1916.	© 2008, The American Physiological Society		✓	✓		
Page 204	Table 14	Am J Physiol Heart Circ Physiol 2008 Nov;295(5):H1905-H1916.	© 2008, The American Physiological Society		✓	✓		

Title:	The Gap Junction Communication Channel
Author:	Nalin M Kumar,Norton B Gilula
Publication:	Cell
Publisher:	Elsevier
Date:	9 February 1996

Copyright © 1996 Cell Press. All rights reserved.

Order Completed

Thank you very much for your order.

This is a License Agreement between Andy Kontogeorgis ("You") and Elsevier ("Elsevier"). The license consists of your order details, the terms and conditions provided by Elsevier, and the payment terms and conditions.

Get the printable license.

License Number	3438210295960
License date	Jul 29, 2014
Licensed content publisher	Elsevier
Licensed content publication	Cell
Licensed content title	The Gap Junction Communication Channel
Licensed content author	Nalin M Kumar,Norton B Gilula
Licensed content date	9 February 1996
Licensed content volume number	84
Licensed content issue number	3
Number of pages	8
Type of Use	reuse in a thesis/dissertation
Portion	figures/tables/illustrations
Number of figures/tables/illustrations	1
Format	electronic
Are you the author of this Elsevier article?	No
Will you be translating?	No
Title of your thesis/dissertation	Murine Gap Junction Remodelling Induced By Subdiaphragmatic Pacing
Expected completion date	Aug 2014
Estimated size (number of pages)	259
Elsevier VAT number	GB 494 6272 12
Permissions price	0.00 USD
VAT/Local Sales Tax	0.00 USD / 0.00 GBP
Total	0.00 USD

ORDER MORE...   CLOSE WINDOW

From: "Jocelyn Kremer" <jocelyn@biopac.com>
Subject: RE: Permission request to use figure on website for PhD Dissertation with Imperial College London.
Date: 29 July 2014 22:13:13 BST
To: <andykontogeorgis1@gmail.com>

Dear Dr Kontogeorgis,

Thanks for using BIOPAC. Please accept this email as authiorization to use BIOPAC images el450.jpg (needle electodes) and mp100sys.jpg (MP100 System) in your dissertation.

For the web links, please use these instead:
· Needle electrodes:
http://www.biopac.com/research.asp?SubCatID=59&Main=Electrodes - this link offers a variety of needle electordes instead of just the 37 mm
· MP Systems -
http://www.biopac.com/Research.asp?CatID=43&Main=Systems - the MP100 System has been updated to the MP150 for quite some time and this link will always show the most recent systsems
Best regards,
 Jocelyn Mariah Kremer

BIOPAC
Systems, Inc.
Registered to ISO 9001:2008

42 Aero Camino, Goleta, CA 93117
Tel 805.685.0066 x128 | Fax 805.685.0067 | www.biopac.com

From: Andy Kontogeorgis   **Sent:** Tuesday, July 29, 2014 10:34 AM **To:** info@biopac.com **Subject:** Permission request to use figure on website for PhD Dissertation with Imperial College London.

Dear Biopac,

I utilised your equipment for my research whilst in Dr Gutstein's Lab at NYU and wanted to use a photograph/figure in my dissertation taken from your website of the needle electrodes-see the link

http://www.biopac.com/needle-electrode-unipolar-37mm.

I also wanted to use the photo on the
page http://www.biopac.com/acqknowledge-mp150-system-guide.

I have of course made reference to the company and both these web
links within my dissertation.

Sincerely and gratefully
Dr Andy Kontogeorgis

From: Marie Carretta <marie@vetequip.com>
Subject: RE: Permission request to use a figure from VetEquip website.
Date: 29 July 2014 19:02:29 BST
To: Andy Kontogeorgis <andykontogeorgis1@gmail.com>

Good afternoon and thank you for contacting us. You are more than welcome to utilize the information and/or photos from our website at your discretion ensuring the source and link are noted, as you have indicated. If there are other, more current products for which you would like photos or information, please don't hesitate to contact me. Thank you again!

Regards,

Marie Carretta,
Co-Owner/President/CEO
VetEquip, Inc.
marie@vetequip.com
800-466-6463
925-463-1828

-----Original Message-----
From: Andy Kontogeorgis [mailto:andykontogeorgis1@gmail.com]
Sent: Tuesday, July 29, 2014 10:27 AM
To: Marie Carretta
Subject: Permission request to use a figure from Vetequip website.

Dear Vetequip,

I utilised your vaporiser equipment for my PhD research and wanted to include a photo in my dissertation taken from your website.
I am writing to request permission in this respect.

The figure in question is at the following link and I will of course make reference and acknowldegment to the company and this link.
http://www.vetequip.com/images/big-901806.jpg

Sincerely and gratefully
Dr Andy Kontogeorgis

Dear Andy,
I am doing well. Hope you are ok. That figure is mine. It'll be fine if you just put something like "courtesy of Dr Rasheda Chowdhury".
Thanks
Rasheda

Dr Rasheda Chowdhury MA (Cantab) MSc (Oxon) PhD

Research Associate

Myocardial Function
National Heart and Lung Institute, Imperial College,
4th floor, Imperial Centre for Translational and Experimental Medicine
Hammersmith Campus
Du Cane Road
London W12 0NN

Tel: 0207 594 3614

From: Kontogeorgis Andy [mailto:A.Kontogeorgis@rbht.nhs.uk] **Sent:** 29 July 2014 16:03 **To:** Chowdhury, Rasheda A **Subject:** Re Figure Permissions.

Hi Rasheda,

Hope that you are well.
I just wanted to check with you regarding a figure I used in my thesis that I had from a previous version of the transfer report which you had given me(it was either yours or Para's).
Where did it originate from and where should I direct my permission request?
This is the figure I am referring to(attached).

From: **Andy Kontogeorgis** andykontogeorgis1@gmail.com
Subject: Permission to use EM figure in my dissertation.
Date: 12 August 2014 21:49
To: pravina.patel@imperial.ac.uk

Dear Pravina,

Hope that you are well.It has been a long time and I'm sorry to be troubling you now.

I wanted to ask if you would be happy for me to include an EM figure in my dissertation that you had emailed me/sent me while I was away in New York?

It is greatly appreciated.

Sincerely and warmest wishes
Andy Kontogeorgis

OXFORD JOURNALS
OXFORD UNIVERSITY PRESS

Title: Biophysical properties of homomeric and heteromultimeric channels formed by cardiac connexins:

Author: Alonso P Moreno

Publication: Cardiovascular Research

Publisher: Oxford University Press

Date: 05/01/2004

Copyright © 2004, Oxford University Press

Order Completed

Thank you very much for your order.

This is a License Agreement between Andy Kontogeorgis ("You") and Oxford University Press ("Oxford University Press"). The license consists of your order details, the terms and conditions provided by Oxford University Press, and the payment terms and conditions.

Get the printable license.

License Number	3438220831217
License date	Jul 29, 2014
Licensed content publisher	Oxford University Press
Licensed content publication	Cardiovascular Research
Licensed content title	Biophysical properties of homomeric and heteromultimeric channels formed by cardiac connexins:
Licensed content author	Alonso P Moreno
Licensed content date	05/01/2004
Volume number	62
Issue number	2
Type of Use	Thesis/Dissertation
Requestor type	Academic/Educational institute
Format	Print and electronic
Portion	Figure/table
Number of figures/tables	1
Will you be translating?	No
Author of this OUP article	No
Order reference number	None
Title of your thesis / dissertation	Murine Gap Junction Remodelling Induced By Subdiaphragmatic Pacing
Expected completion date	Aug 2014
Estimated size(pages)	259
Publisher VAT ID	GB 125 5067 30
Total	0.00 GBP

ORDER MORE... | CLOSE WINDOW

Wolters Kluwer
Health
Lippincott Williams & Wilkins

Requesting permission to reuse content from an LWW publication.

Title: Disturbed Connexin43 Gap Junction Distribution Correlates With the Location of Reentrant Circuits in the Epicardial Border Zone of Healing Canine Infarcts That Cause Ventricular Tachycardia

Author: Nicholas S. Peters, James Coromilas, Nicholas J. Severs, Andrew L. Wit

Publication: Circulation

Publisher: Wolters Kluwer Health

Date: Feb 18, 1997

Copyright © 1997, Wolters Kluwer Health

Order Completed

Thank you very much for your order.

This is a License Agreement between Andy Kontogeorgis ("You") and Wolters Kluwer Health ("Wolters Kluwer Health"). The license consists of your order details, the terms and conditions provided by Wolters Kluwer Health, and the payment terms and conditions.

Get the printable license.

License Number	3438240199473
License date	Jul 29, 2014
Licensed content publisher	Wolters Kluwer Health
Licensed content publication	Circulation
Licensed content title	Disturbed Connexin43 Gap Junction Distribution Correlates With the Location of Reentrant Circuits in the Epicardial Border Zone of Healing Canine Infarcts That Cause Ventricular Tachycardia
Licensed content author	Nicholas S. Peters, James Coromilas, Nicholas J. Severs, Andrew L. Wit
Licensed content date	Feb 18, 1997
Volume number	95
Issue Number	4
Type of Use	Dissertation/Thesis
Requestor type	Individual
Portion	Figures/table/illustration
Number of figures/tables/illustrations	1
Figures/tables/illustrations used	figure 6
Author of this Wolters Kluwer article	No
Title of your thesis / dissertation	Murine Gap Junction Remodelling Induced By Subdiaphragmatic Pacing
Expected completion date	Aug 2014
Estimated size(pages)	259
Total	0.00 GBP

ORDER MORE...   CLOSE WINDOW

RightsLink®

Wolters Kluwer
Health
Lippincott Williams & Wilkins

Requesting permission to reuse content from an LWW publication.
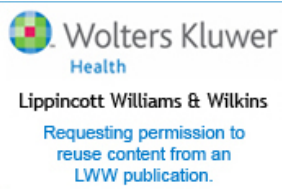
Title: Connexin40 Imparts Conduction Heterogeneity to Atrial Tissue

Author: David E. Leaf, Jonathan E. Feig, Carolina Vasquez, Pamela L. Riva, Cindy Yu, Joshua M. Lader, Andrianos Kontogeorgis, Elvera L. Baron, Nicholas S. Peters, Edward A. Fisher, David E. Gutstein, Gregory E. Morley

Publication: Circulation Research
Publisher: Wolters Kluwer Health
Date: Oct 24, 2008

Copyright © 2008, Wolters Kluwer Health

Logged in as:
Andy Kontogeorgis
Account #:
3000816379

LOGOUT

BACK | CLOSE WINDOW

[278]

RightsLink®

Logged in as:
Andy Kontogeorgis
Account #:
3000816379

LOGOUT

Permission Not Required

Permission is not required for this type of use.

BACK   CLOSE WINDOW

Title: Plasma Membrane Channels Formed by Connexins: Their Regulation and Functions

Author: JUAN C. SÁEZ,VIVIANA M. BERTHOUD,MARÍA C. BRAÑES,AGUSTÍN D. MARTÍNEZ,ERIC C. BEYER

Publication: Physiological Reviews

Publisher: The American Physiological Society

Date: Oct 1, 2003

Copyright © 2003, The American Physiological Society

Permission Not Required

Permission is not required for this type of use.

BACK   CLOSE WINDOW

OXFORD JOURNALS
OXFORD UNIVERSITY PRESS

Title: Gap junction alterations in human cardiac disease:

Author: Nicholas J. Severs, Steven R. Coppen, Emmanuel Dupont, Hung-I Yeh, Yu-Shien Ko, Tsutomu Matsushita

Publication: Cardiovascular Research

Publisher: Oxford University Press

Date: 05/01/2004

Copyright © 2004, Oxford University Press

Order Completed

Thank you very much for your order.

This is a License Agreement between Andy Kontogeorgis ("You") and Oxford University Press ("Oxford University Press"). The license consists of your order details, the terms and conditions provided by Oxford University Press, and the payment terms and conditions.

Get the printable license.

License Number	3438220555528
License date	Jul 29, 2014
Licensed content publisher	Oxford University Press
Licensed content publication	Cardiovascular Research
Licensed content title	Gap junction alterations in human cardiac disease:
Licensed content author	Nicholas J. Severs, Steven R. Coppen, Emmanuel Dupont, Hung-I Yeh, Yu-Shien Ko, Tsutomu Matsushita
Licensed content date	05/01/2004
Volume number	62
Issue number	2
Type of Use	Thesis/Dissertation
Requestor type	Academic/Educational institute
Format	Print and electronic
Portion	Figure/table
Number of figures/tables	1
Will you be translating?	No
Author of this OUP article	No
Order reference number	None
Title of your thesis / dissertation	Murine Gap Junction Remodelling Induced By Subdiaphragmatic Pacing
Expected completion date	Aug 2014
Estimated size(pages)	259
Publisher VAT ID	GB 125 5067 30
Total	0.00 GBP

ORDER MORE...   CLOSE WINDOW

OXFORD JOURNALS
OXFORD UNIVERSITY PRESS

Title: Remodelling of gap junctions and connexin expression in diseased myocardium:

Author: Nicholas J. Severs, Alexandra F. Bruce, Emmanuel Dupont, Stephen Rothery

Publication: Cardiovascular Research

Publisher: Oxford University Press

Date: 10/01/2008

Copyright © 2008, Oxford University Press

Order Completed

Thank you very much for your order.

This is a License Agreement between Andy Kontogeorgis ("You") and Oxford University Press ("Oxford University Press"). The license consists of your order details, the terms and conditions provided by Oxford University Press, and the payment terms and conditions.

Get the printable license.

License Number	3438220690956
License date	Jul 29, 2014
Licensed content publisher	Oxford University Press
Licensed content publication	Cardiovascular Research
Licensed content title	Remodelling of gap junctions and connexin expression in diseased myocardium:
Licensed content author	Nicholas J. Severs, Alexandra F. Bruce, Emmanuel Dupont, Stephen Rothery
Licensed content date	10/01/2008
Volume number	80
Issue number	1
Type of Use	Thesis/Dissertation
Requestor type	Academic/Educational institute
Format	Print and electronic
Portion	Figure/table
Number of figures/tables	2
Will you be translating?	No
Author of this OUP article	No
Order reference number	None
Title of your thesis / dissertation	Murine Gap Junction Remodelling Induced By Subdiaphragmatic Pacing
Expected completion date	Aug 2014
Estimated size(pages)	259
Publisher VAT ID	GB 125 5067 30
Total	0.00 GBP

ORDER MORE... | CLOSE WINDOW

Research article

Short-term pacing in the mouse alters cardiac expression of connexin43

Andrianos Kontogeorgis[14], **Riyaz A Kaba**[34], **Eunice Kang**[1], **Jonathan E Feig**[1], **Pritha P Gupta**[1], **Marc Ponzio**[1], **Fangyu Liu**[1], **Michael J Rindler**[2], **Andrew L Wit**[3], **Edward A Fisher**[12], **Nicholas S Peters**[34] and **David E Gutstein**[12]*

-        * Corresponding author: David E Gutstein
  david.gutstein@nyumc.org

Author Affiliations

[1]

Leon H. Charney Division of Cardiology, Department of Medicine, New York University School of Medicine, New York, NY, USA

[2]

Department of Cell Biology, New York University School of Medicine, New York, NY, USA

[3]

Department of Pharmacology, Columbia University College of Physicians and Surgeons, New York, NY, USA

[4]

Department of Cardiology, St Mary's Hospital, Imperial College London, UK

For all author emails, please log on.

The electronic version of this article is the complete one and can be found online at: http://www.biomedcentral.com/1472-6793/8/8

BioMed Central license agreement

published, constitute a breach of contract or of confidence or of commitment given to secrecy;
• I/we have taken due care to ensure the integrity of the article. To my/our - and currently accepted scientific - knowledge all statements contained in it purporting to be facts are true and any formula or instruction contained in the article will not, if followed accurately, cause any injury, illness or damage to the user.
• I agree to BioMed Central's Open Data policy
3. I, and all authors, agree that the article, if editorially accepted for publication, shall be licensed under the Creative Commons Attribution License 4.0. If the law requires that the article be published in the public domain, I/we will notify BioMed Central at the time of submission upon which the article shall be released under the Creative Commons 1.0 Public Domain Dedication waiver. For the avoidance of doubt it is stated that sections 1 and 2 of this license agreement shall apply and prevail regardless of whether the article is published under Creative Commons Attribution License 4.0 or the Creative Commons 1.0 Public Domain Dedication waiver.

The Creative Commons Attribution License 4.0 provides the following summary (where 'you' equals 'the user')

You are free to:

Share—copy and redistribute the material in any medium or format

Adapt—remix, transform, and build upon the material

for any purpose, even commercially. The licensor cannot revoke these freedoms as long as you follow the license terms.

Under the following terms:

Attribution—You must give appropriate credit, provide a link to the license, and indicate if changes were made. You may do so in any reasonable manner, but not in any way that suggests the licensor endorses you or your use. **No additional restrictions**—You may not apply legal terms or technological measures that legally restrict others from doing anything the license permits.

Notices:

You do not have to comply with the license for elements of the material in the public domain or where your use is permitted by an applicable exception or limitation.

No warranties are given. The license may not give you all of the permissions necessary for your intended use. For example, other rights such as publicity, privacy, or moral rights may limit how you use the material.

[284]

Reprints and permissions

Reprint service

BioMed Central offers a reprint service for those requiring professional quality reproductions of articles.

Open access articles | Other articles | Figures and tables | Reprint service | Commercial reprints

Open access articles

BioMed Central open access articles can be easily identified by looking at the first page of the full text or the PDF, where a logo or bar appears:

The open access logo is also displayed on search results and journal table of contents pages.

Under the terms of BioMed Central's open access charter, all open access articles are made available and publicly accessible via the Internet without any restrictions or payment by the user. PDF versions of open access articles in BioMed Central are available for download and provide a convenient way for users to make printed copies themselves.

As part of our copyright and license agreement, open access articles may be reproduced without formal permission or payment of permission fees. As a courtesy, however, anyone wishing to reproduce large quantities of an open access article (250+) should inform the copyright holder and we suggest a contribution in support of open access publication (see suggested contributions).

Attribution 2.0

License

THE WORK (AS DEFINED BELOW) IS PROVIDED UNDER THE TERMS OF THIS CREATIVE COMMONS PUBLIC LICENSE ("CCPL" OR "LICENSE"). THE WORK IS PROTECTED BY COPYRIGHT AND/OR OTHER APPLICABLE LAW. ANY USE OF THE WORK OTHER THAN AS AUTHORIZED UNDER THIS LICENSE OR COPYRIGHT LAW IS PROHIBITED.

BY EXERCISING ANY RIGHTS TO THE WORK PROVIDED HERE, YOU ACCEPT AND AGREE TO BE BOUND BY THE TERMS OF THIS LICENSE. THE LICENSOR GRANTS YOU THE RIGHTS CONTAINED HERE IN CONSIDERATION OF YOUR ACCEPTANCE OF SUCH TERMS AND CONDITIONS.

1. Definitions

a. **"Collective Work"** means a work, such as a periodical issue, anthology or encyclopedia, in which the Work in its entirety in unmodified form, along with a number of other contributions, constituting separate and independent works in themselves, are assembled into a collective whole. A work that constitutes a Collective Work will not be considered a Derivative Work (as defined below) for the purposes of this License.

b. **"Derivative Work"** means a work based upon the Work or upon the Work and other pre-existing works, such as a translation, musical arrangement, dramatization, fictionalization, motion picture version, sound recording, art reproduction, abridgment, condensation, or any other form in which the Work may be recast, transformed, or adapted, except that a work that constitutes a Collective Work will not be considered a Derivative Work for the purpose of this License. For the avoidance of doubt, where the Work is a musical composition or sound recording, the synchronization of the Work in timed-relation with a moving image ("synching") will be considered a Derivative Work for the purpose of this License.

c. **"Licensor"** means the individual or entity that offers the Work under the terms of this License.

d. **"Original Author"** means the individual or entity who created the Work.

e. **"Work"** means the copyrightable work of authorship offered under the terms of this License.

f. **"You"** means an individual or entity exercising rights under this License who has not previously violated the terms of this License with respect to the Work, or who has received express permission from the Licensor to exercise rights under this License despite a previous violation.

2. Fair Use Rights. Nothing in this license is intended to reduce, limit, or restrict any rights arising from fair use, first sale or other limitations on the exclusive rights of the copyright owner under copyright law or other applicable laws.

3. License Grant. Subject to the terms and conditions of this License, Licensor hereby grants You a worldwide, royalty-free, non-exclusive, perpetual (for the duration of the applicable copyright) license to exercise the rights in the Work as stated below:

   a. to reproduce the Work, to incorporate the Work into one or more Collective Works, and to reproduce the Work as incorporated in the Collective Works;

   b. to create and reproduce Derivative Works;

   c. to distribute copies or phonorecords of, display publicly, perform publicly, and perform publicly by means of a digital audio transmission the Work including as incorporated in Collective Works;

   d. to distribute copies or phonorecords of, display publicly, perform publicly, and perform publicly by means of a digital audio transmission Derivative Works.

   e. For the avoidance of doubt, where the work is a musical composition:

      i. **Performance Royalties Under Blanket Licenses**. Licensor waives the exclusive right to collect, whether individually or via a performance rights society (e.g. ASCAP, BMI, SESAC), royalties for the public performance or public digital performance (e.g. webcast) of the Work.

      ii. **Mechanical Rights and Statutory Royalties**. Licensor waives the exclusive right to collect, whether individually or via a music rights agency or designated agent (e.g. Harry Fox Agency), royalties for any phonorecord You create from the Work ("cover version") and distribute, subject to the compulsory license created by 17 USC Section 115 of the US Copyright Act (or the equivalent in other jurisdictions).

   f. **Webcasting Rights and Statutory Royalties**. For the avoidance of doubt, where the Work is a sound recording, Licensor waives the exclusive right to collect, whether individually or via a performance-rights society (e.g. SoundExchange), royalties for the public digital performance (e.g. webcast) of the Work, subject to the compulsory license created by 17 USC Section 114 of the US Copyright Act (or the equivalent in other jurisdictions).

The above rights may be exercised in all media and formats whether now known or hereafter devised. The above rights include the right to make such modifications as are technically necessary to exercise the rights in other media and formats. All rights not expressly granted by Licensor are hereby reserved.

4. Restrictions. The license granted in Section 3 above is expressly made subject to and limited by the following restrictions:

   a. You may distribute, publicly display, publicly perform, or publicly digitally perform the Work only under the terms of this License, and You must include a copy of, or the Uniform Resource Identifier for, this License with every copy or phonorecord of the Work You distribute, publicly display, publicly perform, or publicly digitally perform. You may not offer or impose any terms on the Work that alter or restrict the terms of this License or the recipients' exercise of the rights granted hereunder. You may not sublicense the Work. You must keep intact all notices that refer to this License and to the disclaimer of warranties. You may not distribute, publicly display, publicly perform, or publicly digitally perform the Work with any technological measures that control access or use of the Work in a manner inconsistent with the terms of this License Agreement. The above applies to the Work as incorporated in a Collective Work, but this does not require the Collective Work apart from the Work itself to be made subject to the terms of this License. If You create a Collective Work, upon notice from any Licensor You must, to the extent practicable, remove from the Collective Work any reference to such Licensor or the Original Author, as requested. If You create a Derivative Work, upon notice from any Licensor You must, to the extent practicable, remove from the Derivative Work any reference to such Licensor or the Original Author, as requested.

   b. If you distribute, publicly display, publicly perform, or publicly digitally perform the

Work or any Derivative Works or Collective Works, You must keep intact all copyright notices for the Work and give the Original Author credit reasonable to the medium or means You are utilizing by conveying the name (or pseudonym if applicable) of the Original Author if supplied; the title of the Work if supplied; to the extent reasonably practicable, the Uniform Resource Identifier, if any, that Licensor specifies to be associated with the Work, unless such URI does not refer to the copyright notice or licensing information for the Work; and in the case of a Derivative Work, a credit identifying the use of the Work in the Derivative Work (e.g., "French translation of the Work by Original Author," or "Screenplay based on original Work by Original Author"). Such credit may be implemented in any reasonable manner; provided, however, that in the case of a Derivative Work or Collective Work, at a minimum such credit will appear where any other comparable authorship credit appears and in a manner at least as prominent as such other comparable authorship credit.

5. Representations, Warranties and Disclaimer

UNLESS OTHERWISE MUTUALLY AGREED TO BY THE PARTIES IN WRITING, LICENSOR OFFERS THE WORK AS-IS AND MAKES NO REPRESENTATIONS OR WARRANTIES OF ANY KIND CONCERNING THE WORK, EXPRESS, IMPLIED, STATUTORY OR OTHERWISE, INCLUDING, WITHOUT LIMITATION, WARRANTIES OF TITLE, MERCHANTIBILITY, FITNESS FOR A PARTICULAR PURPOSE, NONINFRINGEMENT, OR THE ABSENCE OF LATENT OR OTHER DEFECTS, ACCURACY, OR THE PRESENCE OF ABSENCE OF ERRORS, WHETHER OR NOT DISCOVERABLE. SOME JURISDICTIONS DO NOT ALLOW THE EXCLUSION OF IMPLIED WARRANTIES, SO SUCH EXCLUSION MAY NOT APPLY TO YOU.

6. Limitation on Liability. EXCEPT TO THE EXTENT REQUIRED BY APPLICABLE LAW, IN NO EVENT WILL LICENSOR BE LIABLE TO YOU ON ANY LEGAL THEORY FOR ANY SPECIAL, INCIDENTAL, CONSEQUENTIAL, PUNITIVE OR EXEMPLARY DAMAGES ARISING OUT OF THIS LICENSE OR THE USE OF THE WORK, EVEN IF LICENSOR HAS BEEN ADVISED OF THE POSSIBILITY OF SUCH DAMAGES.

7. Termination

a. This License and the rights granted hereunder will terminate automatically upon any breach by You of the terms of this License. Individuals or entities who have received Derivative Works or Collective Works from You under this License, however, will not have their licenses terminated provided such individuals or entities remain in full compliance with those licenses. Sections 1, 2, 5, 6, 7, and 8 will survive any termination of this License.

b. Subject to the above terms and conditions, the license granted here is perpetual (for the duration of the applicable copyright in the Work). Notwithstanding the above, Licensor reserves the right to release the Work under different license terms or to stop distributing the Work at any time; provided, however that any such election will not serve to withdraw this License (or any other license that has been, or is required to be, granted under the terms of this License), and this License will continue in full force and effect unless terminated as stated above.

8. Miscellaneous

a. Each time You distribute or publicly digitally perform the Work or a Collective Work, the Licensor offers to the recipient a license to the Work on the same terms and conditions as the license granted to You under this License.

b. Each time You distribute or publicly digitally perform a Derivative Work, Licensor offers to the recipient a license to the original Work on the same terms and conditions as the license granted to You under this License.

c. If any provision of this License is invalid or unenforceable under applicable law, it shall not affect the validity or enforceability of the remainder of the terms of this License, and without further action by the parties to this agreement, such provision shall be reformed to the minimum extent necessary to make such provision valid and enforceable.

d. No term or provision of this License shall be deemed waived and no breach consented to unless such waiver or consent shall be in writing and signed by the

party to be charged with such waiver or consent.

e. This License constitutes the entire agreement between the parties with respect to the Work licensed here. There are no understandings, agreements or representations with respect to the Work not specified here. Licensor shall not be bound by any additional provisions that may appear in any communication from You. This License may not be modified without the mutual written agreement of the Licensor and You.